EXTRACELLULAR MATRIX-ENHANCED BIOMIMETIC SCAFFOLDS FOR TISSUE-SPECIFIC ORTHOPAEDIC TISSUE ENGINEERING

by

Benjamin B. Rothrauff

BA Psychology, Northwestern University, 2008

MRes Exercise Science, University of Glasgow, 2009

Submitted to the Graduate Faculty of the

School of Medicine in partial fulfillment

of the requirements for the degree of

Doctor of Philosophy

University of Pittsburgh

2016

UNIVERSITY OF PITTSBURGH

SCHOOL OF MEDICINE

This dissertation was presented

by

Benjamin B. Rothrauff

It was defended on

July 25, 2016

and approved by

Alan Wells, MD, DMSc, Professor, Department of Pathology

Harry C. Blair, MD, Professor, Department of Pathology

Volker Musahl, MD, Associate Professor, Department of Orthopaedic Surgery

Alejandro Soto-Gutierrez, MD, PhD, Assistant Professor, Department of Pathology

Dissertation Advisor: Rocky S. Tuan, PhD, Professor, Department of Orthopaedic Surgery

EXTRACELLULAR MATRIX-ENHANCED BIOMIMETIC SCAFFOLDS FOR TISSUE-SPECIFIC ORTHOPAEDIC TISSUE ENGINEERING

Benjamin B. Rothrauff, PhD

University of Pittsburgh, 2016

The work contained herein sought to combine soluble extracellular matrices (ECMs) derived from decellularized musculoskeletal tissues with biomimetic scaffolds for the purpose of orthopaedic tissue engineering. More broadly, tissue engineering combines cells, scaffolds, and biomolecules (e.g., growth factors and cytokines) to restore or replace biological tissues. Scaffolds derived from decellularized tissues provide cells with the biophysical and biochemical motifs that constitute the ECM of the native tissue, in turn promoting homologous (i.e., tissue-specific) cell phenotypes. However, decellularized whole tissues are limited in clinical use due to poor cell infiltration and constrained geometries. On the other hand, decellularized tissues can be pulverized or solubilized to theoretically provide a tissue-specific supplement that, in combination with biomimetic scaffolds, promotes homologous neotissue formation in a tissue defect regardless of shape or size. Nevertheless, the retention of tissue-specific bioactivity following solubilization of ECMs remains uncertain. In particular, few studies have explored the tissue-specific bioactivity of soluble ECM derived from decellularized musculoskeletal tissues.

In this thesis, tendon, hyaline cartilage, and knee menisci were decellularized and solubilized through one of two methods – (1) urea extraction or (2) pepsin digestion. When added as medium supplements to *in vitro* cultures of human mesenchymal stem cells (MSCs) grown on two-dimensional (2D) plastic or as 3D MSC pellets, only urea-extracted ECM

fractions promoted tissue-specific differentiation. Urea-extracted fractions of ECM derived from the inner and outer halves of the meniscus exerted region-specific effects, in agreement with the regional variations in ultrastructure, biochemical composition, and cell phenotype seen in native menisci. The soluble ECMs further enhanced tissue-specific differentiation when combined with biomimetic scaffolds, including aligned electrospun nanofibers to mimic tendon and photocrosslinkable hydrogels to mimic hyaline cartilage and inner meniscus. Additionally, soluble ECMs interacted synergistically with transforming growth factor beta (TGF-β) when provided as an exogenous supplement. Taken together, the work contained herein begins to elucidate the mechanisms by which soluble ECMs promote tissue-specific effects and provides support for their use in orthopaedic tissue engineering.

TABLE OF CONTENTS

PREFACE ..... **XVI**

1.0 INTRODUCTION **1**

1.1 ORTHOPAEDIC SOFT TISSUES **3**

1.1.1 Tendon and Ligament **3**

1.1.1.1 Structure and function **4**

1.1.1.2 Injury and intrinsic healing **6**

1.1.1.3 Current treatment approaches **7**

1.1.2 Articular Cartilage **8**

1.1.2.1 Structure and function **8**

1.1.2.2 Injury and intrinsic healing **10**

1.1.2.3 Current treatment approaches **11**

1.1.3 Meniscus **13**

1.1.3.1 Structure and function **13**

1.1.3.2 Injury and intrinsic healing **14**

1.1.3.3 Current treatment approaches **14**

1.2 MUSCULOSKELETAL TISSUE ENGINEERING **15**

1.2.1 Decellularized Extracellular Matrix as a Biomaterial **17**

1.2.1.1 Whole tissue ECM **18**

1.2.1.2 ECM Powder 19

1.2.1.3 Soluble ECM 20

1.2.2 Biomimetic Scaffolds 23

1.2.2.1 Electrospun nanofibers 23

1.2.2.2 Hydrogels 24

1.3 RESEARCH OVERVIEW 25

2.0 TISSUE-SPECIFIC BIOACTIVITY OF SOLUBLE TENDON- AND CARTILAGE-DERIVED EXTRACELLULAR MATRICES 27

2.1 INTRODUCTION 27

2.2 METHODS 29

2.2.1 Overview 29

2.2.2 Decellularization of tendon and cartilage 30

2.2.3 Solubilization of decellularized ECM 31

2.2.4 SDS-PAGE and growth factory analysis of soluble ECM 32

2.2.5 MSC isolation 32

2.2.6 Bioactivity of soluble ECM in 2-dimensional cell culture 33

2.2.7 Quantitative real-time polymerase chain reaction (qPCR) 33

2.2.8 Bioactivity of pepsin-digested ECM as 3-dimensional hydrogels 34

2.2.9 Bioactivity of urea-extracted ECM in culture of MSC pellets 34

2.2.10 Effect of TGF-β inhibition on urea-extracted ECM bioactivity 35

2.2.11 Histology and immunofluorescence 35

2.2.12 Biochemical composition 36

2.2.13 Bioactivity of ECM in culture of MSC-seeded aligned nanofibers 37

2.2.14 Bioactivity of cartilage ECM as in MSC-seeded GelMA hydrogels..... 38

2.2.15 Statistics 39

2.3 RESULTS 40

2.3.1 Characterization of tendon- and cartilage-derived ECMs..... 40

2.3.2 The effect of soluble ECMs on human MSCs in 2D culture 42

2.3.3 The effect of soluble ECMs on MSC pellets 44

2.3.4 The effect of TGF-β inhibition on soluble ECM bioactivity 47

2.3.5 The effect of soluble ECMs on MSCs seeded on aligned nanofibers 49

2.3.6 The independent and synergistic effects of cECM and TGF-β on chondrogenesis of MSCs seeded in 3D GelMA hydrogels..... 51

2.4 DISCUSSION..... 53

2.5 CONCLUSIONS..... 58

3.0 TENDON TISSUE ENGINEERING – COMBINING A BIOMIMETIC SCAFFOLD WITH SOLUBLE TENDON EXTRACELLULAR MATRIX AND TGF-β . 60

3.1 INTRODUCTION 61

3.2 MATERIALS AND METHODS..... 64

3.2.1 Cell isolation and culture..... 64

3.2.2 Colony forming unit-fibroblast assay..... 64

3.2.3 Flow cytometry..... 64

3.2.4 Preparation of tendon ECM 65

3.2.5 Preparation of scaffold 65

3.2.6 Scaffold characterization..... 66

3.2.7 Differentiation of hASCs 66

3.2.8 Cell proliferation tests 67

3.2.9 Real-time PCR analysis of gene expression 67

3.2.10 Protein extraction and Western blot assay 68

3.2.11 Mechanical testing 68

3.2.12 Matrix deposition and characterization 69

3.2.13 Immunofluorescent staining 69

3.2.14 Statistical analysis 70

3.3 RESULTS 70

3.3.1 Characterization of human ASCs 70

3.3.2 Effect of tendon ECM on ASC behavior in 2D 71

3.3.3 Characterization of the aligned microfiber scaffolds 74

3.3.4 Effect of tendon ECM on ASC behavior in scaffolds 76

3.4 DISCUSSION 80

3.5 CONCLUSIONS 84

4.0 MENISCUS TISSUE ENGINEERING – COMBINING REGION-SPECIFIC BIOACTIVITY OF SOLUBLE INNER AND OUTER MENISCAL-DERIVED EXTRACELLULAR MATRICES WITH PHOTOCURABLE HYDROGELS 85

4.1 REGION-SPECIFIC BIOACTIVITY OF SOLUBLE INNER AND OUTER MENISCAL-DERIVED EXTRACELLULAR MATRICES IN PHOTOCURABLE POLYETHYLENE GLYCOL DIACRYLATE (PEGDA) HYDROGELS 86

4.1.1 Introduction 86

4.1.2 Methods 88

4.1.2.1 Extraction and preparation of mECM 88

4.1.2.2 PEGDA preparation 90

4.1.2.3 Cell isolation 90

4.1.2.4 Fabrication of 3D construct 90

4.1.2.5 Cell viability assay 91

4.1.2.6 Real-time PCR analysis 91

4.1.2.7 Quantification of collagen based on hydroxyproline assay 92

4.1.2.8 Quantification of glycosaminoglycan (GAG) 92

4.1.2.9 Statistical analysis 93

4.1.3 Results 93

4.1.3.1 Decellularization of mECM 93

4.1.3.2 Extraction of mECM 95

4.1.3.3 Cell viability 95

4.1.3.4 Expression profiles of meniscus-associated genes 97

4.1.3.5 Quantification of hydroxyproline and GAG synthesis 98

4.1.4 Discussion 99

4.1.5 Conclusions 103

4.2 REGION-SPECIFIC BIOACTIVITY OF SOLUBLE INNER AND OUTER MENISCAL-DERIVED EXTRACELLULAR MATRICES IN PHOTOCURABLE METHACRYLATED GELATIN (GELMA) HYDROGELS 104

4.2.1 Introduction 104

4.2.2 Methods 106

4.2.2.1 Overview of experimental design 106

4.2.2.2 ECM decellularization 106

4.2.2.3 Histology of native and decellularized ECM 107

4.2.2.4 Biochemical composition of native and decellularized ECM..... 107

4.2.2.5 Solubilization of decellularized ECM..... 108

4.2.2.6 SDS-PAGE and growth factory analysis of ECM..... 111

4.2.2.7 Bioactivity of meniscus ECM extract in 2D culture..... 111

4.2.2.8 Bioactivity of meniscus ECM extract in 3D GelMA hydrogels 112

4.2.2.9 Gene expression and biochemical composition analyses..... 113

4.2.2.10 Histological and immunohistochemical analysis..... 113

4.2.2.11 Compressive mechanical testing..... 114

4.2.2.12 Statistical analyses..... 114

4.2.3 Results..... 115

4.2.3.1 Characterization of inner and outer meniscal ECM 115

4.2.3.2 ECM-induced proliferation and differentiation in 2D culture..... 117

4.2.3.3 Gene expression of MSC-seeded hydrogels enhanced with ECM 119

4.2.3.4 Immunohistochemical and histological staining of hydrogels 120

4.2.3.5 Biochemical composition and compressive moduli of hydrogels.. 125

4.2.4 Discussion..... 126

4.2.5 Conclusions..... 130

5.0 DISCUSSION 131

5.1 SUMMARY..... 131

5.2 FUTURE PERSPECTIVES..... 132

5.2.1 ECM-Enhanced Biomaterials – Getting Closer to Native Structure & Function 132

5.2.2 Top-Down vs. Bottom-Up Tissue Engineering 134

5.2.2.1 Top-down tissue engineering (reverse engineering) 134

5.2.2.2 Bottom-up tissue engineering (developmental engineering) 138

5.2.3 *In Situ* Tissue Engineering 139

5.2.4 Conclusions 141

SUPPLEMENTAL FIGURES 142

SUPPLEMENTAL TABLES 151

BIBLIOGRAPHY 155

LIST OF FIGURES

Figure 1. Overview of tendon tissue architecture. 5

Figure 2. Stress-strain behavior of tendon and ligaments. 6

Figure 3. Intrinsic healing response of tendon and ligament. 7

Figure 4. Hierarchical structure of osteochondral unit 10

Figure 5. The elements of tissue engineering 16

Figure 6. tECM-enhanced hydrogels upregulate tenogenesis 22

Figure 7. Characterization of soluble extracellular matrices 41

Figure 8. The effect of soluble ECMs on human MSCs in 2D culture 43

Figure 9. The effect of soluble ECMs on MSC pellet composition and gene expression 45

Figure 10. The effect of soluble ECMs on MSC pellet protein deposition 46

Figure 11. The effect of TGF-beta inhibition on soluble ECM bioactivity 48

Figure 12. The effect of soluble ECMs on MSCs on aligned nanofibers 50

Figure 13. The effects of cECM and TGF-beta on chondrogenesis of MSC-GelMA hydrogels . 52

Figure 14. Characterization of hASCs 71

Figure 15. Assay of hASC proliferation in 2D cultures 72

Figure 16. Tenogenesis of hASCs in 2D cultures 74

Figure 17. Characterization of electrospun PCL scaffolds 76

Figure 18. Behavior of hASCs seeded on aligned scaffolds 77

Figure 19. Tenogenic differentiation of hASCs seeded on aligned scaffolds 78
Figure 20. Matrix deposition by hASCs cultured on aligned scaffolds 80
Figure 21. Preparation of decellularized mECM 94
Figure 22. Viability of hBMSCs seeded in mECM-enhanced hydrogels 96
Figure 23. The effect of mECM on gene expression 98
Figure 24. The effect of mECM on hydrogel biochemical composition 99
Figure 25. Solubilization of ECM from inner and outer meniscus 110
Figure 26. Characterization of native and decellularized meniscus tissue 116
Figure 27. Bioactivity of soluble ECM extracts on MSCs in 2D culture 118
Figure 28. Gene expression in MSC-GelMA constructs 120
Figure 29. Immunohistochemical staining of collagen type 2 122
Figure 30. Safranin O staining 123
Figure 31. Immunohistochemical staining of collagen type 1 124
Figure 32. Biochemical composition and compressive modulus of MSC-GelMA constructs ... 125
Figure 33. Composite fiber-hydrogel scaffold fabrication 136
Figure 34. Tendon-like features of MSCs encapsulated in composite scaffold 137

LIST OF TABLES

Table 1. Primer sequences for real-time PCR..... 92

Table 2. Growth factor concentrations (pg/mL) in imECM and omECM extracts 117

PREFACE

I would like to begin by thanking my PhD adviser, Dr. Rocky Tuan, for giving me, a psychology major with no wet lab experience, the opportunity to become a tissue engineer. The freedom afforded by Rocky has allowed me to pursue a wide range of questions in orthopaedics and a breadth of experience that no other lab could possibly have matched.

Secondly, thanks to the members of my thesis committee for their thoughtful critiques and encouragement over the years. With a tendency to spread myself too thin, I appreciate their guidance in narrowing the scope of my thesis and providing me, as hopefully conveyed in the subsequent pages, with a coherent narrative.

Thirdly, credit is due to the many lab members of The Center for Cellular and Molecular Engineering. Beyond their collective generosity and patience in teaching me many techniques, they stoically tolerated my 'colloquialisms' and frequent digressions into the esoteric. A special thanks is given to Guang Yang, who has served as my partner in crime on the many tendon projects over the past 4 years.

Lastly, and most importantly, my family is worthy of unending gratitude. From always, my parents have provided me with every opportunity to pursue my interests unimpeded. It is upon this foundation that all past and future success is built.

1.0 INTRODUCTION

The musculoskeletal system is broadly divided into hard (bony) and soft tissues, with injury to these tissues constituting one of the most common causes of pain and disability. The etiology of musculoskeletal disease ranges from acute trauma to chronic degeneration. Treatment options span temporary activity restriction through total tissue replacement (e.g., meniscal allograft transplantation, osteochondral allograft transplantation, etc.). However, barring extensive co-morbidities (e.g., diabetes, chronic smoking, etc.) or massive tissue loss, injuries involving bone typically heal with complete restoration of bony structure and function. Conversely, orthopaedic soft tissues, including muscle, tendon, ligament, hyaline (i.e., articular) cartilage, and fibrocartilage (e.g., menisci, labrum, intervertebral discs), possess a poor intrinsic healing capacity. Also in contrast to bone, orthopaedic soft tissues generally have a limited blood supply and are relatively hypocellular, as individual cells are separated by dense extracellular matrix (ECM). The intraarticular location of many soft tissues may also contribute to their weak healing potential, as the synovial fluid contains fibrinolytic enzymes that degrade the provisional fibrin clot of early wound repair.[1] When healing does occur, it is through a process of scar formation. The healing tissue possesses a disorganized ultrastructure and dysregulated biochemical composition. Even following years of remodeling, the structure and function of the injured tissue is not restored to its native quality, resulting in sustained dysfunction and possible pain. Surgical treatment of ruptured soft tissues may successfully restore continuity of the torn

ends, yet biological limitations impede successful outcomes. As a result, there have been increasing efforts to enhance soft tissue healing by manipulating the innate healing response.

"[Tissue engineering] applies the principles of engineering and life sciences toward the development of biological substitutes that restore, maintain, or improve biological tissue or whole organ function."[2] In an effort to recapitulate the structure and function of native tissues, engineered constructs are comprised of cells, scaffolds, and biomolecules (e.g., growth factors, cytokines, etc.). The use of autologous cells obviates an adverse immune response induced by foreign cells of allografts or xenografts, but mature cells of musculoskeletal soft tissues (e.g., chondroctyes, tenocytes) are not available in large numbers due to the accompanying iatrogenic defect and frequently undergo rapid dedifferentiation upon expansion on culture plastic.[3] Alternatively, mesenchymal stem cells (MSCs) are adult stem cells of the perivascular niche that are abundantly available from multiple tissue sources (e.g., bone marrow, adipose) and are capable of differentiating into all mature cell lineages of the musculoskeletal system.[4,5] As a result, MSCs have been combined with biomimetic scaffolds and biomolecules germane to the development of a particular tissue in an effort to recapitulate the structure and function of native tissue. Unfortunately, the ECM of native tissue is highly complex, rendering current capabilities to faithfully engineer the combined biophysical and biochemical motifs of native tissues exceedingly difficult. On the other hand, decellularization of allografts or xenografts could mitigate immune rejection while preserving the ultrastructural and biochemical cues of native tissues, providing a scaffold capable of directing tissue-specific differentiation of endogenously recruited or exogenously seeded progenitor cells.[6,7]

However, the application of scaffolds derived from decellularized musculoskeletal ECMs is not without challenges. The dense ECM ultrastructure that imparts the unique function of

musculoskeletal soft tissues can necessitate relatively harsh decellularization methods, which may compromise the ultrastructure and biochemical composition of native tissues. Even with sufficient decellularization, infiltration of recruited or seeded cells is often limited, with cells remaining on the graft surface.[8,9] Likewise, grafts of decellularized whole tissue require invasive reconstruction/replacement procedures and the material properties of the graft are relatively immutable. In contrast, tunable biomaterials, including electrospun nanofibers and hydrogels, can be engineered to mimic the ultrastructure and mechanical properties of a particular musculoskeletal tissue while also permitting greater flexibility in terms of controlling degradation rates, cell migration/infiltration, and release of encapsulated growth factors. Nevertheless, the biomolecules traditionally incorporated into biomimetic scaffolds are far fewer than the diverse array of proteins that comprise native tissue and impart a particular phenotype to resident cells. Consequently, the following work has sought to combine soluble extracts of decellularized musculoskeletal tissues with tissue-specific biomimetic scaffolds to more fully recapitulate the native biochemical and biophysical cues that mediate tissue-specific cell phenotypes. This approach has been applied to three tissues that comprise a large percentage of the musculoskeletal disease burden – (1) tendon/ligament, (2) articular (hyaline) cartilage, (3) knee meniscus.

1.1 ORTHOPAEDIC SOFT TISSUES

1.1.1 Tendon and Ligament

The following section contains material from the publication:

Rothrauff BB, Yang G, Tuan RS. 2015. Tendon Resident Cells - Functions and Features in Section I - Developmental Biology and Physiology of Tendons. In: Gomes ME, Reis RL, Rodrigues MT (editors). Tendon Regeneration - Understanding Tissue Physiology and Development to Engineer Functional Substitutes. London, UK: Elsevier; pp. 41-77.

1.1.1.1 Structure and function Tendon and ligament connect muscle to bone or bone to bone, respectively, providing both joint stability and translating muscular contractile forces into joint mobility. Given their similar function, both tissues share a similar structure – a hierarchy of aligned collagen fibrils aggregated into aligned fibers with elongated fibroblasts (i.e., tenocytes) found in the interpositional region (**Figure 1**).[10] Mature tenocytes express the transcription factor Scleraxis (Scx)[11,12] and the cell surface glycoprotein Tenomodulin (Tnmd).[13,14] Tendon and ligament are principally composed of collagen type 1, but additional collagen types and proteoglycans play an essential role in orchestrating and maintaining tissue structure and function.[15] Growth factors and latent metalloproteinases are also localized to the ECM, contributing to tissue homeostasis. The hierarchical structure allows tendon and ligament to resist high tensile loads, with peak forces during running exceeding 12x bodyweight.[16] Although there is heterogeneity among tendons and ligaments, most will fail with strains exceeding 15%. Nevertheless, when testing under uniaxial tension, all tendons and ligament exhibit a characteristic load-elongation (stress-strain) curve (**Figure 2**), divided into the following regions – (a) 0-2% strain = toe region, in which the crimp pattern is slowly removed, (b) 2-8% strain = linear region, in which there is a constant increase in load with a corresponding increase in elongation, (c) >8% strain = plateau, preceding macroscopic failure.[17]

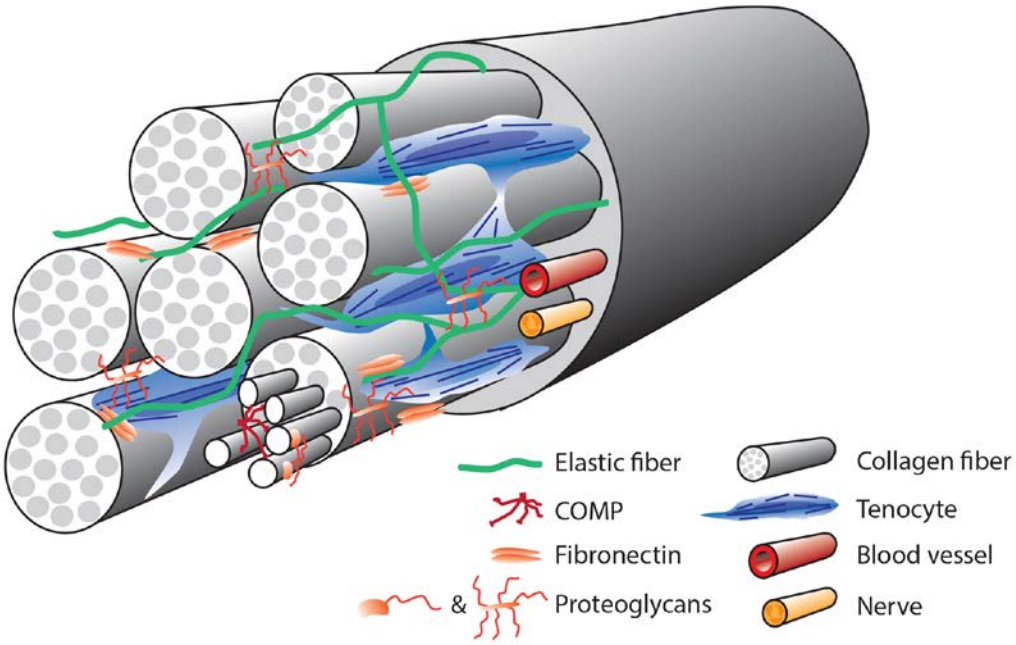

Figure 1. Overview of tendon tissue architecture. . Tenocytes reside between collagen fibers and deposit extracellular matrix proteins into the microenvironment. The proteoglycans, decorin, biglycan, fibromodulin, and lumican, are involved in collagen fibrillogenesis and stem cell niche maintenance. Besides proteoglycans, other types of glycoproteins are also important constituents of tendon for cell adhesion and structural integrity, such as fibronectin, cartilage oligomeric matrix protein (COMP), and lubricin. The collagen fibers are wrapped by a layer of connective tissue known as endotenon that contains blood vessels, lymphatics, and nerves.

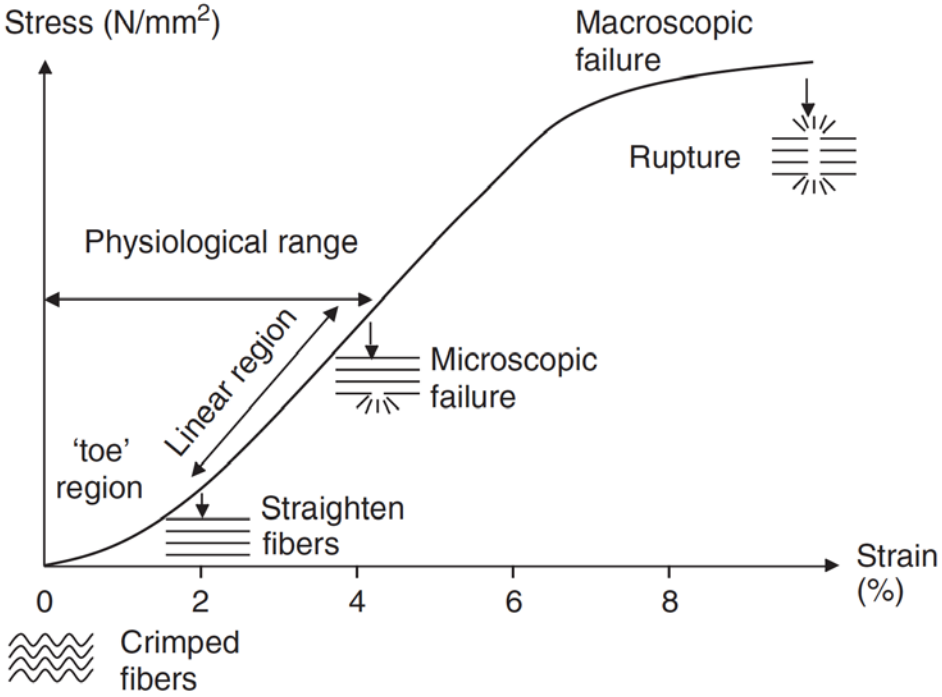

Figure 2. Stress-strain behavior of tendon and ligaments. When elongated under tension, tendons/ligaments exhibit three distinct regions in their stress-strain curves – toe (0-2% strain), linear (2-8% strain), and plateau (>8% strain). Adapted with permission from Wang (2006).[17]

1.1.1.2 Injury and intrinsic healing Of the 32 million musculoskeletal injuries occurring annually in United States, ~45% involve tendon and ligament.[18] While the incidence of injury differs across particular tendons and ligaments, none exhibits a healing response that restores native structure and function. However, tendons and ligaments located extraarticularly (i.e., outside the joint), such as the Achilles tendon and the collateral ligaments of the knee, can be managed conservatively, while those located intraarticularly, such as the rotator cuff tendons of the shoulder and the cruciate ligaments of the knee, display a negligible healing response.[1,19] As a result, intraarticular tendon and ligament injuries require surgical intervention to restore tissue continuity. In particular, over 100,000 anterior cruciate ligament (ACL) reconstructions are performed annually,[20] as are 300,000 rotator cuff repairs.[21] When intrinsic healing does occur, as

seen with tears of the medial collateral ligament (MCL), the process is one of generic wound healing, with sequential but overlapping inflammatory, proliferative, and remodeling phases.[22] The resulting neotissue is a hypertrophic scar with disorganized collagen fibril architecture and perturbations in biochemical composition (**Figure 3**), resulting in sustained decrements in mechanical properties. While numerous growth factors have been identified in this process,[23] in remains uncertain how their manipulation might permit scarless healing, or at minimum, the restoration of native structure and function.[24]

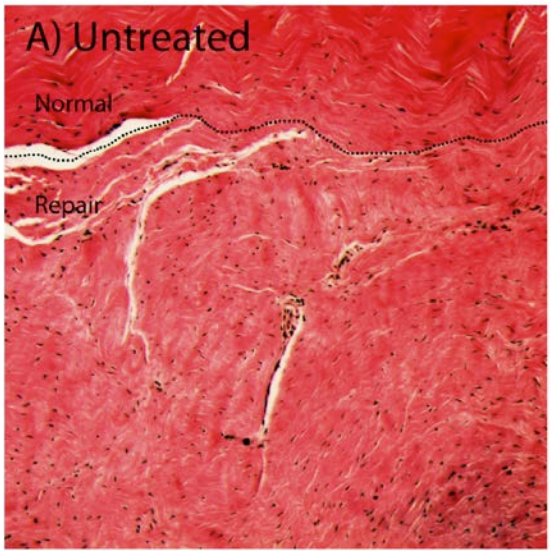

Figure 3. Intrinsic healing response of tendon and ligament. H&E stained section of the interface of native (normal) tendon and the disorganized scar (repair) that forms 12 weeks following removal of the central third of the patella tendon in a rabbit model.

1.1.1.3 Current treatment approaches The ideal treatment strategy for tendon and ligament tears is context dependent, taking into consideration not only the aforementioned differences in the intraarticular and extraarticular microenvironments, but also the state of health of other musculoskeletal tissues and the patient as a whole. For instance, isolated tears of the

MCL are more frequently repaired than are MCL tears in the context of a combined ACL tear.[25] In particular, an ACL reconstruction will render the patient non-weight bearing for several post-operative weeks, protecting the intrinsic healing response of the MCL. Furthermore, there is evidence that the MCL actually heals better in the presence of an ACL reconstruction, presumably due to a greater healing response elicited by concurrent injury. Regardless of the chosen conservative or surgical approach to treat a given tendon or ligament injury, biological impediments still exist. To date, no tissue engineering strategy has become standard of care for tendon and ligament injuries. While there are have been numerous case series on the application of tissue-derived scaffolds for augmented repair of large to massive rotator cuff tears, only two prospective, randomized trials have been performed, with conflicting results.[26,27] Given the paucity of high quality data, coupled with early reports of sterile inflammation, the American Academy of Orthopaedic Surgeons does not currently advocate the use of biologic scaffolds in the management of rotator cuff tears.[28] Clinical studies examining the efficacy of cell therapies in enhancing tendon and ligament healing are even rarer, although there are some promising findings for the application of exogenous MSCs in rotator cuff repair.[29]

1.1.2 Articular Cartilage

1.1.2.1 Structure and function Articular (hyaline) cartilage covers the ends of bone at a joint and serves to distribute loads and allow low friction gliding of articular surfaces. While hyaline cartilage contains a single cell type, the chondrocyte, the osteochondral unit possesses a hierarchical structure. Namely, when moving from superficial to deep, there are four zones – (1) superficial tangential, (2) middle transitional, (3) deep radial, and (4) calcified cartilage (**Figure 4**).[30] Collagen type 2 accounts for 90-95% of all collagen in hyaline cartilage, with the fibrils

organized in different orientations depending on region. Proteoglycans (e.g. hyaluronan, aggrecan, chondroitin/dermatan sulfate, etc.) also comprise a large portion of the cartilage mass, with these highly charged aggregates forming non-covalent bonds with water, thereby allowing cartilage to function in force dissipation.[31] In addition, hyaluronan and proteoglycan 4 (lubricin) are found at high concentrations in the superficial region and serve to minimize friction between articulating surfaces.[32] Devoid of blood vessels, lymphatics, and nerves, chondrocytes of hyaline cartilage are nourished through (hydrostatic) pressure-mediated fluid shifts, as occur with joint motion. Since cartilage can be several millimeters thick, there are both nutrient and oxygen gradients across regions, which can influence chondrocyte behavior.[33]

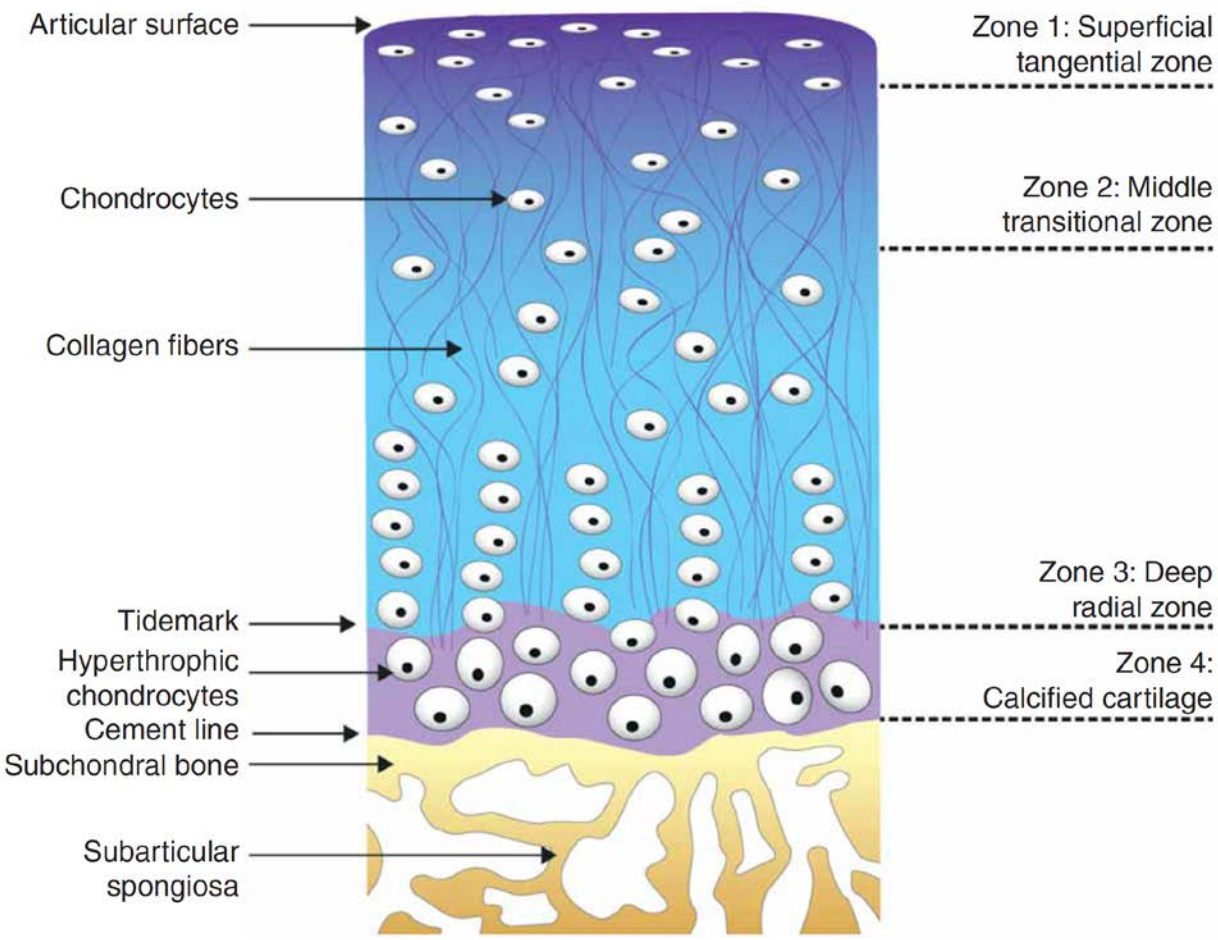

Figure 4. Hierarchical structure of osteochondral unit. Adapted with permission from Gadjankski & Vunjak-Novakovic (2015)[30]

1.1.2.2 Injury and intrinsic healing As of 2005, an estimated 27 million people in the United States had symptomatic joint degeneration (i.e., osteoarthritis, OA), a number expected to rise with an aging population.[34] While ~10% of the population truly constitutes a large disease burden, treating osteoarthritis in the context of an aged joint is a highly formidable challenge, given the diffusivity and chronicity of disease, coupled with systemic impairments in healing experienced with aging. On the other hand, 12% of osteoarthritis is attributable to a distinct

traumatic event (i.e., post-traumatic OA), which is seen more commonly in young patients with healthy joints, excluding the focal chondral defect.[35] Therefore, most of the early efforts to enhance cartilage healing (and subsequent efforts in cartilage tissue engineering) have focused on treating focal lesions, as discussed below.

The hypocellularity and absence of vasculature in cartilage has traditionally been cited to explain the poor intrinsic healing capacity of articular cartilage. Furthermore, it has long been believed that cartilage lacks any stem/progenitor cell population that could aid in tissue repair. However, recent studies have cast doubt on this dogma. Sekiya et al.[36] found an increase in MSCs within the synovial fluid of osteoarthritic joints, as compared to healthy knees, and the MSC number positively correlated with the severity of cartilage degeneration. Similarly, Jiang et al.[37] reported on the emergence of a multipotent cartilage stem/progenitor cell as a subpopulation of culture expanded mature chondrocytes. While the role that these putative progenitor cells play in vivo remains unclear, clinical evidence clearly demonstrates that any intrinsic healing response of cartilage is insufficient to prevent joint degeneration following acute trauma or with age.[38]

1.1.2.3 Current treatment approaches Age-associated OA follows a slow, insidious progression, ultimately causing the patient to present to the clinic complaining of diffuse joint paint made worse with duration and intensity of activity. At present, the standard of care involves analgesics (i.e., oral non-steroidals through intraarticular corticosteroid injections) and possible physical therapy to strengthen the surrounding muscles. However, upon failure of conservative treatment, total joint arthroplasty is typically recommended. Conversely, focal chondral defects in relatively healthy joints have been treated surgically over the past several decades. Namely, microfracture is a procedure in which the subchondral bone of the lesion is

punctured with small holes to allow blood (and with it, progenitor cells) to form a clot and initiate a generic wound healing response. While microfracture produces a fibrocartilaginous neotissue that improves both pain and function in the short-term, the inferiority of this tissue to that of native hyaline cartilage ultimately leads to continued joint degeneration.[39]

In an effort to promote a more hyaline phenotype, autologous chondrocyte implantation (ACI) was developed. ACI is a two-step procedure in which cartilage from a non-weightbearing region is isolated in the first procedure. The cartilage is enzymatically digested to liberate the chondrocytes, which are then expanded and subsequently re-implanted as a cell suspension into the focal defect. The defect is then covered by a collagen-based membrane that is sutured to the cartilaginous ring of the surrounding, healthy cartilage.[40] After undergoing several iterative changes, clinical results have shown promise, yet challenges still exist. In particular, promoting and maintaining a stable (hyaline) chondrogenic phenotype remains a major hurdle.[3] For reasons that are not entirely known, chondrocytes of the neotissue often drift towards a fibrochondrogenic phenotype, as seen with microfracture, or undergo hypertrophy in a process recapitulating endochondral ossification.[41-43]

Further adaptations of ACI have been reported, seeking to maintain a more stable chondrogenic phenotype and/or provide greater mechanical stability (and construct integrity) than a cell suspension covered with a membrane. Other products, utilizing allogeneic chondrocytes or autologous chondrocytes co-cultured with bone marrow cells, seek to obviate the need for a two-step procedure.[44] While these qualities must certainly be addressed in order to make cell-based therapies the standard of care for focal chondral defects, comparisons among products are limited at present by small sample sizes, low-quality clinical studies (i.e., case series), and non-standardized reporting on outcomes.[45] At the same time, and in recognition of

OA as a disease of the osteochondral unit,[46] tissue engineers have begun to fabricate composite constructs with zonal organization mimicking the native osteochondral unit.[30,47,48] Clinical application of these novel constructs are only in the earliest stages.

1.1.3 Meniscus

1.1.3.1 Structure and function The menisci of the knee are crescent-shaped fibrocartilaginous structures interposed between the femoral condyles and tibial plateau.[49] Functioning under a demanding mechanical loading environment of compressive, tensile, and shear stresses, the menisci have a complex, region-specific structure.[50,51] The inner region of the meniscus, when loaded by the articulating femur and tibia during locomotion, experience compressive forces that are translated through radial tie fibers to aligned circumferential collagen 1 fibers of the meniscus periphery.[51,52] Therefore, there is a gradient from the collagen 2- and proteoglycan-rich inner regions towards the collagen 1-rich outer regions.[53-55] The regional variation in structure and biochemistry corresponds to regional differences in cell phenotype – cells of the inner region possess a round morphology and gene expression profile similar to articular chondrocytes while cells of the outer region are interposed between aligned collagen fibers and exhibit a fibroblastic phenotype.[56]

Once thought to be a vestigial tissue, the meniscus is now recognized to be vital to joint health, and in particular, to maintaining the integrity of articular cartilage (i.e., preventing OA). As early as 1948, Fairbank[57] demonstrated that the complete removal of the meniscus (i.e., total meniscectomy) produces instantaneous joint space narrowing in the affected compartment, with subsequent loss of articular cartilage. Fairbank speculated that these destructive changes were attributable to decreased contact surface area, and increased contact stresses, resulting from

meniscectomy. Krause et al.[58] confirmed this impression of altered dynamics in 1976 through biomechanical testing of cadaveric models. Given the catastrophic consequences of total meniscectomy, orthopaedic surgeons thereafter sought to preserve meniscus tissue volume. This approach is further support by recent cadaveric studies. Bedi et al.[59,60] showed that changes in contact stresses, depending on tear morphology, are not seen until the tear size becomes quite large (e.g., 90% the width of the meniscus for radial tears), corroborating the importance of preserving tissue volume.

1.1.3.2 Injury and intrinsic healing The meniscus is the most commonly injured structure of the knee, resulting in over 1,000,000 meniscal procedures performed annually.[61] Much like articular cartilage, the inner 2/3rd of the meniscus is avascular, imparting a limited healing potential on this region. Unfortunately, the avascular region is where the majority of tears occur.[62] When meniscal explants are cultured ex vivo, the emerging cells are capable of forming colonies and undergoing multi-lineage differentiation, suggested either resident meniscal stem cells or dedifferentiation upon culture expansion.[63] Similarly, increased concentrations of MSCs are found in the synovial fluid after meniscus injury.[64] Nevertheless, inconsistent spontaneous healing of tears in the avascular region is seen clinically. In addition, an aberrant phenotype of meniscal cells in seen in the degenerated joint, with a predisposition to undergo osteogenesis.[65] Given the importance of the meniscus in joint integrity, coupled with a growing interest in biologics, primary repairs of meniscus tears are increasingly performed.[66]

1.1.3.3 Current treatment approaches Despite the recent trend to repair isolated meniscus tears,[66] the standard of care remains a partial meniscectomy for tears in the avascular region. Meniscal allograft transplantation is a viable option for a narrow patient population; in particular,

a young, thin patient with neutral knee alignment, healthy articular cartilage, intact (or concurrently repaired) knee ligaments, yet symptomatic meniscus deficiency.[61] In order to expand the number of patients eligible for primary meniscus repair, novel surgical approaches and suture techniques are being actively investigated.[67-69] Some of these techniques have since been translated to the operating room in a limited number of cases.[70,71]

Given the absence of vasculature in the inner meniscal region, surgeons will often place an autologous blood (i.e., fibrin) clot in the defect when performing a repair. While this approach showed early promise in animal models,[72] it has yielded equivocal benefit clinically, possible due to a rapid disintegration by fibrinolytic enzymes of synovial fluild.[1] The provision of vascular channels from the periphery to the tear site (i.e., trephination) has also shown mixed results.[73,74] The application of PRP, while sporadically employed, has also not demonstrated conclusive benefit.[75] Conversely, cell therapies have broadly shown promising results in large animal models,[76,77] yet only one human clinical study has been performed in which adipose-derived MSCs were injected intraarticularly following subtotal meniscectomy.[78,79]

1.2 MUSCULOSKELETAL TISSUE ENGINEERING

The following section contains material from the publication:

Yang G, **Rothrauff BB**, Ling H, Gottardi R, Alexander P, Tuan RS. 2015. Enhancement of tenogenic differentiation of human adipose stem cells by tendon-derived extracellular matrix. *Biomaterials* 34(37): 9295-9306.

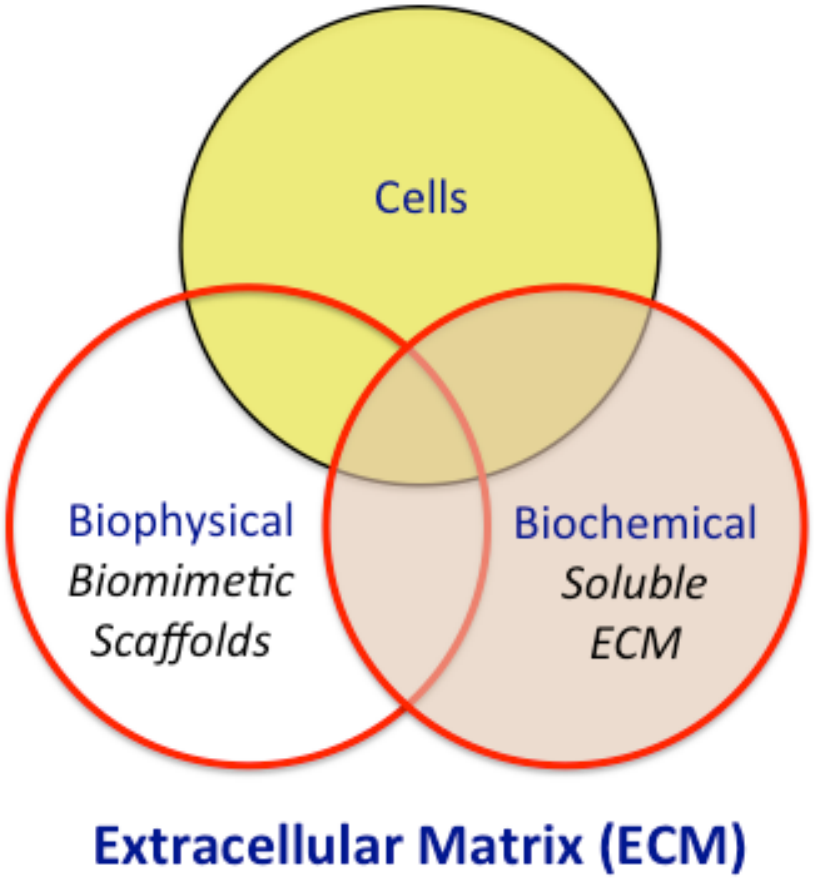

Figure 5. The elements of tissue engineering. Native tissues are comprised of cells and the extracellular matrix, which contains both biophysical and biochemical cues. In combining biomimetic scaffolds with tissue-derived soluble ECMs, it may be possible to replicate the biophysical and biochemical motifs, respectively, of native tissues. These novel biomaterials may then be seeded with patient-derived MSCs to provide an autologous, engineered construct for implantation.

Musculoskeletal tissue engineering, as with all tissues and organs, combines cells, scaffolds, and biomolecules, in an effort to reconstitute the essential elements of native tissue.[2] In native tissues, the ECM provides both biophysical and biochemical cues to the resident cells, which in

turn modify the ECM to maintain homeostasis (**Figure 5**). Thus, cells and ECM exist in a relationship of dynamic reciprocity.[6,80] Biomimetic scaffolds can be engineered to mimic the topographical and mechanical properties of the ECM. Although polymeric materials most commonly utilized for scaffolds are biocompatible, they often lack the bioactive motifs inherent to natural ECM proteins. At the same time, supplementation with exogenous biomolecules (i.e, growth factors) is needed for robust cell differentiation and protein synthesis, yet these growth factors have pleotropic effects that can result in heterologous cell phenotypes.

Alternatively, scaffolds derived from decellularized tissues theoretically possess the precise biophysical and biochemical cues that comprise the resident cell niche. However, ECM-derived scaffolds have several unique limitations, as outlined below, which prevent wider clinical application. Soluble solutions of decellularized ECM have been recently explored to overcome several of these limitations, yet their ability to promote homologous (i.e., tissue-specific) cell phenotypes remains underexplored. The strengths and weaknesses of biomimetic scaffolds and those derived from ECM will be described in sequence with the intention of combining these biomaterials to capture their respective advantages while overcoming their limitations.

1.2.1 Decellularized Extracellular Matrix as a Biomaterial

Far from being a passive 'ground substance', as previously considered, the ECM actively communicates with the resident cells. The ECM is so rich in bioactive information that decellularized whole organs have sustained systemic physiological function when transplanted into animal models following recellularization and pre-conditioning in bioreactors.[81-83] Although whole organs are complex systems with multiple cell types, whose interactions are coordinated

across time and space, the decellularization protocols that must be employed for sufficient removal of their cellular content are more mild than those required to decellularize dense connective tissues.[6,84] Not only does the dense collagenous architecture prevent permeation of cytolytic agents and subsequent extraction of cellular remnants, these tissues are also hypovascular, providing fewer conduits through which the decellularizing agents may be perfused. Nevertheless, several protocols have been shown to successfully decellularize tendon, cartilage, and meniscus, which can be used as (whole) tissue grafts or further processed by milling and solubilization. Each form of decellularized ECM presents unique advantages and limitations, as discussed below.

1.2.1.1 Whole tissue ECM Large explants of tendon, cartilage, and meniscus have been decellularized using assorted protocols, though most include a detergent (e.g., Triton X-100, Sodium Dodecyl Sulfate, etc.) with possible nuclease treatment to follow.[84-86] Decellularization of the whole tissue has been most commonly explored for tendon, with several studies demonstrating the preservation of aligned collagen ultrastructure following decellularization.[85,87-90] The scaffolds are capable of supporting cellular attachment, proliferation, and elongation (parallel to collagen fibers), with corresponding upregulation of tenogenic markers.[85,89,90] The preservation of ultrastructure results in negligible reductions in tensile properties,[88] but highly aligned collagen fibers yield poor suture retention strength, perhaps limiting surgical applicability especially if the graft is intended for mechanical augmentation.[91,92]

Alternatively, decellularization has been found to diminish the compressive modulus of hyaline cartilage ECM, likely due to a significant loss of proteoglycan content.[8,93] Seeded cells are capable of upregulating a chondrogenic phenotype with corresponding deposition of cartilaginous ECM proteins (e.g., Collagen type 2, proteoglycan), but this anabolic effect is

dependent on culture supplementation with exogenous transforming growth factor beta, TGF-β.[8,84,93] Similar observations have been reported for decellularized menisci, although only a few studies have been performed to date.[86,94] Regardless of the proteoglycan loss, decellularized whole cartilage ECM exhibits minimal cell infiltration, with cells localized to the explant surface.[8,93] Limited cell infiltration may adversely affect graft remodeling and integration with native tissues, perhaps explaining the high failure rate of decellularized osteochondral allografts when applied clinically to focal cartilage lesions.[95] Of further concern, limited cell infiltration has also been noted for decellularized whole tendon[9,88] and meniscus.[86]

1.2.1.2 ECM Powder In order to improve cell infiltration and surgical applicability, as needed for small and/or irregularly shaped defects, the decellularized ECM can be milled into a powder. In a series of related studies, Guilak and colleagues fabricated scaffolds of mechanically homogenized cartilage ECM fragments.[96-98] When seeded with MSCs, these constructs supported chondrogenic differentiation and matrix deposition, effects that were enhanced with TGF-β supplementation in the culture medium.[96] However, non-crosslinked scaffolds underwent cell-mediated contractions, limiting their applicability as space-filling constructs, as would be required for repair of focal chondral defects.[96] Chemical or physical methods of crosslinking were able to preserve construct area,[96,97] but increasing crosslinking density lead to decreasing chondroinductivity of the scaffold.[97] Through optimization of the crosslinking agent and density, as well as the concentration of cartilage-derived matrix, anatomically-shaped constructs could be molded.[98] However, the compressive mechanical properties of the constructs were still significantly inferior to native cartilage.[98]In similar but independent studies, Almeida et al.[99-101] fabricated scaffolds of cartilage derived ECM powder

through freeze-drying,[100] dihydrothermal crosslinking,[99] or mixing with fibrin hydrogels.[101] The ECM powder alone supported chondrogenesis of seeded MSCs, but robust chondrogenesis again required TGF-β supplementation. In applying a similar approach to tendon and ligament tissue engineering, Dianne Little's group has mixed pulverized ECM with collagen hydrogels[102] or used it to coat electrospun nanofibrous scaffolds.[103] Compared to studies examining cartilage ECM powder, the effects of tendon/ligament ECM powder were less inspiring, as these powders had little to modest effects on tenogenic differentiation of seeded MSCs.[102,103] With several differences in experimental design, it is not possible to explain the minimal effects of the tendon/ligament powder when applied as a tissue-specific bioactive agent.

1.2.1.3 Soluble ECM Although pulverization of ECM improves cell distribution and expands the forms through which ECM can be incorporated into scaffolds, the constructs must be crosslinked within geometrically defined molds, with a subsequent in vitro culture period required for cell infiltration and attachment. To overcome these limitations, further processing of decellularized ECM into soluble solutions has been explored. Pepsin digestion of ECM in a mildly acidic solution yields a viscous slurry that self-polymerizes when neutralized and heated to body temperature.[104] Pepsin digests of tendon,[105,106] cartilage,[107,108] and meniscus[109] have been reported, with all studies noting excellent cytocompatibility. However, few studies have investigated the tissue-specific bioactivity of these hydrogels despite this putative property being the basis for the use of homologous ECM. Pati et al.[107] reported a very modest (~1.5 fold) increase in Sox9 and Col2 expression in cells seeded in pepsin-digested cartilage ECM, as compared to a purified collagen 1 hydrogel. In similar studies, Beck et al.[110] and Visser et al.[111] found negligible tissue-specificity of pepsin-digested tendon, cartilage, or meniscus. It is possible that pepsin, a non-specific protease, cleaves many of the bioactive proteins of the ECM

that are essential for imparting tissue-specificity. SDS-PAGE gels of pepsin-digested ECM support this hypothesis, with few bands found outside of those corresponding to collagen chains.[107,112]

On the other hand, Zhang et al.[113] demonstrated that 2D culture dishes coated with urea-extracted fractions of liver, skeletal muscle, and skin ECM, promoted homologous cell phenotypes. Similarly, our lab found that the urea-extracted fraction of decellularized MSC sheets, as opposed to pepsin-digested preparations, enhanced MSC attachment, spreading, proliferation, migration, and multi-lineage differentiation.[114] More recently, we showed that urea-extracted tendon ECM, when added to an MSC-seeded collagen hydrogel under static uniaxial tension, upregulated tenogenic differentiation while concurrently downregulating osteogenic markers, suggesting homologous bioactivity inherent in this soluble ECM preparation (**Figure 6**).[115] Based upon these findings, it is possible that urea-extracted fractions of decellularized ECM derived from multiple musculoskeletal tissues can promote tissue-specific differentiation. If so, these soluble ECM preparations may be combined with biomimetic scaffolds possessing topographical and mechanical properties of homologous tissues, providing a tissue engineered construct containing both the biophysical and biochemical motifs of native tissue.

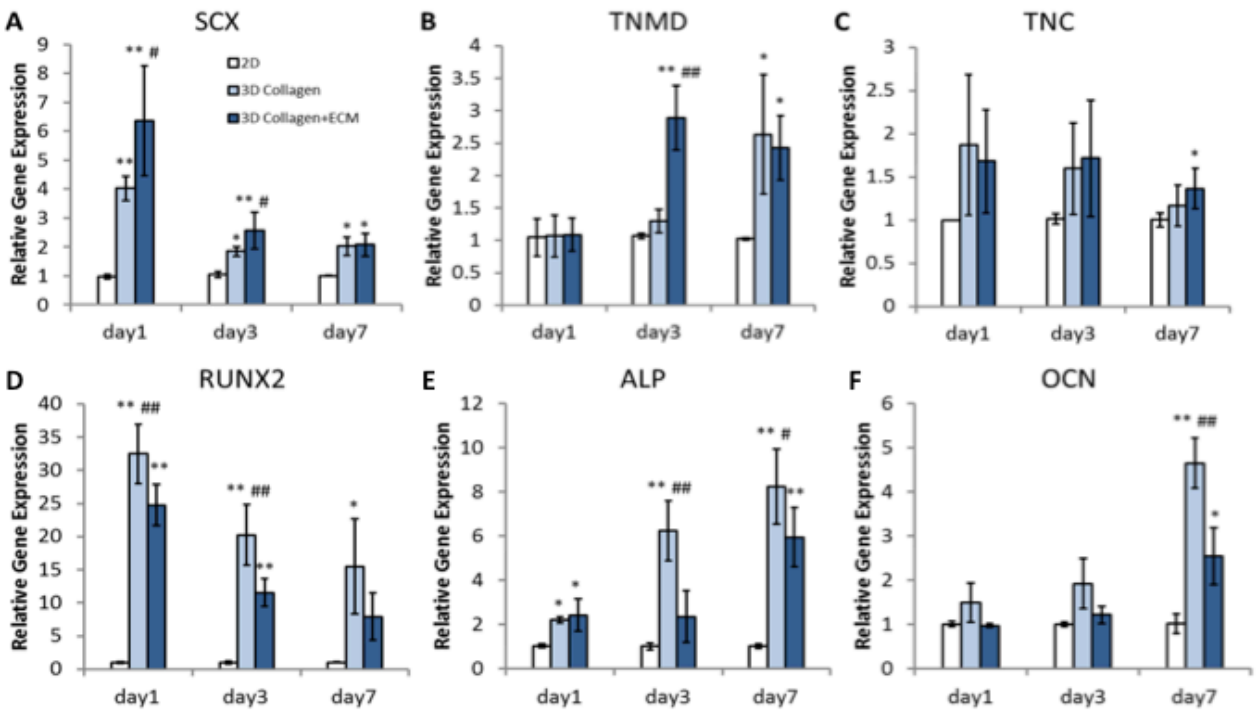

Figure 6. tECM-enhanced hydrogels upregulate tenogenesis. (A-C) Human MSCs seeded in tECM-supplemented scaffolds (3D Collagen+ECM) show higher expression levels of tendon-specific genes (SCX, TNMD, and TNC) compared to both pure collagen scaffolds (3D Collagen) and 2D culture group (2D). (D-F) Osteogenesis-related genes (RUNX2, ALP, and OCN) are expressed at lower levels in MSCs seeded in tECM-supplemented scaffolds compared to the pure collagen scaffold group, although some of them remain still higher than that in 2D culture. * indicates $p < 0.05$ compared to 2D; ** indicates $p < 0.01$ compared to 2D; # indicates $p < 0.05$ compared to the other 3D group; and ## indicates $p < 0.01$ compared to the other 3D group; n = 5

1.2.2 Biomimetic Scaffolds

"Biomimetic scaffolds mimic important features of the extracellular matrix (ECM) architecture and can be finely controlled at the nano- or microscale for tissue engineering."[116] In engineering biologically relevant ECM motifs, cell behavior can be controlled for an intended purpose.[117] The repertoire of materials and methods used for engineering biomimetic scaffolds has rapidly expanded since the inception of tissue engineering. While many have been explored for applications in musculoskeletal tissue engineering, nanofibers and hydrogels have been extensively utilized for tendon and cartilage engineering, respectively.

1.2.2.1 Electrospun nanofibers Electrospinning is a fabrication technique in which a viscous polymer (e.g., polyester) is pushed through a needle under high electrical charge and collected on a rotating mandrel that is electrically grounded.[118] In controlling the parameters of electrospinning, mats of continuous fibers with particular geometries can be created.[119] Electrospun sheets of aligned nano- or microfibers have been exploited to mimic the aligned collagen fibers of the native tendon.[120,121] Interestingly, electrospun fibers with an average diameter of several hundred nanometers (e.g., 320 ± 100 nm) promote greater cell proliferation those with a large diameter (1.8 ± 0.16 μm), which preferentially promote tenogenic differentiation.[122] It is plausible that small diameter fibers mimic the immature collagen fibers of healing or developing tendon, a microenvironment in which cell proliferation would be needed, while large diameter fibers are reminiscent of mature tendon and therefore promote a mature tendon phenotype.[123]

Fiber orientation provides another instructive cue to seeded cells. As compared to randomly oriented fibers, aligned fibers promote elongation of cells in a parallel direction,

resulting in upregulation of tenogenic markers and deposition of aligned ECM.[124,125] Related studies have shown synergism between these biophysical cues and exogenous growth factors[126,127] or mechanical stimulation,[128] although cooperative effects have not been universally reported,[129] with discrepancies likely attributable to variability in polymer composition, culture conditions, and micro- and meso-scale architectural cues.[130] To date, no study has explored the possible synergism between aligned nanofibrous scaffolds and soluble tendon ECM.

1.2.2.2 Hydrogels Hydrogels are networks of crosslinked hydrophilic polymers capable of retaining high water content, bearing resemblance to the water-rich, interconnected collagen/proteoglycan network of hyaline cartilage.[131] Polymers such as agarose and polyethylene glycol (PEG) can form 3D porous structures capable of maintaining cell sphericity and supporting chondrogenic differentiation, but these relatively bioinert molecules lack cell-binding motifs of natural ECM proteins.[131,132] In contrast, gelatin contains the bioactive motifs of native collagen while being highly water-soluble and capable of further functionalization. In particular, the addition of methacrylate functional groups to the gelatin backbone, in the presence of a light-sensitive electron donor (i.e., photoinitiator), is capable of undergoing light-responsive crosslinking that results in a stable hydrogel. These methacrylated gelatin (GelMA) hydrogels allow rapid encapsulation of cells and support robust transcriptional and translational upregulation of chondrogenesis.[133,134] The addition of distinct cartilage ECM proteoglycans (e.g., hyaluronan, chondroitin sulfate, etc.) to GelMA hydrogels has been shown to further enhance chondrogenesis of encapsulated cells.[135] However, the bioactive effect adding soluble cartilage ECM to GelMA hydrogels has not been investigated.

Hydrogels have also been explored in the context of meniscus tissue engineering, but the majority of applications have sought to fabricate a whole engineered meniscus graft as opposed

to delivering cells to the tear site during surgical repair.[136-138] In the few studies in which cell-seeded hydrogels were used to augment suture repair, the hydrogel was made of a collagen slurry, which possesses weak mechanical properties and undergoes fast degradation.[76,139] Given the homology of structure and biochemical composition between hyaline cartilage and the inner meniscal region, which possesses a poor intrinsic healing capacity but where most tears occur, the application of MSC-seeded GelMA hydrogels to meniscal tears may serve to enhance neotissue formation. Further improvement may also be possible by enhancement the GelMA hydrogel with a soluble fraction of the inner meniscal ECM.

1.3 RESEARCH OVERVIEW

The overarching goal of the studies described hereafter is to develop a rational approach to musculoskeletal tissue engineering by combining the tissue-specificity inherent in decellularized extracellular matrix (ECM) with the versatility of engineered biomaterials. The central hypothesis was that urea-extracted soluble ECM preparations derived from decellularized tendon, cartilage, and meniscus, would promote tissue- and/or region-specific differentiation of human mesenchymal stem cells (MSCs), thereby enhancing biomimetic scaffolds fabricated for orthopaedic tissue engineering. The hypothesis was tested through the following specific aims:

Specific Aim 1: Evaluate and compare the tissue-specific bioactivity of soluble tendon and cartilage ECM prepared through two methods – (a) pepsin digestion and (b) urea extraction

Specific Aim 2: Evaluate the effect of combining soluble tendon and cartilage ECM with tissue-appropriate biomimetic scaffolds

Specific Aim 3: Evaluate the region-specific bioactivity of soluble inner and outer meniscal ECM when combined with biomimetic hydrogels.

These aims were addressed through experiments that ultimately comprise the content of four peer-reviewed publications. The evaluation of tissue-specific bioactivity of soluble tendon and cartilage ECM (Aim 1) is described in Chapter 2. The benefit of enhancing biomimetic scaffolds with these soluble ECMs (Aim 2), and their synergistic effects with TGF-β supplementation, are described in Chapters 2 and 3. Finally, the region-specific bioactivity of soluble ECM derived from the inner and outer meniscal regions was explored in two photocurable hydrogels (Aim 3), the results of which are presented in Chapter 4.

2.0 TISSUE-SPECIFIC BIOACTIVITY OF SOLUBLE TENDON- AND CARTILAGE-DERIVED EXTRACELLULAR MATRICES

2.1 INTRODUCTION

Tendon and cartilage are commonly injured musculoskeletal tissues with a poor intrinsic healing capacity. Tissue engineering strategies, which employ the independent or combined application of cells, scaffolds, or biomolecules, have shown promise in restoring the structure and function of both tendon[140,141] and cartilage.[39,142] Biomimetic scaffolds, including aligned electrospun nanofibers[124,125] and hydrogels,[134,143] possess ultrastructural motifs respectively found in native tendon and cartilage, which are capable of directing differentiation of mesenchymal stem cells (MSCs) towards a particular musculoskeletal lineage. These effects are further enhanced by exposure to soluble biomolecules known to orchestrate tendon and cartilage development.[127,131,144] In particular, the transforming growth factor beta (TGF-β) superfamily plays an essential role in both tenogenesis[145] and chondrogenesis,[146] mediating divergent effects depending upon additional microenvironmental cues.[147] At present, an incomplete understanding of the biophysical and biochemical cues governing tendon and cartilage development and homeostasis preclude consistent regeneration of these tissues when employing the aforementioned tissue engineering approaches.[3]

On the other hand, tissues and organs can be decellularized to mitigate an adverse immune response against foreign cells while theoretically preserving the ultrastructural, mechanical, and biochemical motifs of the native tissue.[6] To that end, decellularized tendon and cartilage may serve as the ideal scaffold to promote homologous (i.e., tissue-specific) differentiation of endogenously recruited or exogenously delivered progenitor cells.[84,148] Indeed, decellularized tendon[85,89,90] and cartilage[8,93] tissues have been found to promote tissue-specific differentiation when seeded with MSCs. Nevertheless, the dense collagenous architecture comprising the ECM of these tissues can necessitate the use of relatively harsh decellularization methods, which can compromise native tissue ultrastructure and biochemical composition. Even with sufficient removal of cellular content, the dense ECM serves as a barrier for cell infiltration, with cells often localized to the tissue surface.[8,9] In addition, the use of whole decellularized tissue as grafts requires surgical reconstruction/transplantation (as opposed to repair), with resulting limitations in treating small or irregularly shaped defects.

In an effort to overcome these limitations while retaining the tissue-specific bioactivity inherent in the ECM, decellularized tissues have been processed into powders, which can be molded into distinct geometric shapes,[96,98] or suspended in a hydrogel.[100,101,110] Alternatively, ECM powders can be solubilized with enzymatic or chaotropic agents, resulting in an injectable solution that can be combined with a diverse array of biomaterials. Pepsin-digested tendon[105,106] and cartilage[108,149] hydrogels have been shown to undergo thermoresponsive gelation at body temperature and are cytocompatible. However, the effect of pepsin, a non-specific protease, on the tissue-specific bioactivity of tendon and cartilage ECM remains unknown. While Keane et al.[150] reported that pepsin-digested esophageal ECM hydrogels supported esophageal stem cell migration and organoid formation to greater extent than heterologous ECM hydrogels, Lin et

al.[114] found that a pepsin-digested extract of decellularized MSC sheets provided no additional benefit over type 1 collagen hydrogels; conversely, a urea-extracted fraction enhanced MSC attachment, spreading, proliferation, migration, and multi-lineage differentiation. Similarly, Zhang et al.[113] and Yang et al.[115] independently reported that urea-extracted fractions of decellularized ECM from diverse tissues were capable of promoting tissue-specific differentiation.

In this study, soluble decellularized tendon and cartilage ECMs were prepared by pepsin digestion or urea extraction. In confirming the superiority of urea-extracted over pepsin-digested solutions in terms of proliferation and tissue-specific differentiation of MSCs grown in 2-dimensional (2D) cultures, the bioactivities of urea-extracted ECM solutions were further investigated across several three-dimensional (3D) conditions – pellet cultures, electrospun nanofibers, and photocrosslinked methacrylated gelatin (GelMA) hydrogels. Supplementation of culture medium with TGF-β3 served as a positive control. We hypothesized that urea-extracted ECM fractions would promote homologous differentiation regardless of the 3D condition, while the effect of TGF-β3 would be more strongly mediated by the microenvironment.

2.2 METHODS

2.2.1 Overview

Tendon and hyaline cartilage were procured from bovine hindlimbs and subsequently decellularized and characterized. Tendon and cartilage ECM were then solubilized through either pepsin digestion (tAP, cAP) or urea extraction (tECM, cECM) and their respective effects

on human MSC proliferation and gene expression were determined in 2D culture. MSCs were cultured as pellets, seeded on aligned nanofibrous scaffolds, or encapsulated in GelMA hydrogels, and exposed to media supplemented with TGF-β3, urea-extracted tendon ECM (tECM), or urea-extracted cartilage ECM (cECM). Assays for gene expression, histology, and biochemical composition were performed to assess tissue-specific bioactivities of the supplements. Additionally, the effect of inhibiting endogenous TGF-β found in urea-extracted ECM fractions was explored in pellet cultures by inclusion of small molecule SB-431542.

2.2.2 Decellularization of tendon and cartilage

Patella tendon and articular cartilage were procured from hindlimbs of 6-8 week old cows (Research 87, Boylston, MA, USA) and stored at -20°C in a protease inhibitor solution composed of 1X phosphate-buffered saline (PBS, Gibco, Grand Island, NY, USA) supplemented with 5 mM ethylenediaminetetraacetic acid (EDTA; Sigma-Aldrich, St. Louis, MO, USA) and 0.5 mM phenylmethylsulfonyl fluoride (PMSF; Sigma-Aldrich) until use. Upon thawing, tissues were minced (8-27 mm^3) and cryomilled (Spex Freezer Mill 8670, Metuchen, NJ, USA). 4 g of wet tissue powder was suspended in 40 mL of protease inhibitor solution containing 1% Triton X-100 (Sigma-Aldrich) and agitated for 24 hours at 4°C, followed by three washes for 30 minutes each in 1X PBS. Tissue powders were subsequently exposed to 40 mL of Hanks Buffered Salt Solution (HBSS, ThermoFisher Scientific, Pittsburgh, PA, USA) supplemented with 200 U/mL DNase and 50 U/mL RNase (Worthington, Lakewood, NJ, USA) for 12 hours at room temperature. Decellularized powders were then washed 6 times with 1X PBS and characterized for histological appearance and biochemical composition.

2.2.3 Solubilization of decellularized ECM

Pepsin digestion. Decellularized tendon and cartilage ECM powders (30 mg/mL) were enzymatically digested in a solution of 1 mg/mL porcine pepsin (Sigma-Aldrich) in 0.01 N HCl for 48 hours at room temperature under continuous stirring. If added as a medium supplement, digested tendon and cartilage ECM were neutralized by addition of one-tenth digest volume of 0.1 N NaOH and one-ninth digest volume of 10X PBS while keeping the samples at 4°C. Samples were diluted with 1X PBS. To form 3D hydrogels, pH neutralized digests were warmed to 37°C for 1 hour, as reported previously.[104,150]

Urea extraction. A water-soluble fraction of tendon and cartilage ECM was obtained through urea extraction, as previously described.[115] Briefly, 4 g of wet decellularized ECM powder was agitated for 3 days at 4°C in 40 mL of 3 M urea dissolved in water. The suspension was centrifuged for 20 minutes at 1500g and the supernatant was transferred to benzoylated tubing (Sigma-Aldrich) and dialyzed against ddH_2O for 2 days at 4°C, changing the water every 8 hours. The dialyzed ECM extract was transferred to centrifugal filter tubes (3000 MWCO; EMD Millipore, Billerica, MA, USA) and spin-concentrated approximately 10-fold at 1500g for 60 minutes. The final ECM extract was filter-sterilized through a PVDF syringe filter unit (0.22 μm; EMD Millipore). The total protein concentration was determined by BCA assay (ThermoFisher Scientific) and aliquots of 1000 μg/ml were stored at -80°C until further use. Before use in experimental studies, aliquots prepared from three different batches were pooled.

2.2.4 SDS-PAGE and growth factory analysis of soluble ECM

Samples of native tendon and cartilage ECM, and their corresponding urea-soluble and pepsin-digested extracts were suspended in TM buffer (Total Protein Extraction Kit, EMD Millipore). 30 μg total protein was mixed with LDS loading buffer and reducing agent (NuPAGE; Life Technologies, Carlsbad, CA, USA) and heated for 10 minutes at 70°C. Protein was loaded into a pre-cast 10-well NuPAGE 4-12% Bis-tris Minigel (Life Technologies) and separated by electrophoresis in MOPS running buffer for 50 minute at constant 200V. The gel was washed several times in water and photographed using a CCD camera gel imaging system (FOTODYNE, Hartland, WI, USA).

Additionally, the growth factor contents of the soluble ECM preparations were determined using a Human Growth Factor Array (RayBiotech, Norcross, GA), according to the manufacturer's instructions.

2.2.5 MSC isolation

Human MSCs were obtained as previously described,[114] with Institutional Review Board approval (University of Washington and University of Pittsburgh). MSC populations isolated from individual patients were routinely validated as capable of osteogenic, adipogenic and chondrogenic differentiation (data not shown). All experiments were performed with passage 3 (P3) MSCs. MSCs from 3 patients (56 year old male, 56 year old female, 59 year old male) were pooled for this study.

2.2.6 Bioactivity of soluble ECM in 2-dimensional cell culture

To determine the effect of soluble ECM preparations on MSC morphology and metabolism, 1 x 10^3 cells/cm^2 were suspended in growth medium (DMEM, 10% FBS, 1% Anti-Anti; Life Technologies) and plated in 6-well culture plates. One day following cell seeding, growth medium was replaced with serum-free medium (DMEM, 1% Anti-Anti, 1% Insulin-transferrin-selenium [ITS]; Life Technologies) with or without additional supplementation. There were six medium conditions – (1) serum-free control, (2) 10 ng/mL TGF-β3 (Peprotech, Rocky Hill, NJ, USA), (3) 50 μg/mL tAP, (4) 50 μg/mL tECM, (5) 50 μg/mL cAP, (6) 50 μg/mL cECM. Media were changed every 2 days. On days 1, 3, and 7, an MTS assay (CellTiter 96® AQ_{ueous} Non-Radioactive Cell Proliferation Assay; Promega, Madison, WI, USA) was performed according to manufacturer's instructions. To determine the effects of soluble ECM on gene expression, 2 x 10^4 cells/cm^2 were plated in 6-well culture plates and cultured up to 7 days, as described above. On days 1, 3, and 7, cell lysates were collected for quantitative real-time polymerase chain reaction (qPCR, described below). As significant differences across treatment groups were only seen at day 3, expression levels were normalized against day 3 controls.

2.2.7 Quantitative real-time polymerase chain reaction (qPCR)

In 2D cultures, total RNA was isolated from cells using an RNeasy Plus Mini Kit (Qiagen, Valencia, CA, USA) and reverse transcribed into cDNA through use of SuperScript III first-strand synthesis kit (ThermoFisher Scientific). For 3D cultures, RNA isolation was preceded by homogenization of samples in Trizol (ThermoFisher Scientific). qPCR was performed using SYBR® Green master mix (Applied Biosystems, Foster City, CA, USA) on a StepOnePlus Real-

Time PCR system (Applied Biosystems). Relative expression of each target was calculated using the $\Delta\Delta C_T$ method with the arithmetic average of GAPDH and r18S expression used as the endogenous reference. Primer sequences for gene targets are listed in **Supplemental Table 1**.

2.2.8 Bioactivity of pepsin-digested ECM as 3-dimensional hydrogels

To evaluate the bioactivity of pepsin-digested ECM as 3D hydrogels, 1.0 x 10^6 MSCs/mL were suspended in cold, pH-neutralized hydrogels (5 mg/mL), consisting of the following groups – (1) type 1 collagen (Control; PureCol® EZ Gel, Advanced Biomatrix, Carlsbad, CA, USA) (2) tAP, (3) cAP. To induce thermogelation, MSC-seeded hydrogels were incubated for 1 hour at 37°C, after which reduced-serum medium (DMEM, 2% FBS, 1% Anti-Anti) was added. Constructs were collected on day 7 for qPCR.

2.2.9 Bioactivity of urea-extracted ECM in culture of MSC pellets

2.5 x 10^5 MSCs/mL in 200 μL chondrogenic medium (DMEM, 1% Anti-Anti, 10 μg/ml insulin, transferrin, selenium [ITS+], 0.1 μM dexamethasone, 40 μg/mL proline, 50 μg/mL ascorbate-2-phopshate) were distributed to conical 96-well plates and centrifuged for 10 minutes at 300g. Pellets were cultured for 21 days in one of four medium conditions – (1) Control, (2) 10 ng/mL TGF-β3, (3) 50 μg/mL tECM, (4) 50 μg/mL cECM – with medium changes every 2 days. At day 21, pellets were collected for qPCR, histology, and biochemical analysis.

2.2.10 Effect of TGF-β inhibition on urea-extracted ECM bioactivity

MSC pellets were cultured for up to 21 days in one of four conditions, as described in section 2.3.9. Small molecule SB-431542 (Sigma) was added at a final concentration of 10 μM approximately 1 hour prior to adding the appropriate culture supplement (i.e., 10 ng/mL TGF-β3, 50 μg/mL tECM, 50 μg/mL cECM). Media were changed every 2 days. qPCR, histology, and analysis of biochemical composition were performed on day 21. As supplementation with SB-431542 did not dramatically affect gene expression patterns compared to pellets cultured in control medium (i.e., without SB-431542), relative fold changes are shown normalized against the Control+SB-431542 medium condition for clarity.

2.2.11 Histology and immunofluorescence

All samples collected for histology (excluding electrospun nanofibers, as described in section 2.3.12.) were fixed in 10% phosphate-buffered formalin, serially dehydrated, embedded in paraffin, and sectioned (6 μm thickness) with a microtome (Leica RM2255, Leica Biosystems, Buffalo Grove, IL, USA). Samples were rehydrated and stained with hematoxylin & eosin (H&E, Sigma-Aldrich), Safranin O and Fast Green (Electron Microscopy Sciences, Hatfield, PA, USA) or 4',6-diamidino-2-phenylindole, dilactate (DAPI, Life Technologies, Carlsbad, CA, USA).

For samples undergoing immunofluorescent staining, antigen retrieval entailed incubation with Chondroitinase ABC (100 mU/mL) and Hyaluronidase (250 U/ml) suspended in 0.02% BSA for 30 minutes at 37°. Samples were incubated overnight at 4° with the following

primary antibodies – 1:400 Rabbit Anti-Collagen II (ab34712, Abcam, Cambridge, MA, USA), 1:400 Mouse Anti-Collagen I (5D8-G9/Col1, ThermoScientific), or 1:400 Mouse Anti-Collagen X (ab49945, Abcam). Samples were incubated in one of two secondary antibodies for 1 hour at room temperature – 1:500 AlexaFluor 488 goat anti-mouse or AlexaFluor 594 goat anti-rabbit (Invitrogen, ThermoFisher Scientific).

Samples were photographed using an Olympus SZX16 stereomicroscope with white light (H&E, Safranin O) or fluorescent excitation at 405 nm (DAPI), 488 nm (green), or 594 nm (red) for immunofluorescence.

2.2.12 Biochemical composition

To determine the biochemical composition of tissues and 3D constructs, dry samples were digested overnight at 65°C at a concentration of 10 mg/mL in a digestion buffer (pH 6.0) containing 2% papain (v/v, from Papaya latex, Sigma-Aldrich), 0.1 M sodium acetate, 0.01 M cysteine HCl, and 0.05 M EDTA. Concentrated NaOH was subsequently added to the digestion solution to adjust the pH to 7.0. sGAG content was quantified with a Blyscan Assay according to the manufacturer's instructions (Biocolor, Carrickfergus, UK). dsDNA content was determined using the Quant-iT Picogreen dsDNA assay (Invitrogen). Total collagen was determined using a modified hydroxyproline assay. Briefly, 200 μL of each sample was hydrolyzed with an equal volume of 4 N NaOH at 121°C for 75 min, neutralized with an equal volume of 4 N HCl, and then titrated to an approximate pH of 7.0. The resulting solution was combined with 1.2 mL chloramine-T (14.1 g/L) in buffer (50 g/L citric acid, 120 g/L sodium acetate trihydrate, 34 g/L NaOH, and 12.5 g/L acetic acid) and allowed to stand at room temperature for 30 min. The solution was then combined with 1.2 mL of 1.17 mM p-dimethylaminobenzaldehyde in

perchloric acid and placed in a 65°C water bath for 20 minutes. 200 μL of each sample was added to a clear 96-well plate, in duplicate, and absorbance at 550 nm was read. PureCol bovine collagen (3.2 mg/mL, Advanced Biomatrix) was serially diluted to provide a standard curve ranging from 0 to 1000 μg/ml.

2.2.13 Bioactivity of ECM in culture of MSC-seeded aligned nanofibers

Sheets of aligned nanofibers were fabricated from a solution of poly-ε-caprolactone (PCL, MW = 70k-90k, Sigma-Aldrich) prepared at 15% w/v in 1:1 (v/v) tetrahydrofuran (THF, Sigma-Aldrich):dimethylformamide (DMF, ThermoFisher Scientific). Dissolved PCL was loaded into 10 mL syringes and extruded through an 18-gauge blunt tip needle at 3.0 mL/h using a syringe pump (PY2 70,2209, Harvard Apparatus, Holliston, MA, USA). The needle tip was placed 10 cm from a custom-designed cylindrical mandrel, which rotated at a surface velocity of 10 m/sec. 10-18 kV DC potential (Gamma High Voltage, Ormand Beach, FL, USA) was applied to the polymer solution while an 8 kV potential was applied to two aluminum shields placed perpendicular to the mandrel axis but parallel to the needle axis, narrowing the width of the aligned nanofibrous sheet collected on the grounded mandrel.

6×10^4 MSCs/cm^2 were seeded on PCL nanofibers and cultured for 14 days in serum-reduced (2% FBS) culture medium supplemented with 50 μg/mL ascorbate-2-phosphate (Sigma-Aldrich). There were four medium conditions — (1) Control, (2) 10 ng/mL TGF-β3, (3) 50 μg/mL tECM, (4) 50 μg/mL cECM – with medium changes every 2 days. On day 14, constructs were collected for qPCR or immunofluorescent staining. qPCR was performed as described above. For immunofluorescent staining, constructs were fixed with 4% paraformaldehyde, and

blocked with 1% bovine serum albumin (BSA) and 22.5 mg/ml glycine in PBS-T. Constructs were exposed to goat anti-tenomodulin (Tnmd, 1:50, sc49325 Santa Cruz Biotechnologies, Dallas, TX, USA) overnight at 4°C. AlexaFluor 488 chicken anti-goat (Invitrogen, ThermoFisher Scientific) at a 1:500 dilution was used as the secondary antibody. Constructs were counterstained with DAPI (Invitrogen) and cells were imaged using a confocal microscope (Olympus FluoView 1000).

2.2.14 Bioactivity of cartilage ECM as in MSC-seeded GelMA hydrogels

Methacrylated gelatin (GelMA) was synthesized by adapting a previously established protocol.[134] Briefly, 15 g of gelatin (Type A, from porcine skin, Sigma-Aldrich) was dissolved in 500 mL deionized H_2O at 40°C, and then 15 mL of methacrylic anhydride (Sigma-Aldrich) was added dropwise under vigorous stirring. The mixture was placed at 37°C in an orbital shaker at 150 rpm for 24 h. The resulting GelMA was dialyzed for 4 days against H_2O at room temperature using 2000 NMWCO dialysis tubing (Sigma-Aldrich) to completely remove all low-molecular-weight byproducts, with changes in H_2O twice daily. After lyophilization, the product was stored at -20°C until future use. Prior to use, GelMA was reconstituted at 10% (w/v) in HBSS. 0.25% v/v of visible light-sensitive photoinitiator lithium phenyl-2,4,6-trimethylbenzoylphosphinate (LAP) was then dissolved by gentle shaking at room temperature. Photocrosslinking was induced by exposure to UV light (LED bulbs, 390-395 nm, 0.5 W) for 2 minutes.

MSCs were homogenously suspended in one of two hydrogels – (1) 10% w/v GelMA (Control) or (2) 10% w/v GelMA supplemented with 500 μg/mL cECM (cECM) – at a concentration of 20 x 10^6 cells/mL. Before gelation, MSC-seeded hydrogels (~50 μL) were

distributed to silicone molds measuring 5 mm diameter x 2 mm depth. To induce photogelation, hydrogels were exposed to 2 minutes of visible light (450-490 nm) (**Supplemental Figure 1**). MSC-seeded hydrogels were then removed from silicone molds and transferred to 6 well plates previously coated with silicone (Sigmacote, Sigma-Aldrich) to prevent cell migration and adhesion onto the plastic surface. Constructs were cultured up to 21 days in chondrogenic medium (DMEM, 1% Anti-Anti, 10 μg/ml insulin, transferrin, selenium [ITS+], 0.1 μM dexamethasone, 40 μg/mL proline, 50 μg/mL ascorbate-2-phopshate) with or without additional 10 ng/mL TGF-β3 (Peprotech) supplementation. Medium was changed every 2 days.

2.2.15 Statistics

Comparisons across multiple conditions or time points were made using a one-way or two-way analysis of variance (ANOVA) with Tukey post-hoc testing for multiple comparisons. When comparing two conditions, a Student's t-test was performed. Data are presented as mean ± standard deviation. Experiments were performed with biological triplicates over at least three independent trials. Sample sizes are indicated in figure legends. Statistical significance was considered $p < 0.05$.

2.3 RESULTS

2.3.1 Characterization of tendon- and cartilage-derived ECMs

The decellularization protocol successfully reduced cellular content from both tendon and cartilage, as evidenced by the absence of nuclei on both H&E- and DAPI-stained sections (**Figure 7A-H**), as well as a significant reduction in dsDNA content (**Figure 7I**). The total collagen contents of native and decellularized tendon were equivalent, while decellularized cartilage exhibited a significant increase in collagen content with a corresponding loss in sGAG content (**Figure 7J-K**). The majority of decellularized tissue powder was insoluble in urea (**Figure 7L**) but was homogenously digested by the acid-pepsin solution (**Figure 7M**). As a result, urea-extracted tendon ECM (tECM) and cartilage ECM (cECM) were enriched for low- to moderate-weight proteins, with faint bands corresponding to collagen. Conversely, the pepsin-digested tendon (tAP) and cartilage (cAP) were principally composed of collagen types 1 and 2, respectively, with faint bands found in the low- to moderate-weight regions (**Figure 7N,O**). The prominent streak in the well of native cartilage is an artifact attributable to the high proteoglycan content (**Figure 7O**). tECM and cECM possessed a higher growth factor content than their pepsin-digested counterparts, with notable differences in basic fibroblast growth factor (bFGF) and TGF-β1 (**Supplemental Table 2**).

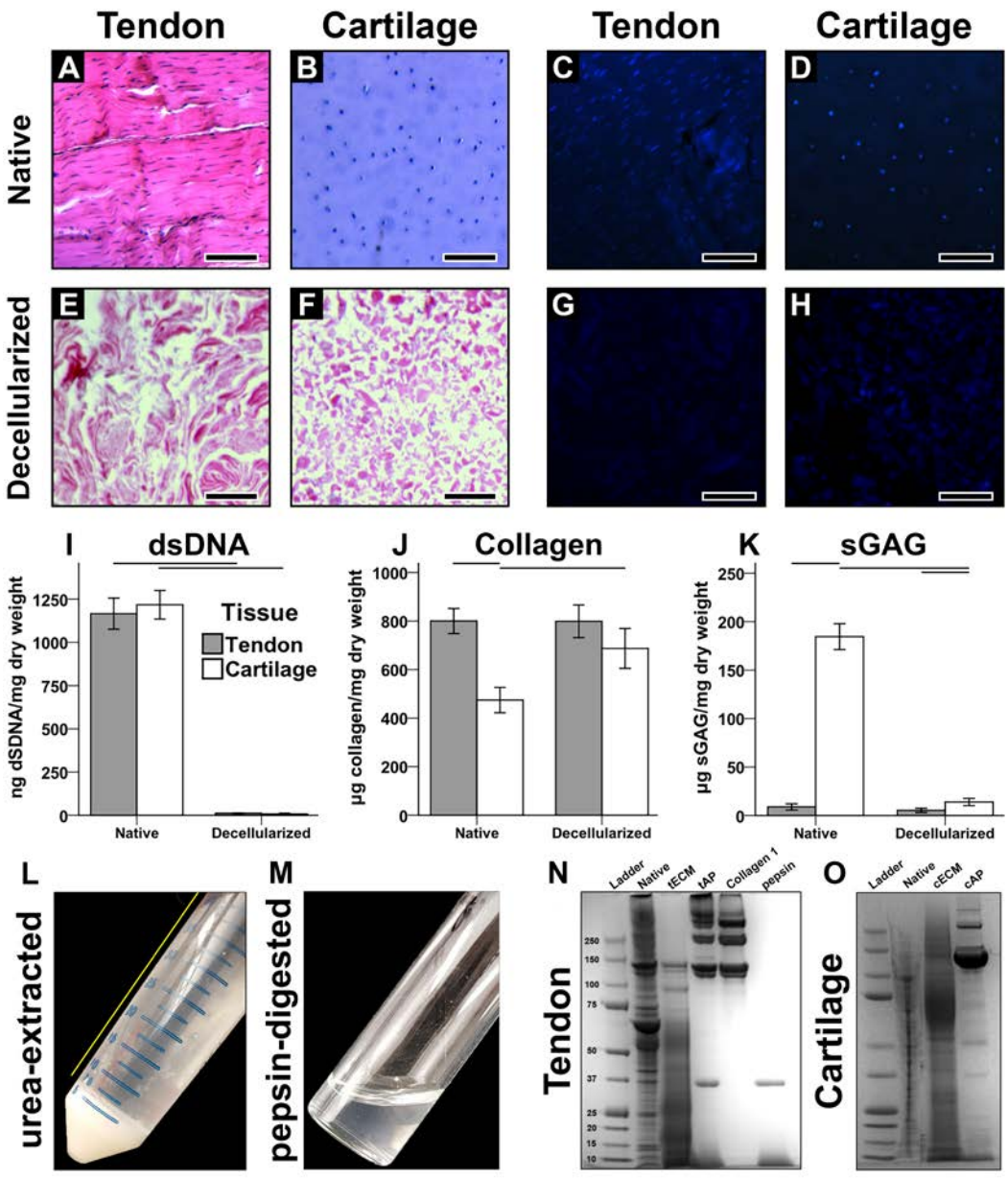

Figure 7. Characterization of soluble extracellular matrices. (A-D) Prior to decellularization, nuclei are clearly present in native tendon and cartilage tissues, as shown through H&E and DAPI staining. (E-H) Following decellularization, no nuclei are visible. (I) dsDNA contents were significantly reduced in decellularized tissues compared to native tissues, $p < 0.001$, n=8. (J) Collagen content in native and decellularized tendon was equivalent, but was increased in decellularized cartilage vs. native cartilage, $p < 0.05$, n=8. (K) sGAG content was higher in

cartilage tissues than tendon tissues, regardless of decellularization step ($p < 0.05$) but decellularized cartilage contained significantly less sGAG than native cartilage ($p < 0.001$, $n=8$). (L) Urea extraction yielded an insoluble and soluble fraction. The soluble supernatant (yellow line) was collected. (M) Pepsin digestion yielded a homogeneous slurry. (N, O) SDS-PAGE gels of tendon (N) and cartilage (O) tissues at different stages of decellularization and solubilization.

2.3.2 The effect of soluble ECMs on human MSCs in 2D culture

Human MSCs were grown on 2D culture plastic in one of six medium conditions (**Figure 8A**). Pepsin-digested and urea-extracted ECM supplementation enhanced cell proliferation, with the urea-extracted groups showing the greatest effect by day 7 (**Figure 8B**). Only the urea-extracted ECMs upregulated tissue-specific transcription factors; tECM preferentially enhanced Scx expression while cECM upregulated Sox9 expression (**Figure 8C**). No soluble ECM preparation affected expression of osteogenic marker, Runx2. Collagen type 2 (Col2) and aggrecan (Acan) expression was not detectable, while collagen type 1 (Col1) was only significantly upregulated by TGF-β3, which also greatly increased Scx expression (**Figure 8C**). MSCs grown in tECM-supplemented medium possessed a spindle-shaped morphology, while cECM and, to a lesser extent, TGF-β3 supplementation produced a cobblestone morphology (**Figure 8D**).

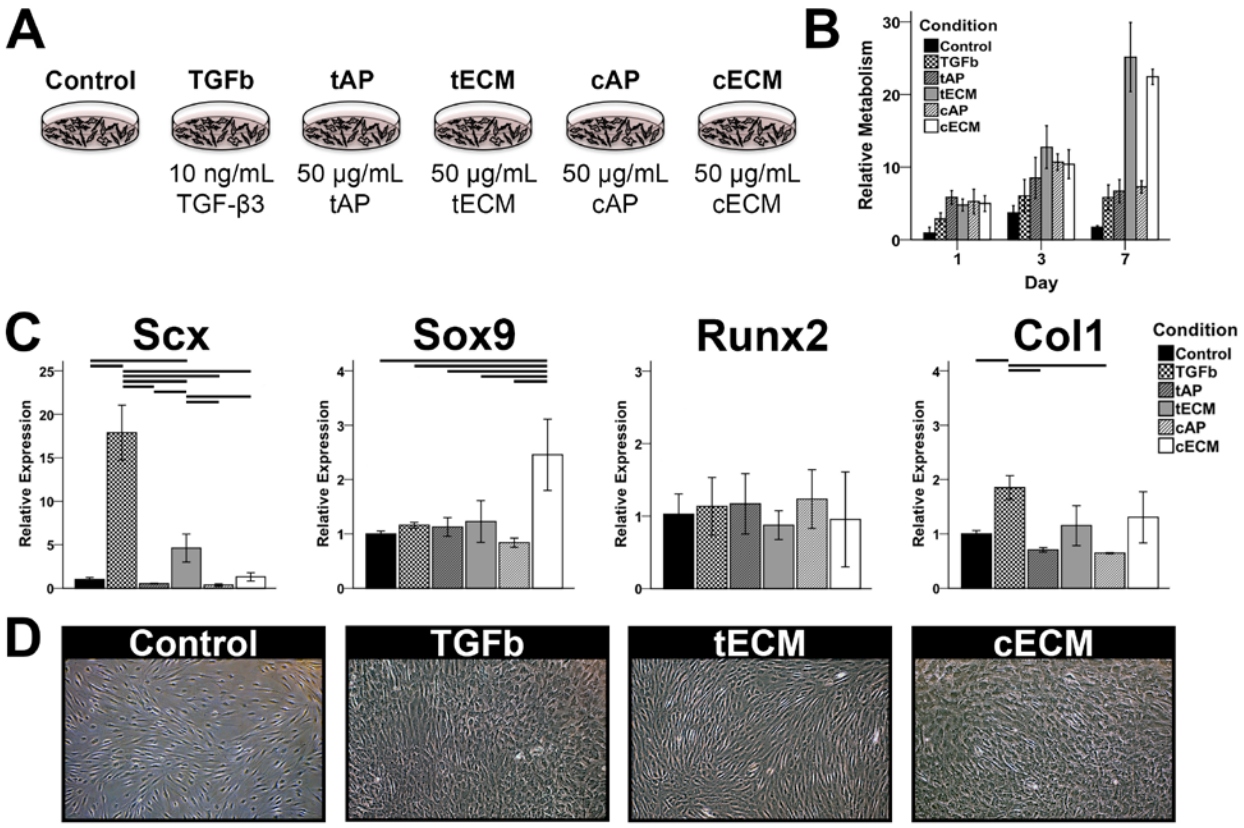

Figure 8. The effect of soluble ECMs on human MSCs in 2D culture. (A) MSCs were cultured up to 7 days on tissue culture plastic in one of six medium conditions. (B) MTS assay showed that all ECM groups enhanced cell metabolism (proliferation), but urea-extracted fractions were the most mitogenic by day 7. (C) Gene expression analysis on day 3 suggested tissue-specific bioactivity of urea-extracted ECM fractions ($p < 0.05$, n=9). (D) Phase contrast microscopy showed spindle-shaped cells in the tECM group but cobblestone morphology with TGF-β and cECM supplementation.

2.3.3 The effect of soluble ECMs on MSC pellets

Total and relative sGAG contents were increased in pellets cultured in supplemented medium (**Figure 9B**). TGF-β3 and cECM supplementation increased total sGAG to a similar extent, but cECM was superior when sGAG content was normalized by dsDNA content (**Figure 9B**). In terms of gene expression (**Figure 9C**), TGF-β3 preferentially promoted a chondrogenic phenotype as shown by increased expression of Sox9, Acan, and Col2. tECM promoted a tenogenic phenotype with robust upregulation of Scx, Mkx, Col3, and Col1, with more modest effects on chondrogenic and osteogenic markers. Similarly, cECM had a negligible or inhibitory effect on tenogenic markers but promoted chondrogenesis to an equivalent or greater degree than TGF-β3. However, cECM also upregulated osteogenic markers most strongly, as seen in expression patterns of Col10 (hypertrophic marker), Runx2, Alp, and Ocn (**Figure 9C**). Histological analysis of pellets showed a pattern that was consistent with assays for biochemical composition and gene expression. Namely, TGF-β3 and cECM enhanced proteoglycan and Col2 deposition while tECM pellets showed the greatest Col1 staining intensity (**Figure 10**).

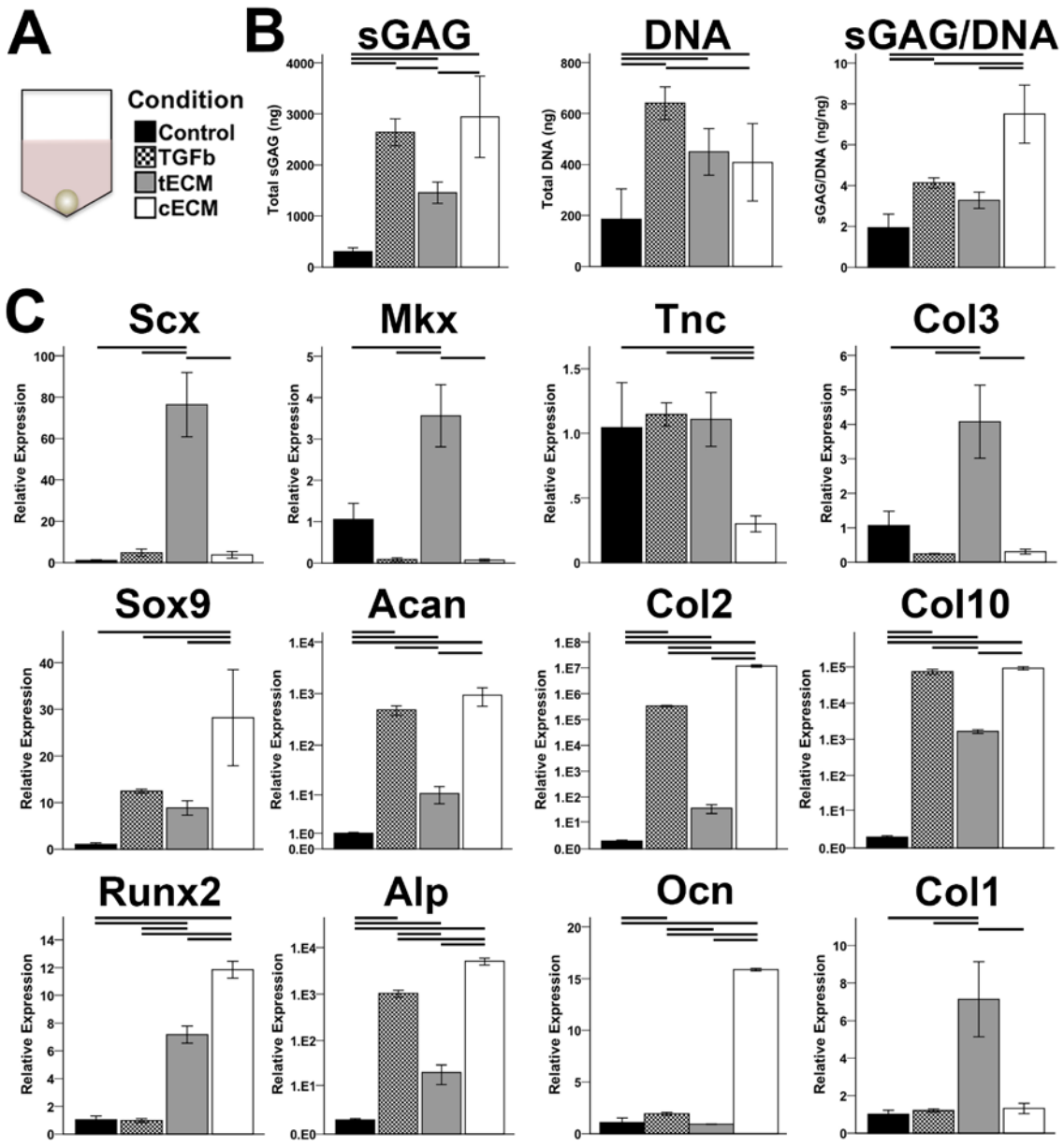

Figure 9. The effect of soluble ECMs on MSC pellet composition and gene expression. (A) MSC pellets were cultured in one of four medium conditions for 21 days. (B) Biochemical composition of pellets reveals anabolic and mitogenic effects for all supplements; cECM promoted the greatest relative sGAG production ($p < 0.05$, n=9). (C) Gene expression analysis on day 21 shows chondrogenic effects of TGF-β, tenogenic effects of tECM, and chondrogenic and osteogenic effects of cECM ($p < 0.05$, n=9).

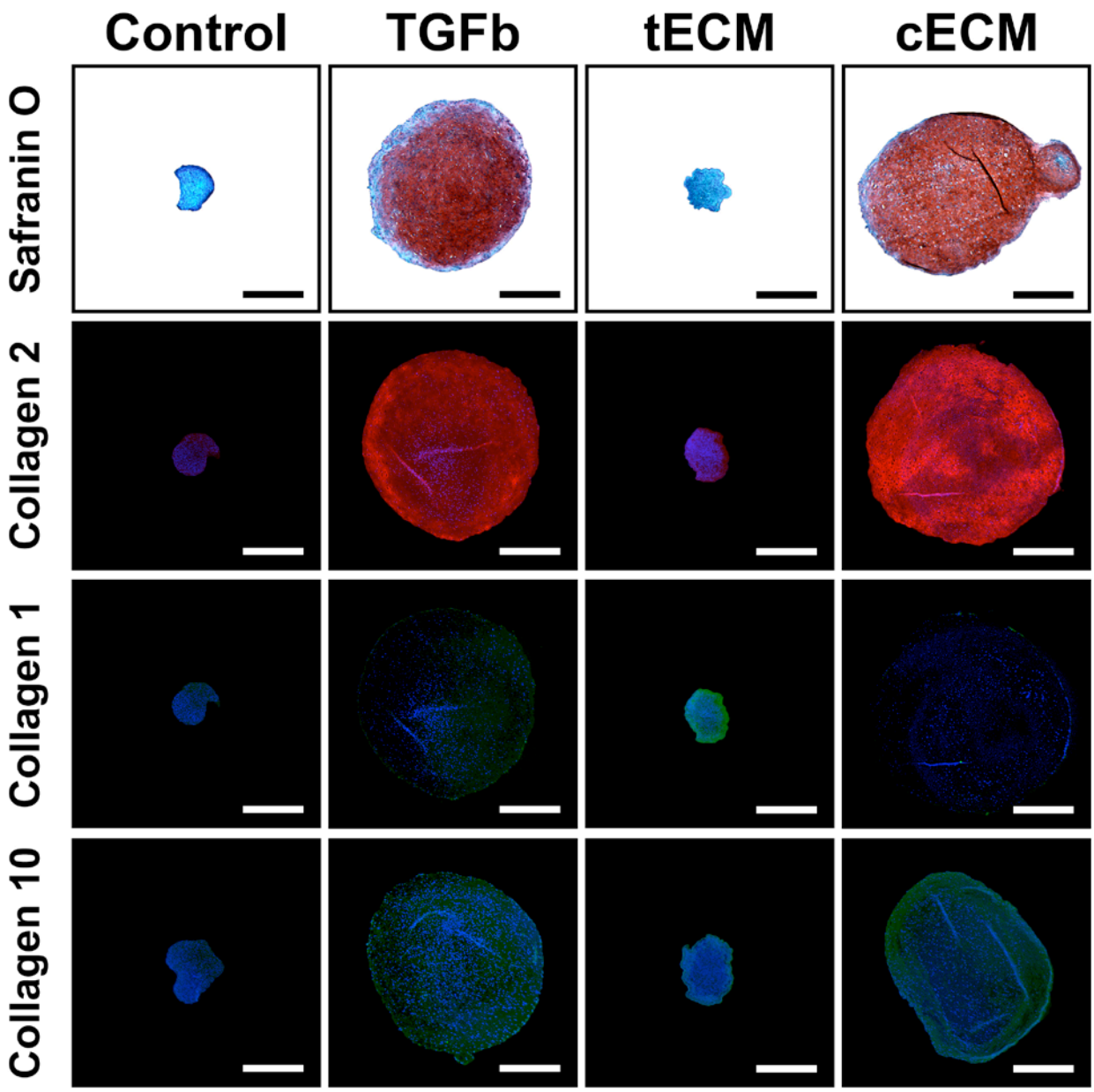

Figure 10. The effect of soluble ECMs on MSC pellet protein deposition. TGF-β and cECM promoted deposition of proteoglycan, Col2, and Col10, while tECM enhanced Col1 synthesis. Proteoglycan (Safranin O) = red, Collagen 2 = red, Collagen 1 = green, Collagen 10 = green, nuclei = blue

2.3.4 The effect of TGF-β inhibition on soluble ECM bioactivity

The effects of endogenous TGF-β in tECM and cECM were blocked by type 1 TGF-β receptor antagonist SB-431542,[151] which was added at 10 μM to pellet culture media (**Figure 11A**). TGF-β inhibition significantly reduced the anabolic effects of TGF-β and cECM on pellets, as evidenced by the loss of proteoglycan staining (**Figure 11B**) and sGAG content (**Figure 11C**, **Supplemental Figure 2**). In analysis of gene expression (**Figure 11D**), SB-431542 eliminated the tenogenic effect of tECM and the chondrogenic effect of TGF-β. Interestingly, cECM supplementation still promoted significant increases in Sox9, Acan, and Col2 expression despite treatment with SB-431542 (**Figure 11D**), although these increases were far weaker than pellets treated with cECM in the absence of SB-431542 (**Figure 9C**). ECM-mediated upregulation of osteogenic markers alkaline phosphatase (Alp) and osteocalcin (Ocn) also persisted in the presence of TGF-β inhibition.

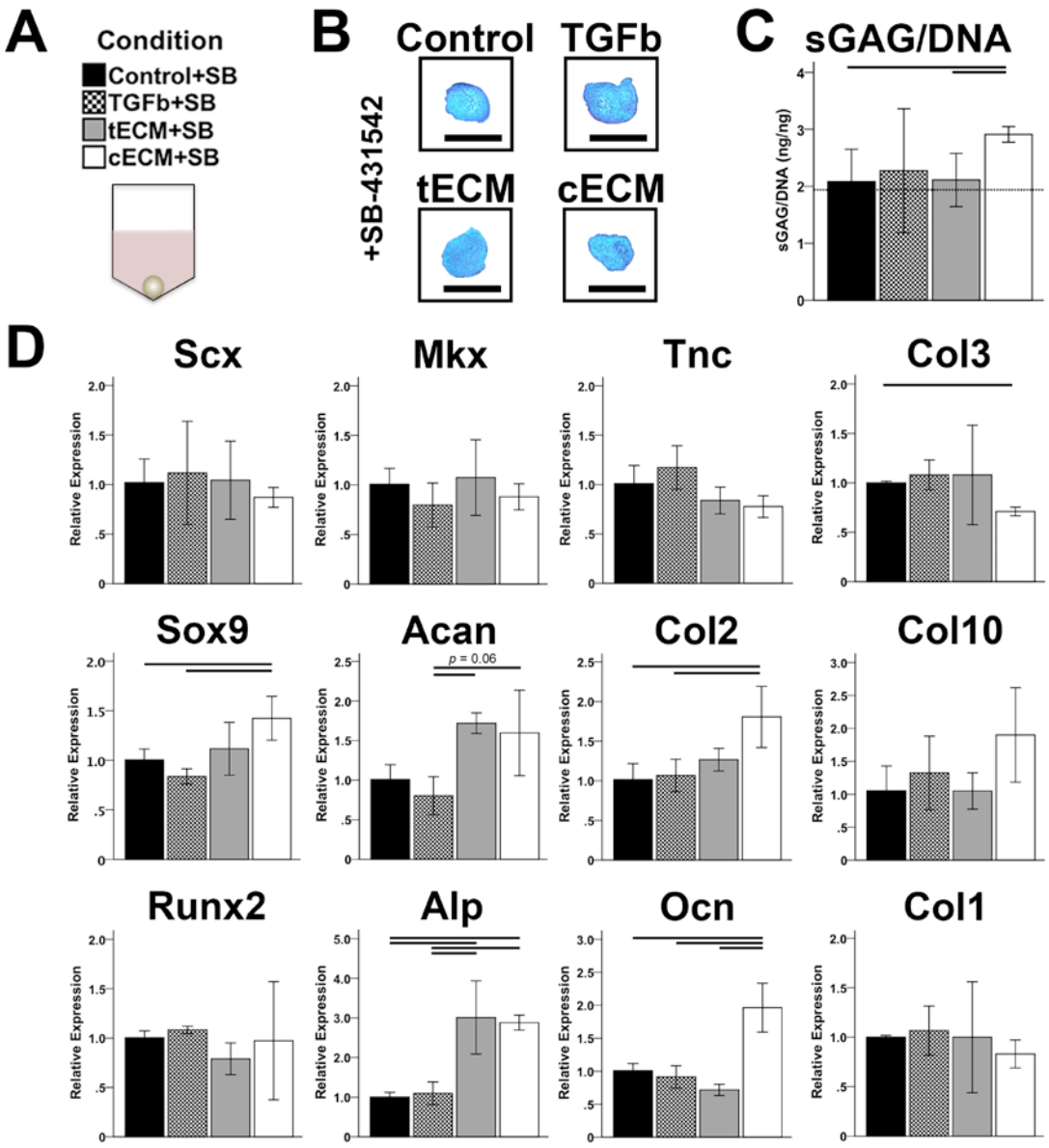

Figure 11. The effect of TGF-beta inhibition on soluble ECM bioactivity. (A) Medium conditions for pellet cultures were further supplemented with 10 μM SB-431542. (B) Safranin O Staining. (C) Normalized sGAG content shows blunted anabolic effects of medium supplements ($p < 0.05$, n=9); dotted line indicates sGAG/dsDNA content of control medium (without SB-431542). (D) Gene expression analysis shows complete inhibition of exogenous TGF-β and blunted tissue-specific bioactivity of ECM supplements ($p < 0.05$, n=9).

2.3.5 The effect of soluble ECMs on MSCs seeded on aligned nanofibers

MSCs seeded on aligned PCL nanofibers (**Figure 12A**) became elongated in the direction of the fibers (data not shown). TGF-β3 supplementation upregulated both tenogenic (Scx, Tnc, Col3, Col1) and chondrogenic (Sox9, Col10) markers, while tECM supplementation enhanced expression of tenogenic markers only (**Figure 12B**). cECM modestly increased tenogenic markers (Scx, Tnc, Col3) but upregulated chondrogenic markers (Sox9, Col2, Col10) to an equivalent or greater extent than TGF-β3. cECM also upregulated Runx2. All supplements decreased gene expression of cartilage proteoglycan Acan and bone protein osteocalcin (Ocn). Paralleling the expression pattern of Scx, an upstream driver of tenodmodulin (Tnmd)[12], confocal microscopy revealed the greatest staining intensity for Tnmd in the TGF-β3 group. However, tECM enhanced Tnmd translation to a greater extent than cECM (**Figure 12C**).

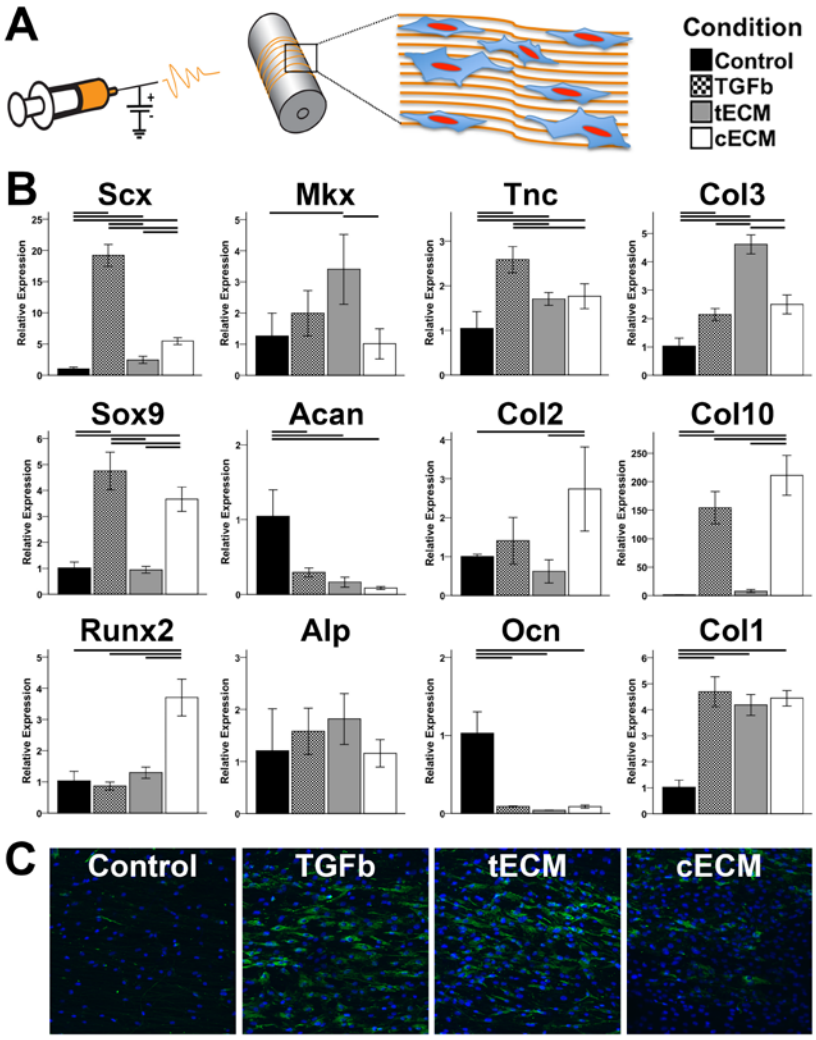

Figure 12. The effect of soluble ECMs on MSCs on aligned nanofibers. (A) MSCs were cultured on aligned PCL nanofibers in one of four medium conditions. (B) Gene expression analysis on day 14 showed tenogenic and chondrogenic effects due to TGF-β supplementation. tECM supplementation promoted a tenogenic phenotype while cECM upregulated chondrogenic markers and Runx2. Both TGF-β and cECM increased expression of hypertrophic marker, Col10 ($p < 0.05$, $n=9$). (C) Immunofluorescent staining of tenomodulin shows increasing intensity in the following order: Control < cECM < tECM < TGF-β; Tnmd = green, nuclei = blue.

2.3.6 The independent and synergistic effects of cECM and TGF-β on chondrogenesis of MSCs seeded in 3D GelMA hydrogels

MSCs were seeded in photocurable GelMA hydrogels and cultured in chondrogenic medium (with or without TGF-β supplementation) for up to 21 days (**Figure 13A**). On day 7, the inclusion of cECM within the hydrogels had independently upregulated chondrogenic markers Sox9, Acan, and Col2, as well as the ratio of Col2:Col1, despite a more modest increase in Col1 (**Figure 13B**). Runx2 expression was also upregulated by cECM on day 7, but was equivalent to controls (and returned to baseline) by day 21. Supplementation of culture medium with TGF-β dramatically enhanced the expression of chondrogenic markers, compared to controls, on days 7 and 21. The effect was further enhanced when cECM was mixed with the GelMA hydrogel, suggesting a synergistic effect between the cECM and TGF-β (**Figure 13B**). This synergistic effect was also confirmed when analyzing the biochemical composition of MSC-seeded hydrogels (**Figure 13C**). Importantly, acellular cECM-containing GelMA hydrogels had negligible sGAG content (data not shown), suggesting that the observed group differences are attributable to the effects of cECM on MSCs rather than sGAG contained within cECM solution.

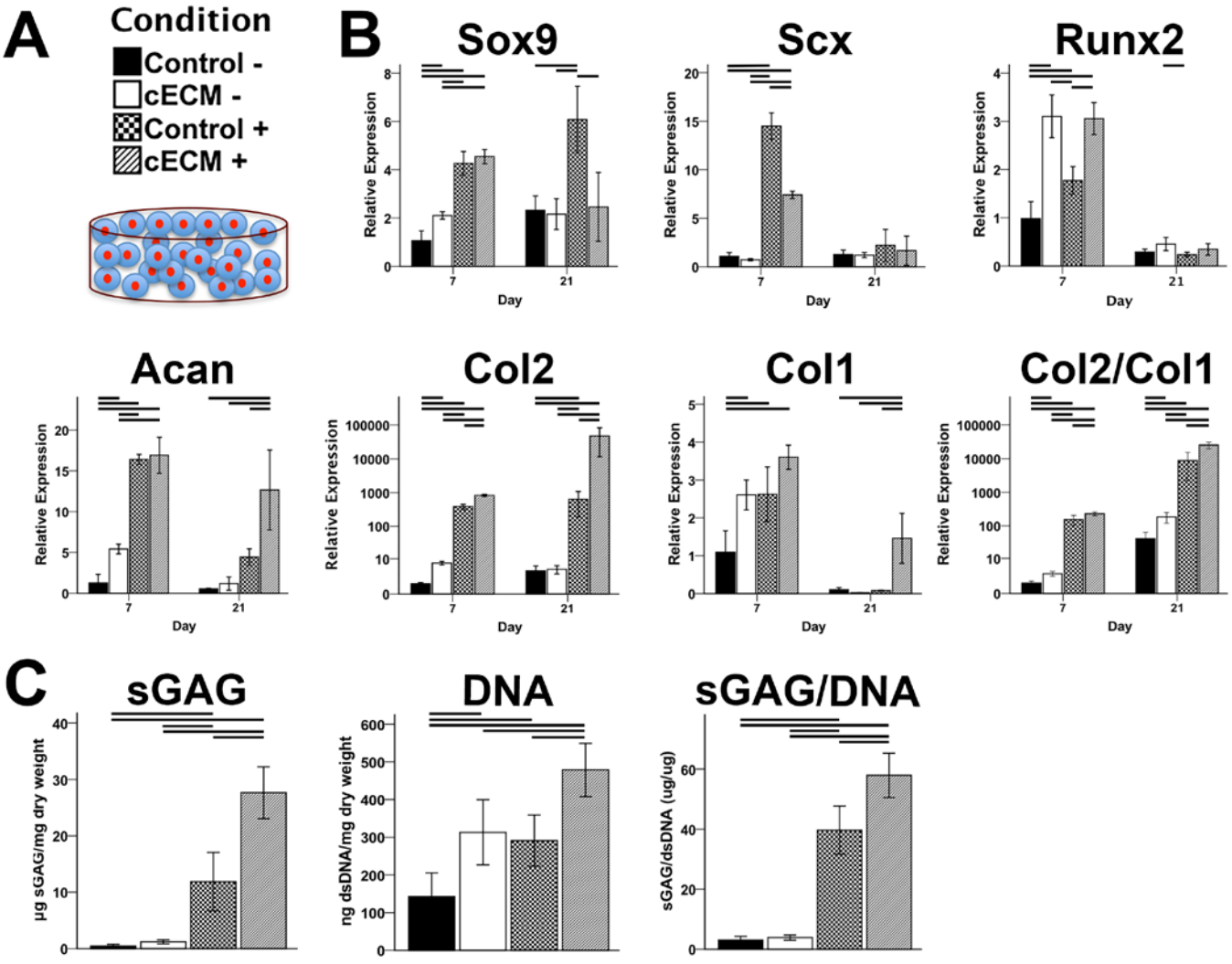

Figure 13. The effects of cECM and TGF-beta on chondrogenesis of MSC-GelMA hydrogels. (A) MSC-seeded GelMA hydrogels, with or without cECM enhancement, were cultured in chondrogenic medium, with or without TGF-β supplementation, for up to 21 days. (B) Gene expression analysis shows independent and synergistic effects of cECM and TGF-β ($p < 0.05$, n=9). (C) Biochemical composition shows synergistic effect of cECM and TGF-β in enhancing absolute and normalized sGAG production ($p < 0.05$, n=9).

2.4 DISCUSSION

Given the conservation of ECM proteins across species, the utility of decellularized tissues as biomaterials capable of promoting tissue-specific cell phenotypes is theoretically and empirically supported.[7,152] Nevertheless, there is an inherent trade-off between tissue processing and retention of bioactive cues.[6] While sufficient decellularization is required to mitigate an adverse immune response to the implanted scaffold,[153] it is uncertain which elements of the ECM must be preserved to retain homologous bioactivity. Pepsin digestion of decellularized ECMs yields viscous slurries capable of undergoing thermoresponsive gelation when pH balanced,[104,154] providing an attractive biomaterial for minimally invasive cell delivery to irregularly shaped defects. On the other hand, characterization of pepsin-digested ECMs is seldom performed. Our group[114] and others[112,149] have recently reported that pepsin solubilization produces digests composed principally of structural ECM proteins, especially collagen. A similar finding was seen in this study. Additionally, the tissue-specific bioactivity of pepsin-digested tendon[105,106] and cartilage ECM[84,108] remains relatively unexplored. Pati et al.[107] reported an ~ 1.5-fold increase in Sox9 and Col2 expression when human MSCs were seeded in cAP hydrogels, as compared to collagen 1 hydrogels. Conversely, two related studies[110,111] found a negligible effect of pepsin-digested cartilage ECM, compared to controls, in enhancing chondrogenesis. A similar (null) effect was found in this study when pepsin-digested ECMs were added as a culture supplement (**Figure 8**) or seeded with MSCs as 3D thermoresponsive hydrogels (**Supplemental Figure 3**).

In contrast, we previously found that urea-extracted tendon ECM (tECM) upregulated expression of tenogenic markers, with concurrent downregulation of osteogenic markers, in MSCs cultured in a hydrogel under static uniaxial tension.[115] Zhang et al.[113] reported similar

findings when coating tissue culture dishes with urea-extracted ECM derived from skin, skeletal muscle, and liver. Building on these findings, this study found that urea-extracted tECM and cECM upregulated homologous transcription factors (i.e., Scx and Sox9, respectively) in MSCs grown on 2D plastic, while exogenous TGF-β3 preferentially upregulated Scx alone. Furthermore, tECM and cECM enhanced cell proliferation to a greater extent than TGF-β3, tAP, or cAP, and mediated differences in cell morphology. However, these effects were not sustained beyond 7 days, likely attributable to the stress of sustained serum-starvation coupled with the non-physiologic biophysical microenvironment (i.e., 2D plastic). Therefore, we explored the tissue-specific bioactivity of tECM and cECM in two different 3D microenvironments – cell pellets and aligned electrospun nanofibers.

Pellet cultures were employed as an in vitro assay to replicate the early condensation, and subsequent tenogenesis and chondrogenesis, of mesenchymal cells in limb formation. In this context, TGF-β3 preferentially promoted chondrogenesis, while tECM and cECM promoted homologous gene expression (i.e., tenogenesis and chondrogenesis, respectively). TGF-β is essential for mediating both tenogenesis and chondrogenesis in vivo,[146,155] yet its in vitro effect is variable, depending on other microenvironmental cues. For instance, Lorda-Diez et al.[156,157] identified several downstream regulators of TGF-β signaling that mediated either fibrogenic or chondrogenic differentiation. Interestingly, in this study, inhibition of TGF-β type 1 activin receptor-like kinase receptors ALK4, ALK5, and ALK7 by SB431542[151] abolished the tissue-specific bioactivity of tECM and cECM, suggesting that TGF-β signaling is necessary, but not sufficient, to explain their tissue-specific effects. It is always noteworthy that the concentrations of endogenous TGF-β found in tECM and cECM were in the pg/mL range, yet supplementation

with these extracts promoted homologous bioactive effects equaling or exceeding those produced by 10 ng/ml exogenous TGF-β.

A growth factor array further revealed differences in composition between tECM and cECM; it is possible that the greater concentrations of bFGF, BMP-5, and BMP-7, found in cECM mediated the cartilage-specific effects. But given their role in bone formation,[158] the additional BMPs found in cECM may also have contributed to the noted upregulation of hypertrophic and osteogenic markers seen in this study, although TGF-β alone induced some degree of hypertrophy in pellet cultures. The finding of cartilage ECM-induced hypertrophy has also been recently reported in similar studies.[159,160] Indeed, the stability of the chondrogenic phenotype remains a persistent challenge in cartilage tissue engineering.[3] It is possible that the use of cECM derived from adult animals could promote chondrogenic differentiation with less hypertrophy, as the delineation between articular cartilage and subchondral bone (with obvious vasculature) is apparent (**Supplemental Figure 4**), allowing for the isolation of cartilage ECM alone. As shown in the growth factor array (**Supplemental Table 2**), cECM from 2-3 year old animals contains a lower concentration of growth factors than cECM from 6-8 week old animals (as used in this study), but also greatly reduced levels of BMPs. Clearly, further elucidation of soluble ECM composition, and the interactions among these elements, will be necessary to expand on the findings obtained herein, thereby furthering our understanding of cell-matrix interactions.

However, based upon these promising results that suggested tissue-specific bioactivity of urea-extracted ECMs, we sought to explore if additive or synergistic effects were possible when combining these soluble extracts with biomimetic scaffolds. Electrospun nanofibers mimic the structural proteins of musculoskeletal tissue ECM (e.g., collagen) and are capable of directing

cell behavior.[161] In particular, aligned nanofibers, reminiscent of the aligned collagen 1 fibrils of native tendon, have been shown to promote tenogenic differentiation of seeded stem cells.[121,124,125] Furthermore, Leung et al.[127] reported that supplementation with TGF-β3 further enhanced tenogenesis in MSCs seeded on aligned chitosan-PCL nanofibers while Kishore et al.[129] found no additional effect of BMP-12 supplementation with MSCs seeded on electrochemically aligned collagen threads. Similarly, nonaligned PCL nanofibers coated with pulverized tendon ECM showed little benefit over nanofibers alone in promoting a tenogenic phenotype of seeded MSCs.[103] These conflicting results suggest a complex interaction between biophysical and biochemical cues in directing cell differentiation. Nevertheless, in this study, tECM supplementation further upregulated expression of tenogenic markers, with negligible or inhibitory effects on chondrogenic and osteogenic expression in MSCs seeded on aligned nanofibers. cECM affected expression of chondrogenic markers to a similar extent as TGF-β3, with a relatively diminished effect on tenogenic markers. Of note, Scx is known to cooperatively regulate Sox9 and Col2 expression in the context of chondrogenesis,[162] despite its common categorization as a tendon-specific marker,[11] perhaps explaining the small but significant upregulation of Scx mediated by cECM. In contrast, TGF-β3 upregulated markers of both tenogenesis and chondrogenesis.

Given the tissue-specific bioactivity of soluble ECMs exerted on MSC-seeded nanofibers, we sought to explore the possible benefit of including cECM within a photocrosslinkable hydrogel, a biomimetic scaffold often used for cartilage tissue engineering. Of additional consideration, the inclusion of cECM within the hydrogel itself, as opposed to the culture medium, makes its application more clinically relevant. The provision of cartilage ECM structural proteins such as collagen type VI,[163] collagen type II, and proteoglycans,[164,165] within

MSC-seeded hydrogels has been found to enhance chondrogenic differentiation. Similarly, Almeida et al.[99,101] reported similar improvements when using decellularized cartilage ECM particles. In this study, cECM was mixed with photocrosslinkable GelMA hydrogels, a biomaterial which we previously found to support robust chondrogenesis.[134] cECM independently enhanced chondrogenesis at day 7, but the chondroinductive effect decreased by day 21. Rather, medium supplementation with TGF-β was required for sustained upregulation of chondrogenic markers, with a corresponding deposition of cartilage ECM proteins; this finding agrees with related work.[99-101] Despite the apparent necessity of exogenous TGF-β for robust cartilage formation, cECM within the hydrogel interacted synergistically with the supplemented TGF-β, as demonstrated by the greatest increases in chondrogenic gene expression and sGAG deposition seen in this group. Given these results, we are now developing cECM-enhanced hydrogels with controlled release of encapsulated TGF-β, potentially obviating the need for medium supplementation and improving the translational applicability of this approach. Taken together with the results of MSC-seeded nanofibers, these findings support the tissue-specific bioactivity of urea-extracted ECMs when cells are seeded on biomimetic surfaces. The results parallel those of Sun et al.,[166] who reported increased osteogenesis when gelatin nanofibers were enhanced with noncollagenous proteins extracted from bone using a similar method to this study.

Although this study found that urea-extracted ECM, rather than pepsin-digested ECM, is capable of promoting tissue-specific cell phenotypes across multiple culture conditions, we did not explore the many other benefits reported for pepsin-solubilized ECM. In particular, pepsin ECM digests have been found to enhance in vitro cell migration,[150] proliferation,[167] and macrophage polarization,[168] effects mediated by tissue source,[169] animal age,[170] and fraction.[171] In vivo, ECM-mediated effects on macrophage polarization, and the broader inflammatory

response, at least partially explain the benefit of ECM in promoting constructive remodeling (i.e., improved healing).[172,173] To what extent in vitro assays for tissue-specific differentiation are predictive of enhanced in vivo healing remains unknown. For instance, Keane et al.[150] and Wolf et al.[154] found that ECM hydrogels derived from esophagus and skeletal muscle, respectively, promoted tissue-specific differentiation of cells in vitro, but their effects in vivo were not superior to ECM hydrogels derived from heterologous tissues. The effects of urea-extracted ECM fractions on macrophage polarization and in vivo healing were beyond the scope of the present investigation, but certainly worthy of future inquiry. Indeed, it is self-evident that successful regeneration of musculoskeletal tissues will require a greater understanding of the intersection of biomimetic biomaterials that are capable of guiding tissue-specific cell phenotypes, with the resulting inflammatory response elicited when such constructs are implanted in vivo.

2.5 CONCLUSIONS

In this chapter, decellularized tendon and cartilage ECMs were solubilized either by pepsin digestion or urea extraction. The effects of these preparations on human MSC behavior were evaluated in 2D and 3D cultures. Pepsin-digested tendon and cartilage ECMs did not promote tissue-specific differentiation, as compared to controls, while urea-extracted fractions were mitogenic and upregulated homologous cell phenotypes. When MSCs were cultured as pellets, inhibition of endogenous TGF-β by small molecule SB431542 largely negated the tissue-specific inductivity of urea-extracted ECMs, suggesting that endogenous TGF-β is necessary, but not sufficient, to explain the homologous bioactivity of tECM and cECM. When added as a

component of a photocurable GelMA hydrogels, cECM independently upregulated early chondrogenesis of encapsulated MSCs, and synergistically enhanced chondrogenesis when exogenous TGF-β was added as a medium supplement. Therefore, urea-extracted ECM fractions may be a promising biomaterial, which when combined with tunable scaffolds, can guide tissue-specific cell differentiation. However, our results, and those of others,[99-101,110,159,174] suggest that robust neotissue formation likely requires supplementation with exogenous growth factors (e.g., TGF-β). Building on the finding of synergism between cECM and TGF-β in inducing chondrogenesis in MSC-seeded GelMA hydrogels, we explored similar effects for tendon tissue engineering, as described in Chapter 3.

3.0 TENDON TISSUE ENGINEERING – COMBINING A BIOMIMETIC SCAFFOLD WITH SOLUBLE TENDON EXTRACELLULAR MATRIX AND TGF-β

As shown in the previous chapter, MSCs cultured on aligned PCL nanofibers further upregulated tenogenic markers when the medium was supplemented with urea-extracted tECM. In a subsequent experiment, MSC-seeded GelMA hydrogels demonstrated independent and synergistic enhancement of chondrogenesis when supplemented with cECM (in the hydrogel) and/or TGF-β3 (in the culture medium). In the following chapter, we explore the possible synergism between tECM and TGF-β3 as promoters of tenogenic differentiation of MSCs grown on both 2D plastic and aligned fibrous scaffolds. As native tendon tissue is principally composed of type 1 collagen, this specific protein was included as a distinct experimental group to discern the bioactivity of collagen 1 (of tendon ECM) compared to that of the diverse protein composition found in urea-extracted tECM. Of clinical relevance, the MSCs used herein were derived from human adipose tissue rather than bone marrow, as the former is abundant, contains a higher proportion of MSCs, and causes minimal donor site morbidity.

The following section contains material from the accepted publication:

Yang G, **Rothrauff BB**, Lin H, Yu S, Tuan RS. 2016. Tendon-Derived Extracellular Matrix Enhances TGF-β3 Induced Tenogenic Differentiation of Human Adipose-Derived Stem Cells. *Tissue Engineering Part A*. [**Accepted**]

3.1 INTRODUCTION

Tendon injuries occur frequently in sports and daily activities due to excessive load or overuse. Tendinopathies and tendon tears account for over 30% of all musculoskeletal consultations.[175] Unfortunately, the natural healing process of tendons is slow and insufficient, resulting in fibrotic scar formation and inferior mechanical strength at the injured sites.[141] Current clinical outcomes of tendon repair remain unsatisfactory due to limitations including donor site morbidity, risk of injury recurrence, and limited long-term functional recovery.[176-178] Therefore, tissue engineering approaches, which use a combination of cells, scaffolds, and bioactive molecules, are gaining increasing research interest as a promising alternative strategy to treat tendon injuries.

The use of adult mesenchymal stem cells (MSCs) as the cellular component for tendon tissue engineering has been increasingly explored in recent years.[179-181] Compared with other cell sources, adipose-derived mesenchymal stem cells (ASCs) are abundant and can be isolated by minimally invasive approaches.[182,183] Although a variety of growth factors are able to induce expression of tenogenic markers in ASCs, no single growth factor has been found to exclusively promote tenogenic differentiation. For instance, in addition to its tenogenic effect,[184,185] growth differentiation factor 5 (GDF-5) is also capable of stimulating ASC differentiation towards other mesenchymal lineages, such as osteogenesis[186,187] and chondrogenesis.[188] Likewise, transforming growth factor-β1 (TGF-β1) exhibits both tenogenic and chondrogenic effect for ASCs.[189,190] Rather, the evolving microenvironment produced by progenitor cells plays an important role in mediating cell responses to growth factors, which induce proliferation and tissue-specific differentiation during development and tissue repair.[191-193] However, there is still limited

understanding regarding how the biochemical and biophysical cues of the tendon microenvironment promote a tendon-specific cell phenotype.

Studies in tendon development have revealed the complexity of tendon differentiation. As shown across several animal models, members of the TGF-β superfamily are actively involved in tendon development and healing in a spatiotemporally specific manner. For example, mouse patellar tendon cells were found to respond to TGF-β signaling at developmental stages starting at gestation day 17.5 and ending at postnatal day 14.[194] Consistent with this finding, micromass culture of chick embryonic limb bud mesodermal cells with TGF-β demonstrated significant up-regulation of tendon markers, scleraxis (SCX) and tenomodulin (TNMD), with concurrent reduction in cartilage markers.[195] Conversely, disruption of TGF-β signaling resulted in the loss of most tendons and ligaments in a SCX-GFP mouse model.[196] When injured, high levels of TGF-β expression and activity were also seen throughout the healing period.[197-199]

Concurrently, recent research has illustrated the pivotal role of the extracellular matrix (ECM) in tendon differentiation.[200,201] ECM is composed of the structural and signal molecules secreted by the resident cells of each tissue. While the ECM of most tissues share highly conserved structural proteins (e.g., collagen, proteoglycans), it is the unique biophysical arrangement of these proteins, and the highly orchestrated deposition and presentation of soluble cues that serve to promote and maintain a particular cell phenotype.[202,203] Tendon is rich in ECM components, and many of the tendon ECM proteins have been found to play important roles in tendon differentiation and organization.[204-206] As proof, tendon-derived stem/progenitor cells (TSPCs) seeded on decellularized tendon/ligament ECM demonstrated improved proliferation and tendon cell phenotype.[207] Taken together, it is reasonable to assume that the presence of

native tendon ECM may be beneficial to TGF-β induced tenogenic differentiation of MSCs for tendon repair.

In addition to biochemical cues, scaffolds are also utilized in tendon tissue engineering to provide mechanical support as well as topographical cues that mimic the architecture of native tendon. Because tendon is primarily composed of aligned collagen fibers, scaffold anisotropy is an important topographical characteristic to consider in tendon tissue engineering. For instance, human tendon fibroblasts seeded on aligned microfibrous scaffolds exhibited increased expression of tendon phenotype markers.[123] In this study, we have therefore prepared and employed aligned poly-ε-caprolactone (PCL) scaffolds to partially reproduce the biophysical features of native tendon ECM.

The objective of this study was to investigate the effect of native tendon ECM components and TGF-β on the tenogenesis of human ASCs (hASC). A soluble extract of decellularized tendon ECM (tECM) was prepared as described previously.[115] The individual and combined effects of tECM and TGF-β3 on hASC behavior, including proliferation and differentiation, were analyzed by using tECM as a medium supplement for ASCs cultured with or without TGF-β3 for up to 2 weeks on 2D tissue culture plastic or aligned PCL scaffolds. We hypothesized that tECM is able to enhance the proliferation and TGF-β3-induced tenogenesis of ASCs in vitro, and that tECM modulates matrix deposition and organization of ASCs on scaffolds.

3.2 MATERIALS AND METHODS

3.2.1 Cell isolation and culture

hASCs were obtained from lipoaspirates of two donors (34 years old male and 38 years old female) using an automated cell isolation system (Tissue Genesis Inc.), with University of Pittsburgh Institutional Review Board approval. Isolated hASCs were cultured in growth medium (GM) consisting of DMEM-high glucose (Gibco), 10% fetal bovine serum (FBS), and penicillin/streptomycin (P/S). hASCs between passage 2 and 4 (P2-P4) were used for experiments.

3.2.2 Colony forming unit-fibroblast assay

The colony forming unit-fibroblast (CFU-F) assay was performed using an established method described elsewhere with culture time extending up to 14 days.[208] hASCs from each donor at P2 were plated separately in 100 mm dishes (Falcon) in triplicate at densities of 100 cells per dish and cultured in GM. The cultures were stained with 0.5% crystal violet solution in methanol and visible colonies were scored.

3.2.3 Flow cytometry

hASCs at P2 were detached by trypsin-EDTA and incubated with propidium iodide (PI) and PE- or FITC-conjugated mouse (IgG1, κ) anti-human antibodies for 30 min at 4 C°. Antibodies include mouse anti-human CD31, CD34, CD44, CD45, CD73, CD90, CD105 (BD Biosciences).

Dead cells were excluded by positive PI staining. PE- or FITC-conjugated isotype-matched IgGs (BD Biosciences) were used as controls. After washing, the cells were sorted using the FACSAria II SORP flow cytometer (BD Biosciences), and data analyzed with DiVa v6 software.

3.2.4 Preparation of tendon ECM

A soluble fraction of tendon ECM (tECM) was prepared using our previously reported protocol.[115] The proximal part of superficial digital flexor tendons was harvested from hind legs of 2-3 months old calves purchased from a commercial abattoir (Research 87 Inc.), pulverized, and decellularized by 1% Triton X-100 (Sigma-Aldrich). After nuclease treatment (200 U/ml DNase, Worthington), the acellular tissue was extracted in 3 M urea (Sigma-Aldrich) for 3 days. Urea was removed by dialysis in 3,500 MWCO cassettes (Thermo Scientific) against water for 2 days, and then the tECM extract was spin-concentrated, sterilized using 0.22 μm PVDF syringe filter units (Millipore), and stored as 1 mg/ml stock at -20 °C until use.

3.2.5 Preparation of scaffold

Aligned microfibers were fabricated by electrospinning. A solution of PCL (MW = 70k-90k, Sigma-Aldrich) prepared at 18% w/v in 1:1 (v/v) dimethylformamide (DMF) and tetrahydrofuran (THF) (Fisher Scientific) was loaded into a 10 mL syringe and extruded at 2 mL/h through a 22-gauge blunt-tip needle using a syringe pump (PY2 70-2209, Harvard Apparatus). A 10 kV DC potential (Gamma High Voltage) was applied to create an electrostatic field with a distance of 15 cm between the needle tip and a custom designed rotating mandrel. Electrospinning was performed for 2 hours per scaffold to form the scaffold sheet, which was

trimmed to 4 cm in width and dried in vacuum overnight to remove residual organic solvent. Scaffolds were cut into 20 mm x 5 mm rectangular pieces, hydrated and sterilized in 75% ethanol, and then soaked in GM overnight. The scaffolds were secured to the bottom of culture wells in customized incubators for cell seeding.

3.2.6 Scaffold characterization

Both aligned and non-aligned scaffolds were dried in vacuum, mounted on aluminum stubs, sputter-coated with 3.5 nm gold, and examined by a scanning electron microscope (SEM, field emission, JEOL JSM6335F) operated at 3 kV accelerating voltage and 8 mm working distance. The external surface of the central part of the constructs was selected for imaging. Fiber diameter and degree of alignment was quantified from the SEM images (n=4/group). Briefly, the diameters of 50 randomly selected fibers in each image were measured by ImageJ, and average fiber diameter calculated. The angle between fiber and horizontal orientation was measured by ImageJ (50 fibers counted in each image). The thicknesses of the scaffolds were measured by digital calipers (n=30).

3.2.7 Differentiation of hASCs

Differentiation along mesenchymal lineages, including osteogenesis, adipogenesis and chondrogenesis, was performed to assess the multipotency of the isolated hASCs using an established protocol with slight modifications.[208] Briefly, 10 ng/ml bone morphogenetic protein 6 (BMP-6) was added into the standard chondrogenic medium to improve TGF-β driven chondrogenesis of hASCs.[209] To induce tenogenesis, hASCs at P3 were serum-starved overnight

at a density of 1×10^4 cells/cm^2 in plate culture and at 6×10^4 cells/cm^2 in scaffold culture, respectively. Cells were then treated with or without 10 ng/ml TGF-β3 (PeproTech) in basal medium (BM) consisting of high glucose DMEM, 1x Insulin-Transferrin-Selenium-X (ITS) and P/S (Gibco), and supplemented with 10% v/v of 1 mg/ml tECM, 1 mg/ml collagen type I solution (Col I, PureCol Advanced Biomatrix) or FBS for up to 14 days.

3.2.8 Cell proliferation tests

hASCs at P3 were plated on culture plastic and scaffolds at a density of 0.5×10^4 cells/cm^2 and 4×10^4 cells/cm^2, respectively. Twenty-four hours after initial seeding, cells were fed with BM containing one of the following supplements at 10% v/v: 1 mg/ml tECM, 1 mg/ml Col I solution, or FBS. DMEM supplemented with 10% v/v Hanks' Balanced Salt Solution (HBSS, Gibco) was used as a negative control. On days 0, 3 and 7, MTS assays (CellTiter 96 Assay, Promega) were performed to spectrophotometrically determine metabolic activity of cells from each group. Additionally, cells were nuclear stained by 4, 6-diamidino-2-phenylindole, dilactate (DAPI, Life Technologies) at each time point and imaged using an Olympus CKX41 inverted fluorescent microscope equipped with a CCD camera to reflect cell nuclei density.

3.2.9 Real-time PCR analysis of gene expression

Total cellular RNA was isolated on days 3, 7 and 14, after differentiation treatment (RNeasy, Qiagen) and first-strand cDNA was synthesized using the SuperScript III First-Strand cDNA synthesis kit (Invitrogen). Real-time PCR was performed using SYBR green Supermix in a Step One Plus real-time PCR system (Applied Biosystem, Life Technologies). The targets and

sequences of primers are shown in **Supplemental Table 3**. Relative expression level of each gene was normalized to that of 18S rRNA and calculated using the ΔΔCt method.

3.2.10 Protein extraction and Western blot assay

Eight days after differentiation induction, total protein was extracted from each group by TM buffer (Total Protein Extraction Kit, Millipore) and concentrations were measured by BCA assay. Equal masses of reduced protein samples of the same concentration (~800 μg/ml) were electrophoretically separated in NuPAGE Bis-Tris Mini Gel (Life Technologies), and transferred onto PVDF membranes (iBlot dry blotting system, Invitrogen) for incubation with rabbit anti-scleraxis (SCX) or anti-glyceraldehyde-3-phosphate dehydrogenase (GAPDH) primary antibody (Abcam) at 4˚C overnight. Western blots were developed using horseradish peroxidase (HRP)-conjugated donkey anti-rabbit IgG secondary antibodies (GE Healthcare Bio-Sciences) and West Dura Extended Duration Substrate (Thermo Scientific).

3.2.11 Mechanical testing

Tensile properties of scaffolds were analyzed using the Bose 3230 mechanical tester. Scaffolds were securely mounted between two clamps at 10 mm and loaded with uniaxial force applied at a displacement rate of 0.2 mm/s until 10 mm displacement. The tensile force and the displacement were recorded, and the slope of the linear portion of the stress–strain curve was calculated as Young's modulus.

3.2.12 Matrix deposition and characterization

hASCs were seeded on PCL scaffolds at a density of 6×10^4 cells/cm^2 and cultured with BM supplemented with either 2% FBS or 2% FBS plus 10% tECM (v/v), in the presence of 50 μg/mL ascorbate-2-phosphate (Sigma-Aldrich), for 3 weeks. Negative controls consisted of cell-free scaffolds treated under the same conditions. Collagen content in each group was quantified using the Chloramine T-based hydroxyproline assay. Briefly, cell-seeded scaffolds were papain digested at 60 °C overnight, reacted with 4N NaOH, and then neutralized with HCl. The samples were then reacted with Chloramine T reagent (Fisher Scientific) and subsequently Ehrlich's reagent (Sigma-Aldrich). Absorbance at 550 nm was measured spectrophotometrically by a microplate reader (BioTek).

3.2.13 Immunofluorescent staining

Cell-seeded scaffolds were washed in PBS, fixed in 4% paraformaldehyde, and blocked with 1% bovine serum albumin (BSA) and 22.52 mg/ml glycine in PBS-T. Primary antibodies used included goat anti-tenomodulin (Tnmd, 1:50, sc49325 Santa Cruz), or rabbit anti-Col I (1:500, ab34710 Abcam), with overnight incubation at 4 °C. Alexa Fluor 488 chicken anti-goat or Alexa Fluor 488 goat anti-rabbit were used as secondary antibodies at 1:500 dilution (Life Technologies). For F-actin staining, fixed cells were permeabilized in 0.1% Triton X-100 and then incubated with Alexa Fluor 488 phalloidin for 30 min at room temperature (Life Technologies). After nuclear counterstaining with DAPI (Life Technologies), cells were imaged using a confocal microscope (Olympus FluoView 1000).

3.2.14 Statistical analysis

Data are presented as mean ± standard deviation (SD). All quantitative assays were performed for no less than three times independently (N equals to the number of independent tests in figure legends). In each replicate, cells from two donors were treated and analyzed separately in duplicate, and data were combined. One-way ANOVA with Bonferroni post hoc test and Student's t-test were performed with SPSS (SPSS Statistics software 21, IBM) to determine statistical significance. Significance was considered at $p<0.05$.

3.3 RESULTS

3.3.1 Characterization of human ASCs

After 14 days of culture, 28.83 ± 3.31% of the adherent cells isolated from the stromal vascular fraction (SVF) of adipose tissue were found proliferating by CFU assay, indicating a self-renewal capability within the cell population. Upon induction of differentiation, the cultured cells at P2 were able to undergo differentiation toward multiple mesenchymal lineages, including adipogenesis, osteogenesis, and chondrogenesis (**Figure 14A**). Moreover, the phenotypic analysis by flow cytometry suggested a relatively homogeneous population that expressed mesenchymal cell markers (CD44, CD73, CD90 and CD105) while free of hematopoietic and endothelial markers (CD31, CD34, CD45) (**Figure 14B**).[210] Taken together, these results confirmed that the cell population used for subsequent experiments exhibited characteristics consistent with ASCs derived from subcutaneous lipoaspirate.

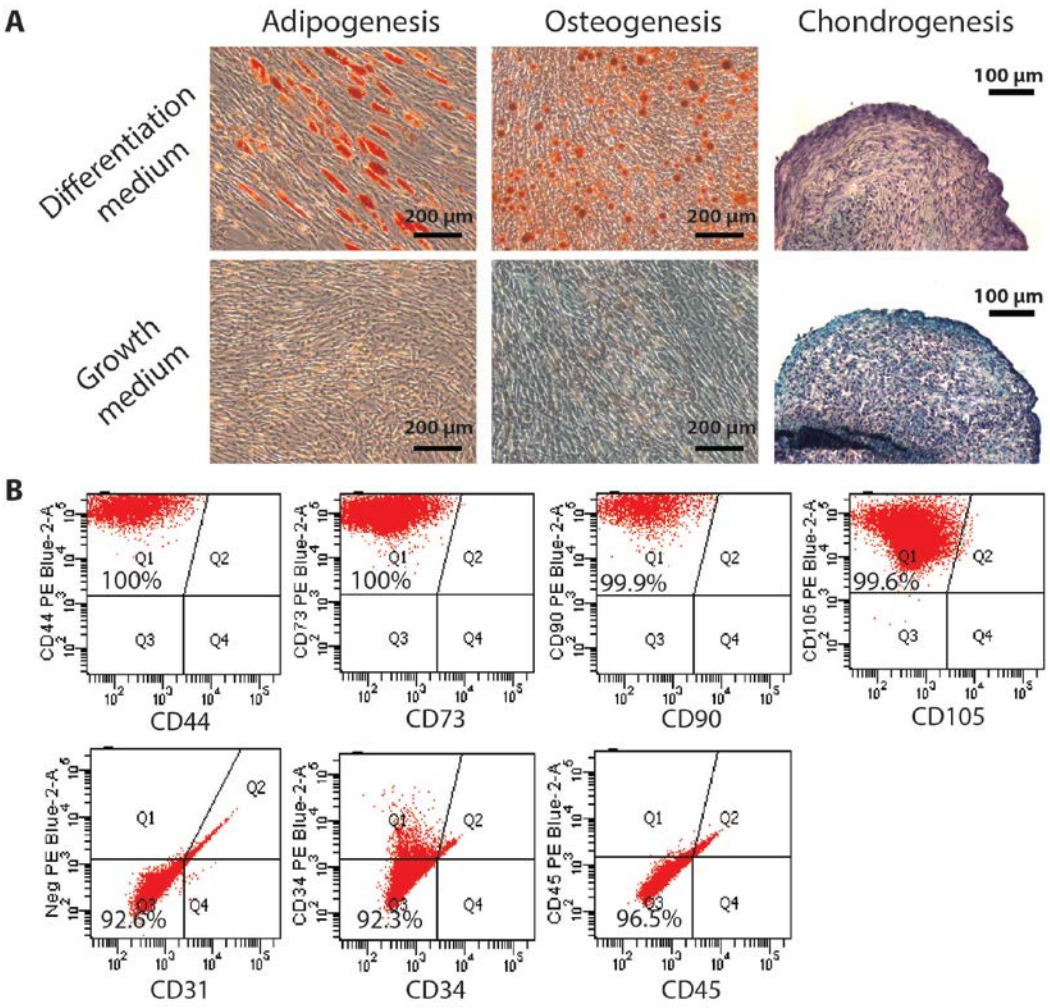

Figure 14. Characterization of hASCs. (A) Histological detection of ASC multipotency: Adipogenesis by Oil Red staining (red), osteogenesis by Alizarin Red staining (red), and chondrogenesis by Safranin-O staining (red). (B) Flow cytometry analysis of the cell surface markers characteristic for mesenchymal stem cells, hematopoietic and endothelial cells.

3.3.2 Effect of tendon ECM on ASC behavior in 2D

In order to investigate the role of tendon ECM in regulating ASC behavior, we extracted the soluble fraction of decellularized tendon ECM (tECM) from juvenile bovine SDF tendons. As

previously reported, the tECM solution prepared by this method is cell-free and rich in non-collagenous ECM proteins, with a constant yield rate and consistent composition (**Supplemental Figure 5**).[115] tECM or Col I solution were used at 1 mg/ml as medium supplements at 10% v/v to treat ASCs on 2D tissue culture plastic for up to 7 days. ASCs cultured with HBSS-supplemented medium or FBS-supplemented medium (10% v/v) were used as negative and positive controls, respectively (**Figure 15A**). At days 0, 3, and 7, cell density and metabolic activity were determined by DAPI staining and MTS assay. After 7 days of culture, higher cell density in tECM and FBS-treated groups was clearly visualized by DAPI staining (**Figure 15B**). ASCs cultured with tECM for 7 days demonstrated significantly higher metabolic activity than those with Col I, the most abundant structural ECM protein in tendon tissue, but slightly lower than those cultured with FBS (**Figure 15C**).

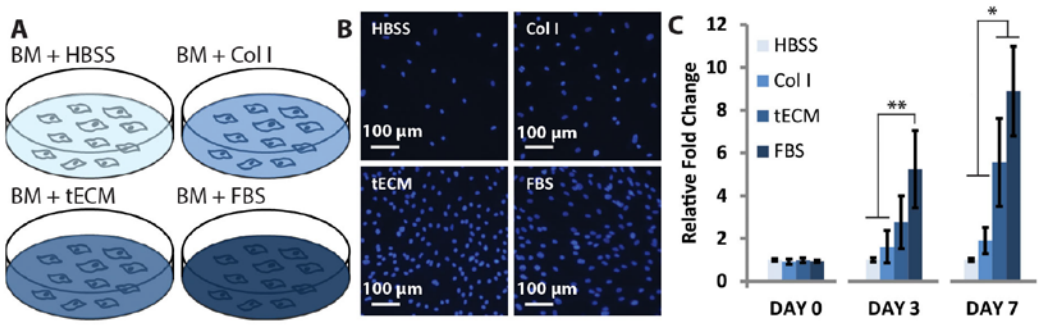

Figure 15. Assay of hASC proliferation in 2D cultures. (A) hASCs were plated on 2D tissue culture plastic, and treated with basal medium (BM) containing one of the following supplements at 10% v/v: HBSS, 1 mg/ml tECM solution (tECM), 1 mg/ml collagen type I solution (Col I) or FBS. (B) After 7 days of culture, DAPI nuclear staining showed high cell density in tECM- and FBS-treated groups. (C) MTS assay revealed elevated cellular metabolic activity in tECM- and FBS-treated groups. *, $p<0.05$; **, $p<0.01$; N=3.

The individual and combined effect of tECM and TGF-β3 on hASC tenogenesis was analyzed at the mRNA and protein level. Three types of medium (BM supplemented with 10% v/v FBS, Col I, or tECM) were prepared, with or without 10 ng/ml TGF-β3, in which ASCs were cultured for up to 14 days (**Figure 16A**). Real-time PCR analysis showed that treatment with tECM alone did not significantly increase the expression of SCX, the primary marker for early tendon differentiation. However, tECM combined with TGF-β3 gave rise to significantly higher levels of SCX expression than all other groups tested at days 3 and 7 (**Figure 16B**). The difference in SCX expression among the groups was confirmed at the protein level by Western blot (**Figure 16D**). Interestingly, unlike SCX, TNC expression was up-regulated by tECM treatment in the absence of TGF-β3 after 7 and 14 days of culture, while the combined treatment of tECM and TGF-β3 led to the highest level of TNC mRNA among all groups (**Figure 16C**). ASCs treated with TGF-β3 in the presence of Col I again showed delayed upregulation of tendon markers compared to the tECM plus TGF-β3 treatment (**Figure 16C**). Taken together, these data suggested that tECM treatment in 2D resulted in partial adoption of the tendon cell phenotype in the absence of other inductive cues, and enhanced tenogenesis of ASCs induced by TGF-β3. Moreover, tECM exhibited no such inductive effect on chondrogenesis of ASCs in 2D culture, suggesting a tissue-specific functionality of the tECM (**Supplemental Figure 6**).

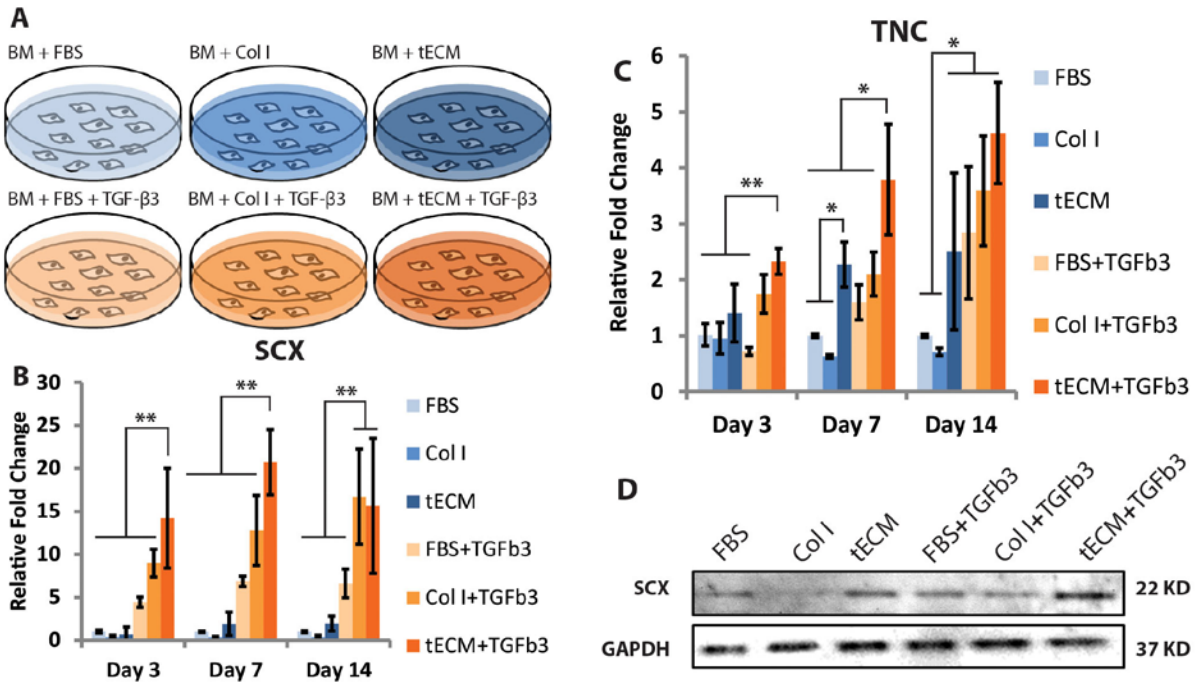

Figure 16. Tenogenesis of hASCs in 2D cultures. (A) hASCs were plated on 2D tissue culture plastic, and treated with or without 10 ng/ml TGF-β3 in basal medium (BM) containing one of the following types of supplements at 10% v/v: FBS, 1 mg/ml tECM solution (tECM) and 1 mg/ml collagen type I solution (Col I). (B, C) Real-time PCR analysis of (B) scleraxis (SCX) and (C) tenascin-C (TNC) expression levels. tECM treatment up-regulated SCX expression in the presence of TGF-β3, and increased TNC expression with or without TGF-β3. (D) Western blot assay showed consistent difference in SCX protein. *, $p<0.05$; **, $p<0.01$; N=3.

3.3.3 Characterization of the aligned microfiber scaffolds

We next attempted to generate a physical scaffold environment that mimics the structural features of tendon. A microfibrous PCL scaffold was fabricated by electrospinning (**Figure 17A**). Aligned scaffolds exhibited highly uniaxial fiber orientation: most fibers were oriented at

between 80° and 100° with respect to cross axis (**Figure 17D,F**), in contrast to the random orientation seen in the non-aligned scaffolds (**Supplemental Figure 7**). The mean thickness of aligned scaffold was 103.3 ± 18.9 μm (n=30). No significant difference in fiber diameter was found between aligned and random scaffolds (**Figure 17E**, 1.26 ± 0.51 μm vs. 1.29 ± 0.34 μm). When tension was applied in the direction of fibers, the aligned scaffolds displayed 2.5-fold higher tensile strength as compared to the randomly oriented scaffolds (**Figure 17B,C**). Anisotropy of the aligned scaffolds was confirmed by tensile testing along two planes: the elastic modulus along the axis of fibers (longitudinal) was 10-fold higher than that in the perpendicular direction (cross), as expected from the uniform orientation of fibers (**Figure 17B,C**). hASCs seeded on aligned scaffolds adopted elongated morphology and were orientated in the direction of fibers after 3 days of culture. In contrast, hASCs seeded on random scaffolds exhibited a polygonal shape without uniformity in orientation (**Supplemental Figure 7**).

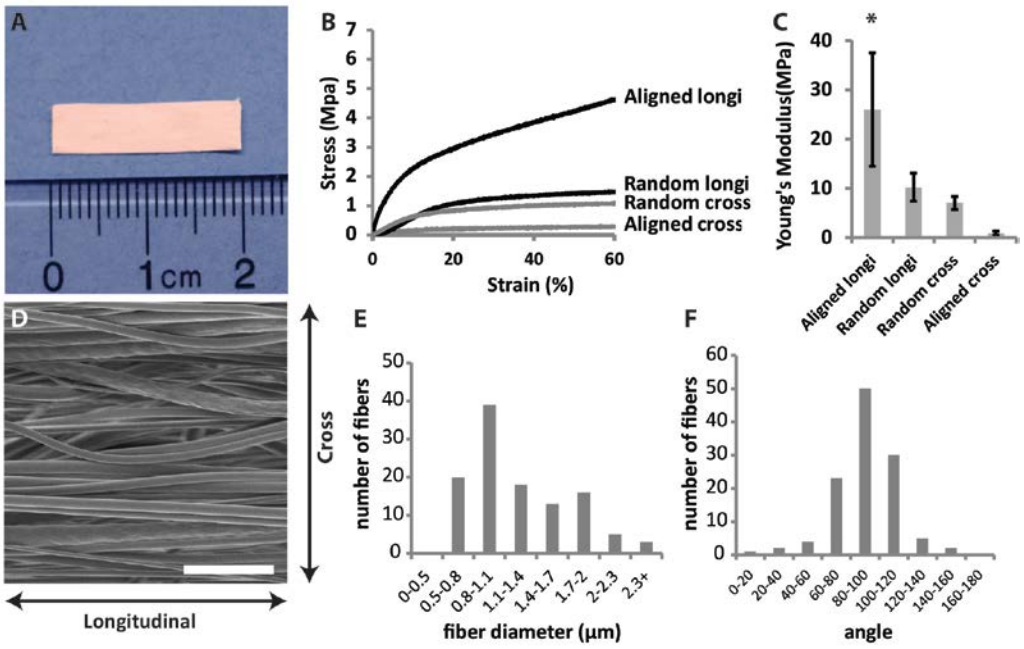

Figure 17. Characterization of electrospun PCL scaffolds. (A) Gross appearance of scaffold. (B) Strain-stress curves indicated dramatic difference in tensile strength between aligned and random scaffolds; anisotropy in tensile strength was found in aligned scaffolds (Aligned longi *vs.* Aligned cross). (C) In aligned scaffolds, the elastic modulus was the highest in the longitudinal direction (Aligned longi *vs.* Aligned cross), which was also significantly higher than that of randomly-oriented scaffolds (Random longi, Random cross). *, $p<0.05$; N=3. (D) SEM image of aligned microfibrous PCL scaffolds. (E) Distribution of fiber diameters. (F) Most fibers in the aligned scaffold were oriented at between 80° and 100° with respect to cross axis.

3.3.4 Effect of tendon ECM on ASC behavior in scaffolds

ASCs seeded on aligned scaffolds were treated for one week in BM supplemented with 10% v/v FBS, Col I, or tECM. No observable differences in cell shape were found among groups; most ASCs cultured on the aligned scaffolds were elongated and aligned in the direction of the

surrounding fibers regardless of treatment method, as indicated by immunofluorescent staining of F-actin (**Figure 18A**). Nevertheless, cell metabolic activity differed greatly among groups: the tECM-treated group exhibited enhanced metabolic activity compared to Col I- or HBSS-treated groups. At day 7, the metabolic activity of tECM-treated cells remained significantly higher than Col I- or HBSS-treated cells, and was comparable to FBS-treated cells (**Figure 18B**).

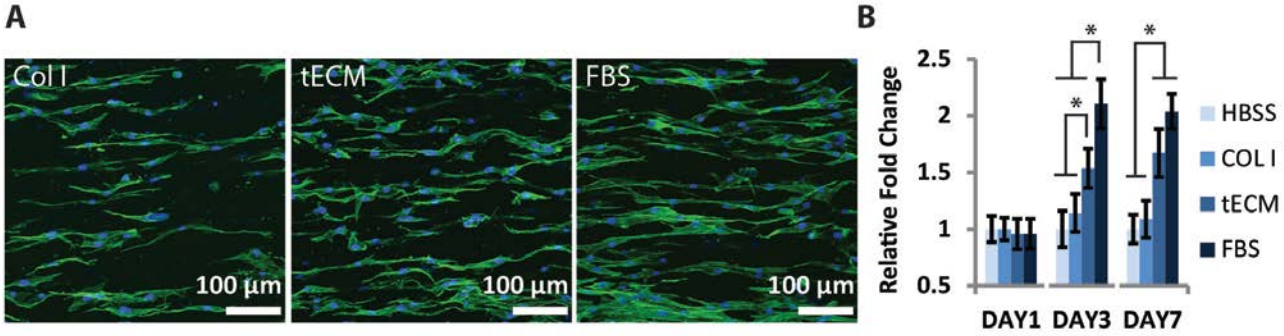

Figure 18. Behavior of hASCs seeded on aligned scaffolds. Cultures were treated with basal medium (BM) containing 10% v/v FBS, Col I, or tECM. (A) After 3 days of culture, most ASCs cultured on aligned scaffolds were elongated and aligned regardless of treatment condition. Green: F-actin; blue: DAPI. (B) MTS assay showed enhanced cellular activity in the tECM-treated group compared to Col I- or HBSS-treated groups, which was comparable to FBS-treated cells at day 7. *, $p<0.05$; N=3.

Given the established positive influence of fiber alignment on tenogenic differentiation, analysis of gene expression and matrix deposition were only performed on aligned microfibrous scaffolds. When cultured in BM with TGF-β3 and 2% FBS, SCX expression in hASCs was increased by the presence of tECM on days 3, 7 and 14, whereas in the Col I group the up-regulation in SCX was not seen until day 14 (**Figure 19A**). Similarly, tECM supplementation

resulted in significantly higher TNC levels compared to controls at all three time points tested. In contrast, Col I treatment did not significantly up-regulate TNC levels although there was a trend of increase (**Figure 19A**). To further investigate the extent of tECM-mediated tenogenesis, we analyzed the presence of Tnmd, a tendon-specific membrane glycoprotein found in the late phase of differentiation, by immunofluorescent staining. Compared to other treatment groups, an evidently higher density and intensity of staining for Tnmd (green) was seen in the tECM-treated group (**Figure 19B**).

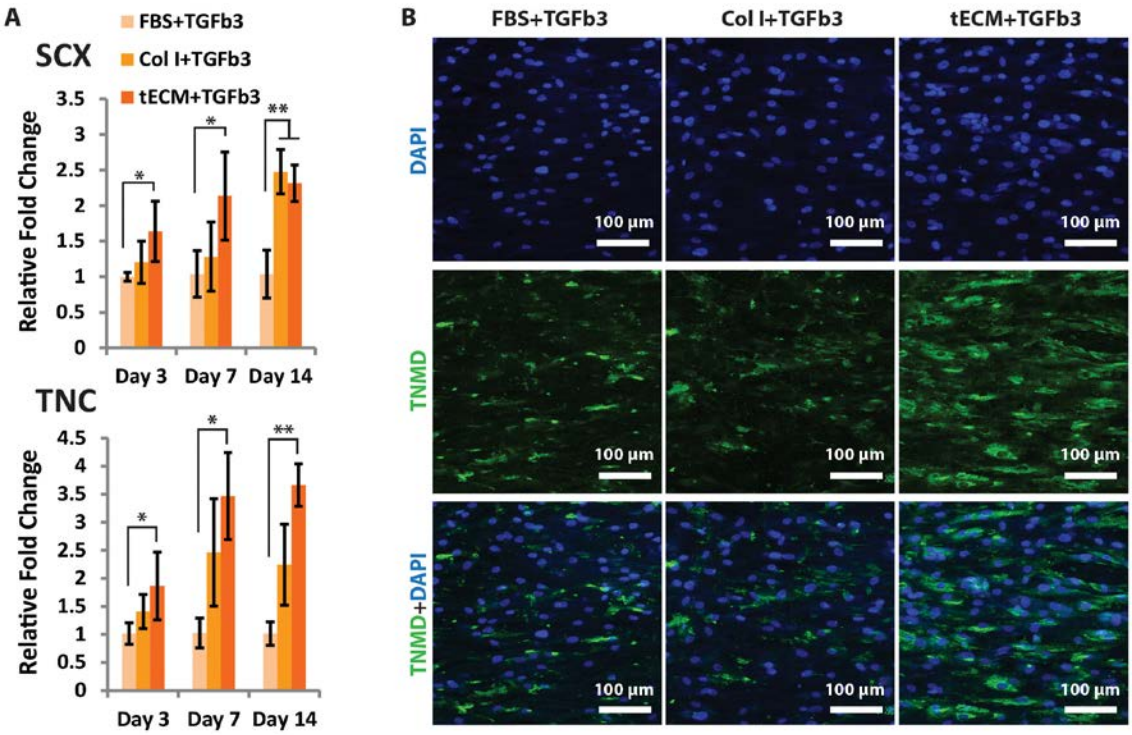

Figure 19. Tenogenic differentiation of hASCs seeded on aligned scaffolds. (A) Real-time PCR assay showed that scleraxis (SCX) and tenascin C (TNC) expression was significantly increased in the presence of tECM. (B) Immunofluorescence showed that staining for tenomodulin (Tnmd) was denser and more intense (green) in tECM-treated group. *, $p<0.05$; **, $p<0.01$; N=4.

We next examined the influence of tECM on the synthesis and organization of collagen, the primary structural protein of tendon tissue. Cells seeded on PCL scaffolds were treated with L-ascorbate 2-phosphate for 3 weeks to accelerate collagen synthesis. Immunofluorescent staining of Col I on the surface of scaffolds qualitatively confirmed the presence of newly-synthesized matrix in both the control and tECM-treated groups, revealing arrays of collagen fibrils extended in the direction of the PCL fibers. Interestingly, denser collagen fibrils were found on scaffolds treated with tECM (**Figure 20A**) compared to those treated with FBS only, while the amount of collagen presented by tECM alone on the acellular scaffolds was negligible. (**Figure 20A**). This was expected, as tECM is composed of a high ratio of non-collagenous proteins (**Supplemental Figure 5**). The observed difference in collagen content was confirmed quantitatively by hydroxyproline assay. In the presence of tECM, hASCs produced a 2.4-fold higher amount of collagen per scaffold than controls (86.54 ± 7.46 *vs*. 36.79 ± 2.49 μg/scaffold). This pattern persisted when collagen content was normalized against double stranded DNA (dsDNA) content, with a 1.8-fold higher collagen content per unit weight of dsDNA (145.05 ± 17.46 *vs*. 80.02 ± 17.77 μg/μg DNA) in the tECM-treated group *vs.* control group.

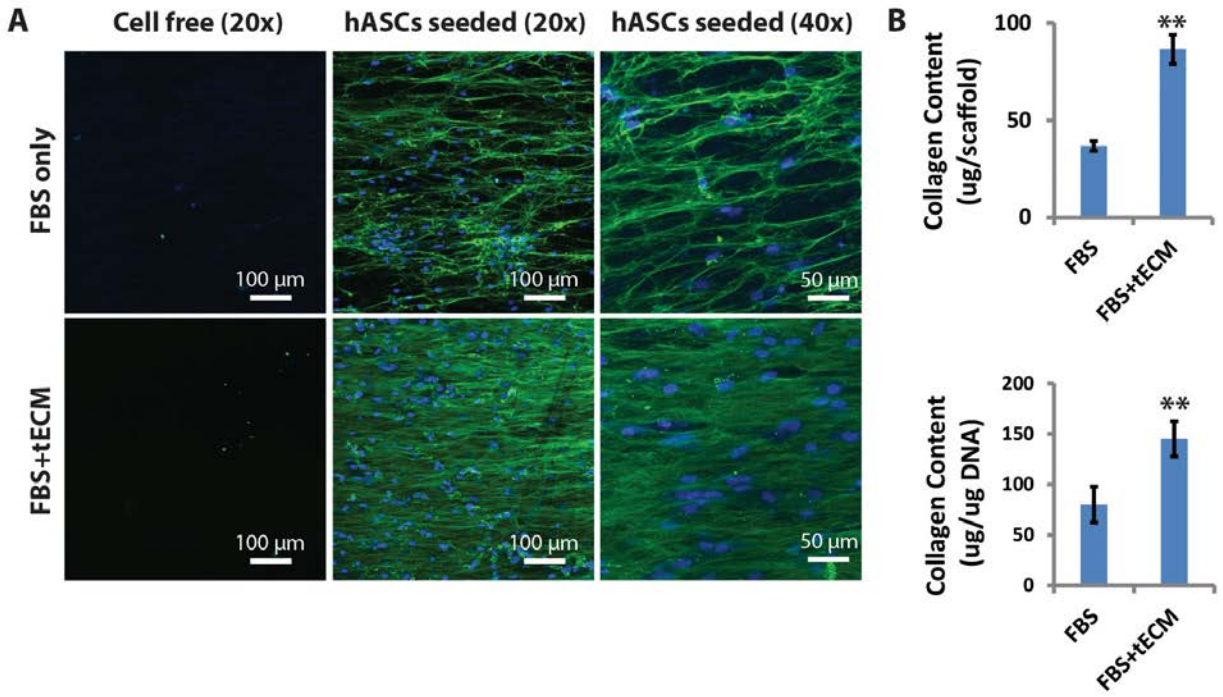

Figure 20. Matrix deposition by hASCs cultured on aligned scaffolds. (A) Immunofluorescent staining for collagen type I (green) found denser collagen fibrils deposited by cells treated with tECM compared to the control group. (B) Hydroxyproline assay showed higher collagen content in the tECM-treated group. Collagen content of each group was normalized to that of the corresponding cell-free group. **, $p<0.01$; N=3.

3.4 DISCUSSION

The goal of this study was to investigate the modulatory effect of soluble tendon ECM (tECM) on known biochemical (i.e. TGF-β3) and biophysical cues that promote tendon differentiation, in order to advance the development of functional engineered tendon grafts. Human ASCs were prepared and characterized, and individual and combined effects of tECM and TGF-β3 on cell behavior, including proliferation and differentiation, were examined. We found that: (1) tECM

enhanced TGF-β3-induced tenogenesis of hASCs in both 2D plastic and 3D scaffold cultures, and (2) tECM favorably modulated matrix deposition and organization by hASCs seeded on microfibrous scaffolds.

In the native tendon microenvironment, dense ECM surrounds the tendon cell. Tendon stem/progenitor cells (TSPCs) exhibited impaired proliferative and tenogenic potential in the absence of critical ECM proteins,[201] and showed reduced TNMD expression when seeded on tissue culture plastic, as compared to tendon ECM.[211] The tECM prepared in our study increased hASC proliferation and TNC expression when used as a culture supplement in the absence of other inductive cues. Expression of both TNC and SCX was further enhanced when treated concomitantly with TGF-β3, as shown in both 2D plastic and 3D scaffold cultures. Our findings indicate that the regulatory effects of tECM on tendon cell behavior also apply to ASCs. Consistent with our results, Little et al.[102] found increased proliferation and partial adoption of tendon phenotype by ASCs seeded on acellular tendon/ligament matrix. The tECM contains not only collagen but also a number of non-collagenous proteins, including fibronectin, fibromodulin, biglycan and decorin, all of which are known to regulate MSC activities, such as adhesion, proliferation, stemness, and differentiation.[212-215] In addition, a variety of growth factors, such as TGF-β, IGF-1, VEGF, and CTGF, were found embedded in the decellularized tECM.[216] How these bioactive molecules, along with other yet-to-be-identified components in the tECM, contribute to the bioactivity of the tECM in our results remains to be investigated. The enhancement of ASC tenogenesis by tECM combined with TGF-β3 treatment exemplifies the complexity in the fine control of tissue differentiation – tECM may serve as a reservoir of signals by itself or, not mutually exclusively, exert a regulatory effect on exogenous inductive cues.[214] Moreover, we found little inductive effect of tECM on chondrogenesis, in agreement with our

earlier work (Chapter 2). This finding further highlights the tissue specificity of the derivation of ECM in influencing MSC differentiation.

To date, ASCs are widely used for scaffold recellularization and as a means to improve vascularization, matrix deposition, and implant integration,[217-220] whereas optimization of tendon-specific differentiation of seeded ASCs remains elusive. On one hand, ASCs isolated from a variety of animal species have been reported to upregulate tenogenic markers *in vitro* under specific treatments,[184,185,189,191,221] suggesting the tenogenic potential of ASCs. On the other hand, Eagan et al. questioned the suitability of hASCs for tendon tissue engineering and reported the lack of any significant and consistent upregulation in the expression of COL I, TNC, or SCX, in hASCs treated for up to 4 weeks with TGF-β1 or IGF1.[222] In addition, hASCs showed lower SCX expression compared to TSPCs when cultured *in vitro*.[223] Incorporating tissue-specific ECM molecules into differentiation protocols represents an alternative approach to develop a robust tenogenesis strategy for ASCs in order to better exploit the regenerative potential of ASCs applied to tendon tissue engineering. In future studies, more tendon phenotypic markers, such as Mohawk (MKX), and ECM protein encoding genes should be analyzed to advance our knowledge of the pro-tenogenic effect of tECM.[224]

As noted above, the scaffold is another key component in tendon tissue engineering by creating a proper microenvironment for mechanical support and tissue regeneration. Therefore we prepared electrospun, aligned fibrous PCL scaffolds consisting of microfibers (~1.3 μm) to simulate the size of collagen fibrils in natural tendon tissue.[225] The diameter of fibers has been found to have an influence on seeded cells; compared with nanofibers, microfibers promoted the expression of phenotypic markers of tendon fibroblasts, possibly due to the resemblance of the healthy, mature matrix with micron-sized collagen fibrils.[226,227] A promising future prospect

based on this work is the application of dynamic/cyclic stretch to cell-seeded scaffolds to simulate the loading of native tendon during motion.[228] Moreover, the PCL scaffold used here may be further modified to address some of the current limitations. For instance, although the aligned scaffold demonstrated anisotropy similar to that of tendon tissue, improvements in tensile strength is clearly needed if intended to be used as a clinical tendon graft.[229] In addition, a functional implant will likely require a scaffold that sufficiently retains bioactive agents. For this purpose, scaffold surface modification may be carried out to immobilize bioactive macromolecules contained in tECM.[230] Likewise, scaffold thickness and porosity may need to be improved to allow sufficient cell infiltration.[231]

We examined the influence of tECM on collagen synthesis and organization by hASCs seeded on aligned scaffolds. Consistent with previous studies, collagen fibrils were aligned in the direction of the PCL fibers.[231] More abundant and homogenous distribution of collagen fibrils were found in cells treated with tECM. The tECM-induced enhancement of collagen fibrillogenesis may be due to the bioactivity of small leucine-rich proteoglycans (SLRPs) and glycoproteins in tECM, such as decorin, biglycan, lumican, and collagen oligomeric matrix protein (COMP). These proteins are able to bind non-covalently to collagen molecules at specific sites in the gap region of fibrils and therefore facilitate collagen fibrillogenesis and stabilization.[232-235] Acellular scaffolds possessed negligible collagen content when treated with tECM. This confirms that the tECM acts by promoting collagen production in ASCs rather than by merely adsorbing to the scaffold.

3.5 CONCLUSIONS

In this study, a bioactive, soluble fraction of tendon ECM (tECM) was prepared, characterized and incorporated into growth/differentiation medium to treat ASCs. We demonstrated that tECM treatment enhanced the proliferation and tenogenic capacity of hASCs. Moreover, when cultured on scaffolds that mimic the architecture of native tendon tissue, hASCs treated with tECM exhibited increased Col I matrix synthesis and improved organization. These findings provide new insights into the role of tissue-specific ECM in guiding site-appropriate cell responses in terms of connective tissue differentiation and healing. In addition to serving as an *in vitro* differentiation model, the design attributes of the scaffold culture system developed in this study are applicable to functional tendon tissue engineering that aims at simultaneous induction of phenotypic markers and enhanced matrix deposition. Our findings highlight the importance of reproducing the native tissue microenvironment as a design principle for eliciting desired cellular responses for tissue regeneration.

4.0 MENISCUS TISSUE ENGINEERING – COMBINING REGION-SPECIFIC BIOACTIVITY OF SOLUBLE INNER AND OUTER MENISCAL-DERIVED EXTRACELLULAR MATRICES WITH PHOTOCURABLE HYDROGELS

As shown in the preceding chapters, urea-extracted fractions of decellularized tendon and cartilage ECMs are able to promote tissue-specific cell phenotypes in various culture microenvironments. In these experiments, the entire tissue was homogenized prior to decellularization and solubilization, without regard to any regional differences in ultrastructure or biochemical composition. However, the meniscus contains profound regional differences when moving radially from the central to peripheral zones. In particular, the central region more closely resembles hyaline cartilage while the peripheral region resembles tendon/ligament. In this chapter, we explore the region-specific bioactivity of urea-extracted fractions derived from ECM of the inner and outer meniscal regions. In **Section 4.1**, soluble meniscal ECM from either region was added to photocrosslinkable polyethylene glycol diacrylate (PEGDA) hydrogels seeded with human bone marrow MSCs. PEG provides a 3D structure in which MSCs can deposit matrix, but it lacks bioactive motifs (e.g., cell-binding domains) found in natural ECM structural proteins (e.g., collagen). As a result, PEGDA hydrogels serve as a relatively inert 3D microenvironment in which any differences between groups can be attributed to the urea-extracted meniscus ECM. **Section 4.2** expands on the results of **Section 4.1** through additional

characterization of the soluble ECM fractions. GelMA hydrogels are used in place of PEGDA, as we've previously shown the former to support roust chondrogenesis in seeded MSCs.[134] As GelMA contains cell-binding domains found in native collagen, it may possess an inherent bioactivity that could influence the region-specific effects of soluble meniscus ECM. Collectively, the work presented in this chapter demonstrates the homologous bioactivity of urea-extracted fractions of soluble ECM derived from the inner and outer meniscal regions, which may serve to enhance hydrogels intended for meniscus tissue engineering.

4.1 REGION-SPECIFIC BIOACTIVITY OF SOLUBLE INNER AND OUTER MENISCAL-DERIVED EXTRACELLULAR MATRICES IN PHOTOCURABLE POLYETHYLENE GLYCOL DIACRYLATE (PEGDA) HYDROGELS

The following section contains material from the accepted publication:

Shimomura K, **Rothrauff BB**, Tuan RS. 2016. Region-specific effect of decellularized meniscus extracellular matrix on mesenchymal stem cell-based meniscus tissue engineering. *American Journal of Sports Medicine.* [**Accepted**]

4.1.1 Introduction

The meniscus plays important roles in the knee joint, including force transmission, shock absorption, joint lubrication, and provision of joint stability.[236-240] Unfortunately, many athletes suffer injury to the knee meniscus, and the effective repair of such injuries remains a challenge in such a young and active population.[241-243] Importantly, it is widely accepted that a meniscal tear

does not heal spontaneously owing to limited blood supply.[244-246] Without effective long-term repair for these injuries, the damage to the knee may compromise athletic careers and lead to osteoarthritis (OA) at an early age.[247,248] Therefore, the development of novel therapeutic methods for meniscal repair is both timely and necessary.

Recently, tissue engineering approaches that involve the use of adult tissue-derived multipotent mesenchymal stem cells (MSCs) and biomaterial scaffolds have gained increasing attention as potential regenerative therapies, including musculoskeletal regeneration. While a number of meniscal biomaterial scaffolds have been developed and shown promise, complete meniscal regeneration remains challenging because of the difficulty in reproducing the anatomically complex meniscal structure composed of region-specific matrix organization and biochemical composition.[249-251] Recently, decellularized, tissue-derived extracellular matrices (ECMs) have been tested as candidate scaffolds because they are considered potentially beneficial to tissue development via regulation of cell proliferation and differentiation by providing specific molecules that guide cell behavior and morphogenesis.[6,252] It is also generally assumed that tissue-derived ECMs retain bioactivities specific to their tissue origin.[115] A 3D collagen-based scaffold combined with water-soluble decellularized ECMs derived from native tendon tissue has been recently developed, and proved its feasibility in developing an MSC-seeded, tendon ECM-containing construct for tendon tissue engineering.[115] Considering the structural similarities between tendons and menisci, including dense ECM components as well as their hypocellular and hypovascular nature, meniscus-derived ECM (mECM) may offer similar benefit for meniscus tissue engineering.

It is noteworthy that menisci have different characteristics across the inner and outer regions. In particular, there are regional differences in collagen ultrastructure and biochemical

composition, with resident meniscal cells having distinct morphologies and biological properties dependent on their location.[253,254] Histological and immunohistochemical analyses by Chevrier et al.[255] on human, sheep, and rabbit menisci showed that collagen type I appeared throughout most of the meniscus, while collagen type II was present primarily in the inner main meniscal body. The inner region of menisci was also the glycosaminoglycan (GAG)-rich area. These studies therefore indicate that the inner region of menisci should be considered to have a fibrocartilaginous phenotype, while the outer region of menisci exhibits a fibroblastic phenotype. In applying mECM for meniscus tissue engineering, it is important to consider these differences in structural and biochemical features between the inner and outer regions.

This study investigates the feasibility of applying water-soluble mECM combined with a polyethylene glycol diacrylate (PEGDA) hydrogel-based scaffold for meniscal tissue engineering, specifically comparing the effects of region-specific mECMs on 3D constructs using multipotent, human bone marrow-derived MSCs (hBMSCs). PEDGA provides a cytocompatibility 3-dimensional microenvironment without additional cell-binding motifs found on other hydrogel polymers (e.g., collagen, fibrin). As a result, differences in hBMSC behavior can be attributed to compositional differences between region-specific mECM extracts. It is hypothesized that mECM derived from the inner or outer region will direct the differentiation of hBMSCs in a regionally specific manner. In turn, this region-specific bioactivity may be utilized for future applications in meniscal tissue engineering.

4.1.2 Methods

4.1.2.1 Extraction and preparation of mECM Meniscal tissue specimens were harvested from the hind-leg stifle of 2- to 3-year-old cows within 24 hours of slaughter (JW Trueth and

Sons, Baltimore, MD). Bovine menisci have been shown to have homologous structure and function to human menisci[52,256] and the relatively large size[257] provides a inexpensive source of meniscal ECM. Preparation of mECM was carried out using the recently published protocol for tendon ECM.[115] The menisci were divided precisely along the midline separating the inner and outer halves. The tissues were then minced separately into small pieces (~8 mm^3), decellularized by incubation in 1% Triton X-100 (Sigma-Aldrich, St. Louis, MO) in phosphate-buffered saline (PBS; pH 7.4) under continuous agitation at 4 °C for 3 days, followed by three washes, 30 min each, in PBS. The decellularized material was then treated with 200 U/ml DNase and 50 U/ml RNase (Worthington, Lakewood, NJ) solution at 37°C for 24 h and then washed in PBS (6 times, 30 min for each wash). After nuclease digestion, decellularization was verified by the lack of cell nuclei using DAPI staining and by the reduction in double-stranded DNA content using PicoGreen® dsDNA Quantitation Reagent and Kits (Invitrogen, Carlsbad, CA), compared to that of native meniscal tissues. After the confirmation of successful decellularization, each tissue was cryomill-powderized using Freezer/Mill® (SPEX Sample Prep, Metuchen, NJ), and then extracted with 3 M urea (Sigma-Aldrich, St. Louis, MO) in water (25 mg mECM powder/ml) with gentle agitation at 4°C for 3 days. The suspension was then subjected to centrifugation for 30 min at 1,500 x g to collect the extract supernatant. Urea was removed by dialysis in 2000 MWCO dialysis tubing (Sigma-Aldrich, St. Louis, MO) against deionized water at 4°C for 2 days. Water was changed every 4 h. The dialyzed mECM extract was transferred into centrifugal filter tubes (3000 MWCO, Millipore, Carrigtwohill, Ireland) and spin-concentrated for 30 min at 1,500 x g. The final mECM solution was filter-sterilized through PVDF syringe filter units (0.22 μm, Millipore, Billerica, MA), and the total protein concentration determined using the BCA

assay (Thermo Fisher Scientific, Waltham, MA). The mECM preparations were stored as aliquots of 600 μg/ml at -20 °C until use.

4.1.2.2 PEGDA preparation 5 g polyethylene glycol (PEG, 4 kd, Fluka, Milwaukee, WI) was dissolved in 15 ml anhydrous dicholoromethane (DCM) followed by the addition of 0.44 ml methacrylic anhydride (MA), 0.25 ml triethylamine (TEA), and 3 g molecular sieves. The solution was thoroughly mixed and protected from light, and allowed to react at room temperature for 4 days. The final PEGDA suspension was filtered to remove the solvent and dried overnight under high vacuum. The dried PEGDA was then dissolved in H_2O at 30% concentration (w/v) and dialyzed in 2000 MWCO dialysis tubing (Sigma-Aldrich) against H_2O to completely remove all low-molecular-weight contaminants.

4.1.2.3 Cell isolation hBMSCs were isolated from bone marrow aspirate from the femoral head of three patients undergoing total hip arthroplasty with Institutional Review Board approval (University of Pittsburgh) and cultured in growth medium (DMEM-high glucose, 10% fetal bovine serum, 100 units/ml penicillin and 100 μg/ml streptomycin, Invitrogen, Carlsbad, CA) and passaged. All experiments were performed with hBMSCs at passages 3-5.

4.1.2.4 Fabrication of 3D construct hBMSCs were trypsinized from cell culture flasks and mixed at 1 x 10^6 cells/ml with 10% PEGDA, containing a final concentration of either 60 μg/ml (see below) inner mECM or outer mECM. A control group was prepared without mECM supplementation. These solutions (500 μl per construct in 24 well culture plates) were mixed with 0.125% lithium phenyl-2,4,6-trimethylbenzoylphosphinate (LAP) as used in a previous study,[258] and then photocrosslinked to fabricate hydrogel scaffold-based 3D constructs. The cell-

seeded constructs were cultured with chondrogenic medium containing Dulbecco's Modified Eagle's Medium (DMEM)-high glucose (Invitrogen), containing 100 units/ml penicillin and 100 μg/ml streptomycin, ITS Premix (BD Biosciences, Franklin Lakes, NJ), 50 μg/ml ascorbic acid 2-phosphate (Sigma-Aldrich), 40 μg/ml L-proline (Sigma-Aldrich), 100 μg/ml sodium pyruvate (Life Technologies, Carlsbad, CA), 0.1 μM dexamethasone (Sigma-Aldrich), and 10 ng/ml recombinant human transforming growth factor-β3 (TGF-β3; PeproTech, Rocky Hill, NJ).

4.1.2.5 Cell viability assay On culture days 1 and 7, the 3D constructs (n = 2 per group) were washed twice with PBS and cell viability was assessed with the Live/Dead stain (Invitrogen, San Diego, CA), and examined by epifluorescence microscopy (live cells stained green, dead cells stained red). Using four different microscopic views of the samples from each group, live and dead cells were counted to calculate cell viability, represented as the percentage of number of live cells as a function of total number of cells (live plus dead).

4.1.2.6 Real-time PCR analysis On culture days 1, 3, and 7, total RNA was isolated from the 3D constructs (n = 4 or 5 per group, per culture day) using an RNA extraction Kit (Qiagen, Valencia, CA) according to the manufacturer's protocol. First-strand cDNA was synthesized with random primers using a cDNA synthesis kit (Invitrogen, Carlsbad, CA). Quantitative real-time PCR (qRT-PCR) was performed using SYBR green Supermix in a Step One Plus real-time PCR system (Applied Biosystem, Life Technology) and then analyzed by comparative Ct quantification (delta delta Ct method). Primers used for meniscus-associated gene expression included those for collagen type I, collagen type II, aggrecan, and Sox 9. The targets and sequences of primers are shown in **Table 1**. The expression level of each gene was normalized to GAPDH.

Table 1. Primer sequences for real-time PCR

Gene	Primer sequence (5'-3')		Product size (bp)
GAPDH	Forward	CAAGGCTGAGAACGGGAAGC	194
	Reverse	AGGGGGCAGAGATGATGACC	
Collagen I	Forward	TAAAGGGTCACCGTGGCT	355
	Reverse	CGAACCACATTGGCATCA	
Collagen II	Forward	GGATGGCTGCACGAAACATACCGG	157
	Reverse	CAAGAAGCAGACCGGCCCTATG	
Aggrecan	Forward	AGTCACACCTGAGCAGCATC	147
	Reverse	AGTTCTCAAATTGCATGGGGTGTC	
Sox 9	Forward	CTGAGCAGCGACGTCATCTC	72
	Reverse	GTTGGGCGGCAGGTACTG	

4.1.2.7 Quantification of collagen based on hydroxyproline assay On culture day 28, the collagen content of 3D constructs (n = 4 per group) was estimated by hydroxyproline quantification. The constructs were digested with papain (Sigma-Aldrich) at 60°C overnight. After treatment with 4N sodium hydroxide, the samples were heated to 120 °C for 20 min, and then neutralized with 4N hydrochloric acid. The samples were then oxidized with chloramine-T at room temperature for 20 min, and reacted with Ehrlich's reagent at 65°C for 20 min, following which A_{550} of each sample was measured spectrophotometrically. Hydroxyproline contents were calculated based on a calibrated standard curve.

4.1.2.8 Quantification of glycosaminoglycan (GAG) On culture day 28, the sulfated GAG (sGAG) content of 3D constructs (n = 4 per group) was determined. Papain-digested samples (see above) were reacted using a Blyscan Glycosaminoglycan Assay Kit (Biocolor Ltd, Carrickfergus, United Kingdom) according to the manufacturer**'**s protocol. Dilutions of provided

chondroitin 4-sulfate were used to generate a standard curve. The Blyscan dye reagent, containing 1,9-dimethylmethylene blue (DMMB), binds proportionately to the sGAG in the sample. Absorbance of each sample was measured at 656 nm with a spectrophotometer, and the sGAG contents of 3D constructs were calculated from the standard curve.

4.1.2.9 Statistical analysis Statistical analysis was performed using analysis of variance (ANOVA) followed by post-hoc testing for DNA contents, qPCR, and quantification of hydroxyproline and GAG synthesis. The results are presented as mean ± SD. The data were analyzed with SPSS 21.0 (IBM SPSS, Chicago, IL) and significance was set at $p < 0.05$.

4.1.3 Results

4.1.3.1 Decellularization of mECM Decellularization after Triton X-100 and subsequent nuclease treatment was verified by the absence of cell nuclei using DAPI staining (**Figure 21A-D**). Also, the DNA contents of meniscal tissues from both the inner or outer regions were significantly reduced by Triton X-100 and subsequent nuclease treatment, compared to that of original meniscal tissues (native *versus decellularized* inner meniscus: 168±87 ng/mg versus 22±15 ng/mg, p=0.0056; native *versus* decellularized outer meniscus: 133±40 ng/mg *versus* 12±7 ng/mg, p=0.0004 (**Figure 21E**).

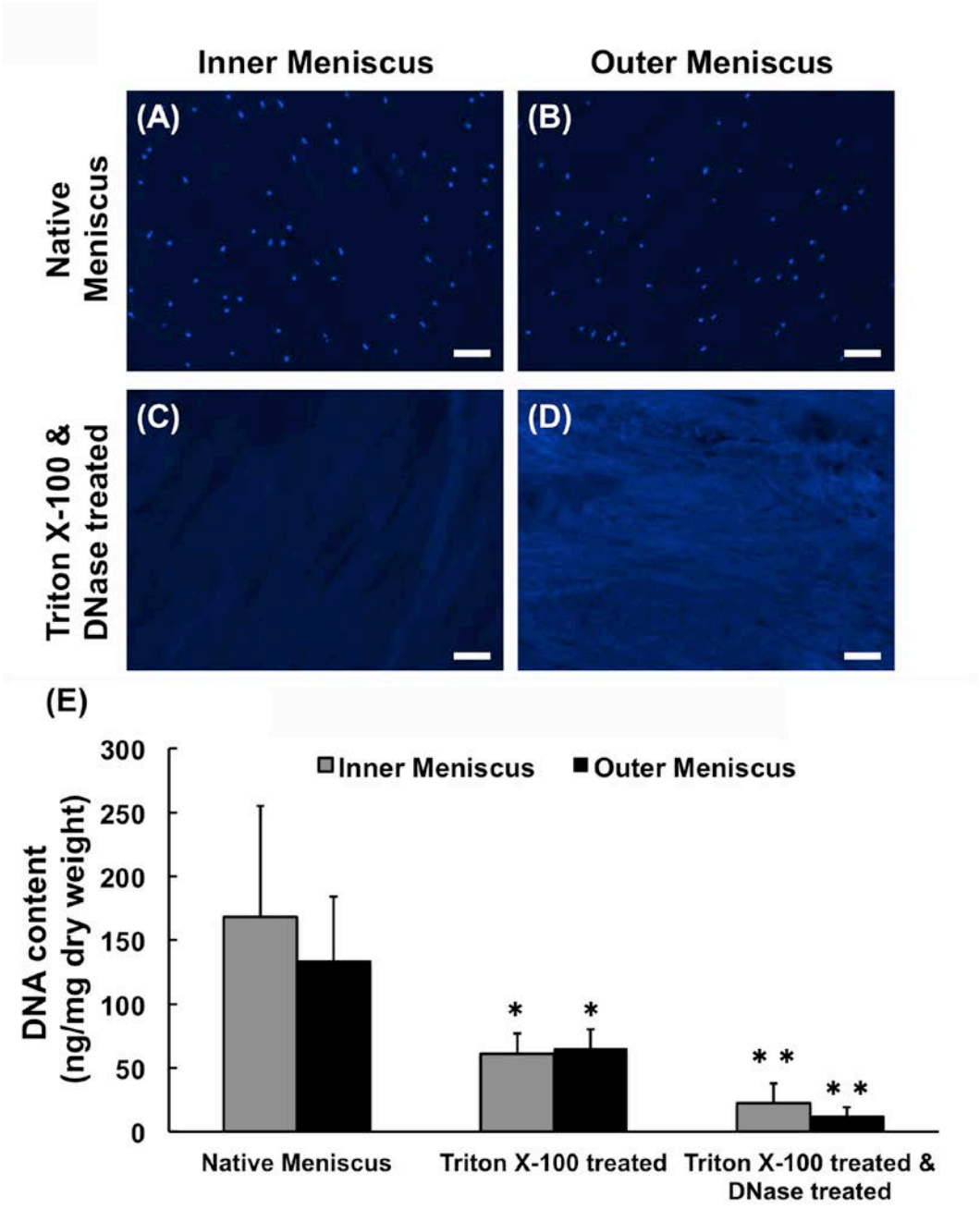

Figure 21. Preparation of decellularized mECM. DAPI staining of meniscal tissues from inner region (A, C) and outer regions (B, D). Meniscal tissues in both groups (A, B) were successfully decellularized after sequential treatment with Triton X-100 and subsequent nuclease digestion (C, D). Scale bar = 100 μm. Also, DNA contents of meniscal tissues in both groups were

substantially reduced by combined Triton X-100 and nuclease treatment (E). *, $p<0.05$; **, $p<0.01$.

4.1.3.2 Extraction of mECM After the decellularization process, the extraction of water-soluble mECM with urea was verified by the BCA assay, in which the amount of total protein was stably obtained at > 600 μg/ml. Based on these results, we set the concentration of mECM at 60 ug/ml for the production of 3D constructs based upon the 10% v/v supplementation ratio used in our previous study on soluble tendon ECM.[115]

4.1.3.3 Cell viability Live/Dead assay demonstrated that high percentages of viable cells were seen on day 1 in each group (control, 90.5%±4.5%; inner, 87.1%±6.9%; and outer, 79.4%±2.0%) (**Figure 22A,C**), indicating that the mECM solution was non-toxic to cells. After 7 days of culture, cells continued to retain a high rate of viability in each group (control, 93.5%±1.0%; inner, 91.7%±4.5%; and outer, 88.2%±8.2%) (**Figure 22B, C**).

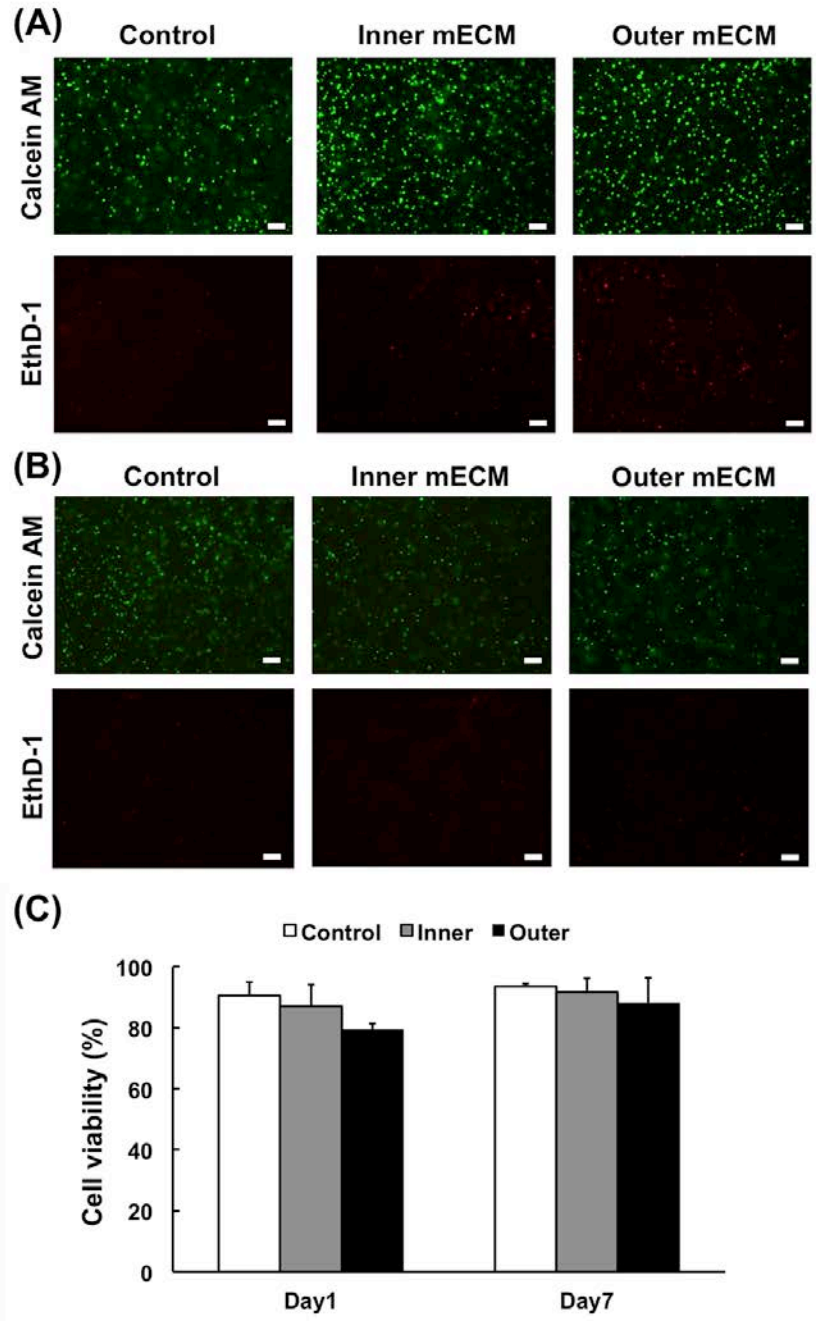

Figure 22. Viability of hBMSCs seeded in mECM-enhanced hydrogels. Live/Dead cell viability staining (green, live cells; red, dead cells) showed a high percentage of viable cells in all culture groups (control, inner ECM, and outer ECM) on culture day 1 (A) and day 7 (B). Scale bar = 100 μm. (C) Quantification of cell viability. A high percentage of viable cells was seen in all groups.

4.1.3.4 Expression profiles of meniscus-associated genes qPCR showed that supplementation with mECM increased the relative level of collagen type I mRNA on culture day 7, with the outer mECM group producing a higher level of collagen type I than the inner mECM group (9.8±6.0 *versus* 5.2±1.2, p=0.0378) and the control group (9.8±6.0 *versus* 1.0±0.78, p=0.0033) (**Figure 23A**). On the other hand, the level of collagen type II mRNA in the inner mECM group was significantly higher than that in the outer mECM group (3.1±1.1 *versus* 1.4±0.52, p=0.0092) and control group (3.1±1.1 *versus* 1.0±0.18, p=0.0019) at day 7 (**Figure 23B**). Similar to the expression of collagen II, the level of aggrecan mRNA in the inner mECM group was significantly higher than that in the outer mECM group (2.6±0.52 *versus* 1.8±0.33, p=0.0308) and control group (2.6±0.52 *versus* 1.0±0.16, p=0.0006) at day 3, and remained higher than the control group (3.0±1.5 *versus* 1.0±0.24, p=0.0159) by day 7 (**Figure 23C**). Finally, the mRNA level of Sox9 was significantly increased in both inner (2.3±0.59 *versus* 1.0±0.35, p=0.0070) and outer mECM group (2.6±0.15 *versus* 1.0±0.35, p=0.0028) at day 3, compared with control group, and then decreased to a similar level to the control group at day 7 (**Figure 23D**).

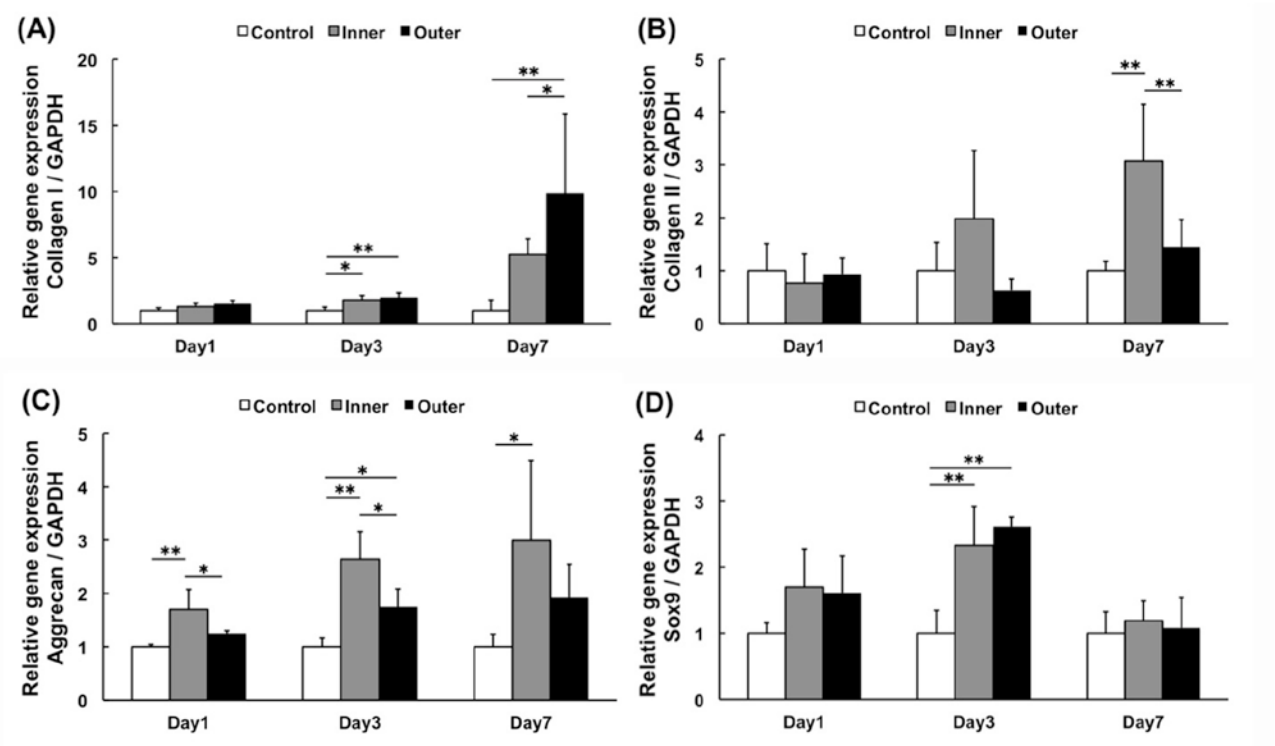

Figure 23. The effect of mECM on gene expression. Expression of meniscus-associated genes in chondrogenic cultures of hBMSC-seeded hydrogel constructs analyzed by real time qPCR at days 1, 3, and 7. (A) Collagen type I, (B) collagen type II, (C) aggrecan, and (D) Sox9. Note that collagen type I expression was significantly higher in the outer mECM group, while the expression of collagen type II and aggrecan in the inner mECM group was significantly higher than in other groups. *, $p<0.05$; **, $p<0.01$.

4.1.3.5 Quantification of hydroxyproline and GAG synthesis Supplementation with mECM increased hydroxyproline content, which was higher in the outer mECM group compared with the inner mECM group (21.7±5.9 μg/culture *versus* 12.5±3.3 μg/culture, p=0.0408) and control group (21.7±5.9 μg/culture *versus* 7.0±3.7 μg/culture, p=0.0029) (**Figure 24A**) on day 28. At the same time, increases in GAG content were also observed upon treatment with mECM, with both inner (21.8±6.1 μg/culture versus 6.7±3.8 μg/culture, p=0.0131) and outer mECM groups

(20.4±7.0 μg/culture versus 6.7±3.8 μg/culture, p=0.0214) being significantly higher than that of the control group (**Figure 24B**).

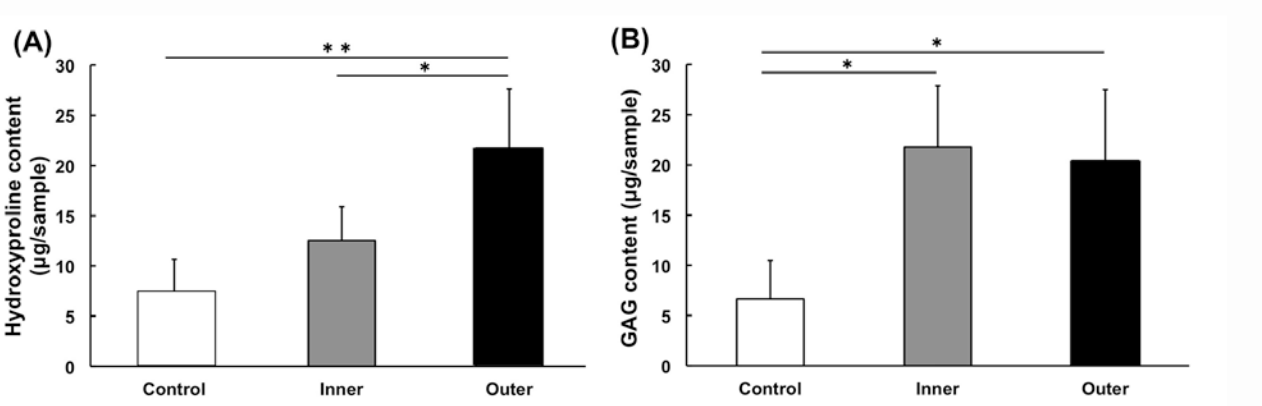

Figure 24. The effect of mECM on hydrogel biochemical composition. Collagen (hydroxyproline) and GAG contents in long-term chondrogenic cultures of hBMSC-seeded hydrogel constructs at day 28. (A) Hydroxyproline content in the outer mECM group was significantly higher than that of other groups. (B) GAG content in the inner and outer mECM groups were both significantly higher than that of the control group. *, $p<0.05$; **; $p<0.01$.

4.1.4 Discussion

The findings reported here demonstrated that 3D constructs produced using hBMSCs seeded in a photocrosslinked hydrogel scaffold and treated with the chondrogenic agent, TGF-β3, actively responded to treatment with mECM. Exposure to mECM did not compromise cell viability and resulted in long-term gain in collagen and GAG production. Interestingly, inner and outer regions of the meniscus appear to produce ECM with different compositions. Gene expression analysis of genes showed that supplementation with inner mECM increased the mRNA

expression level of collagen type II and aggrecan, associated with a cartilaginous phenotype, as well as Sox 9, a transcription factor associated with chondrogenic induction. On the other hand, the supplementation with outer mECM more strongly increased the mRNA expression level of collagen type I. In addition, collagen (hydroxyproline) content was highest in the outer mECM group, while sGAG content was equally elevated by both mECM groups, compared to control. Based on these findings, we concluded that inner mECM enhances fibrocartilaginous differentiation of hBMSCs, while outer mECM promotes a more fibroblastic phenotype.

Although the importance of preserving the meniscus for optimal knee joint function is well recognized,[246,259-261] meniscectomies remain the gold standard for meniscal tears given the poor intrinsic healing capacity of the meniscus.[244,262] Therefore, a new therapeutic method for meniscal repair or regeneration with high clinical relevance is urgently necessary. Nevertheless, meniscal regeneration has remained highly challenging. It is technically difficult to artificially reproduce meniscal structure because of the highly complex biochemical and anatomical features of the meniscus.[255] In particular, the meniscus is known to exhibit regional structural, biochemical, and cellular differences between its fibrocartilaginous inner and fibroblastic outer zones.[253,255] In this study, we have successfully extracted water-soluble mECM, similar to recent work on tendon ECM,[115] and demonstrated that the application of both inner and outer mECM to meniscal tissue engineering could contribute to the production of such biphasic meniscal structure, correspondent with previous morphological and biological studies.[253-255]. Taken together, these results suggest the feasibility of fabricating bioactive scaffolds using region-specific meniscus ECM preparations for meniscus tissue engineering, which may have significant clinical relevance.

A number of meniscal implants have recently been developed, and some of them are already used in clinical practice.[263-267] These implants are commonly monophasic implants that do not take into account the differences between the inner and outer regional structural and biological properties as mentioned above, although the consideration of these regional differences should be critical for complete meniscus regeneration. We believe that zonal regeneration of inner and outer regions is needed to improve repair quality, i.e., engineered implants should be fabricated such that the inner and outer regions are already pre-arranged and pre-formed in a structurally relevant manner.

Recent work of tendon-derived ECM (tECM) revealed that soluble tECM isolated from bovine tendons contains not only collagen but also numerous low molecular-weight, non-collagenous proteins, including fibronectin, fibromodulin, biglycan and decorin, all of which are known to regulate MSC behavior.[115] Considering the structural and compositional similarities between tendons and menisci, it is likely that the cocktail of low molecular-weight, non-collagenous components derived from mECM may serve important signaling activities to promote meniscal morphogenesis in a regional specific manner. While identification of the numerous proteins comprising the mECM extracts was beyond the scope of the study, it is likely that unique combinations of growth factors found in each are responsible for directing the noted region-specific differentiation of hBMSCs. Equally plausible, components of the mECM extract may bind to cell adhesion receptors (e.g., integrins) and/or modify growth factor receptor activity (e.g., TGF-β receptor) to modulate the specific bioactivity of exogenous growth factors added as medium supplements. Future studies will explore both the composition of mECM extracts and the mechanisms underlying their region-specific effects.

Decellularized ECM scaffolds have been previously applied as regenerative medicine strategies for tissue and organ replacement, and some of them, including ECM products derived from dermis, urinary bladder, small intestine, mesothelium, pericardium, and heart valves, are already used in clinical practice.[6] Numerous decellularization techniques have been explored (e.g., chemical, enzymatic, and physical), the optimal combination of which depends on the tissue cellularity and structure.[115,268-270] Successful decellularization has been defined as <50 ng dsDNA per mg ECM dry weight and lack of visible nuclear material in tissue sections stained with DAPI or H&E.[6] Our decellularization technique, combining a detergent and nucleases, significantly reduced the DNA content and showed the absence of cellular nuclei by DAPI staining. Therefore, it should be considered as a suitable technique for meniscal decellularization.

Our findings suggest that inner and outer mECM preparations may be applied, e.g., using PEG-based hydrogel, in a regionally defined manner, to engineer a meniscus-like tissue that mimics the anatomy and biochemistry of native meniscus. With recent advancements of scaffold fabrication techniques, including 3D printing,[258,271] we are working to combine region-specific mECM with printable polymers to fabricate an anatomic meniscus substitute. To that end, hBMSCs could be homogenously distributed within a meniscus-shaped hydrogel with subsequent adoption of a region-appropriate cell phenotype guided by the surrounding mECM extract. Ultimately, we hope to leverage this technology to develop novel grafts and/or in situ biologics capable of enhancing meniscus healing and preserving joint health.

In order to achieve these future directions, several limitations of the present study must be addressed. First, we did not perform biomechanical testing on the constructs. Sufficient mechanical integrity will be necessary to achieve sustained integration within the joint,

especially with progressively increasing weight-bearing activities. Secondly, cell differentiation was evaluated principally by analysis of gene expression, which may differ from changes in protein translation. While biochemical assays (i.e., hydroxyproline and sGAG content) demonstrated changes that were broadly congruent with mECM-mediated changes in gene expression, future studies will include Immunohistochemical staining and/or Western Blotting to confirm parallel changes in protein production. As mentioned above, additional investigation is underway to determine compositional differences between mECM extracts that may account for the region-specific bioactivities. At the same time, it is important to consider the age of the ECM source. Tottey et al.[170] and Sicari et al.[272] have shown that the age of the animal from which ECM biomaterials are derived can have significant effects on in vitro stem cell behavior and in vivo wound healing, respectively. While similar studies have not been performed using meniscal ECM as a biomaterial, other studies have shown that the phenotype of ECM changed as part of meniscal degenerative changes with aging.[273,274] For these reasons, mECM of this study was derived from young, adult cows without macroscopic evidence of joint injury or degeneration. Whether use of tissues from younger animals would provide greater biologic effect is a subject of ongoing research.

4.1.5 Conclusions

In conclusion, mECM represents a highly bioactive tissue extract that promotes differentiation towards region-specific cell phenotypes. Using a 3D hBMSC-based hydrogel construct in vitro, the inner mECM was found to enhance fibrocartilaginous differentiation, while the outer mECM promoted a more fibroblastic phenotype. Taken together, these results suggest the feasibility of

fabricating bioactive scaffolds using region-specific meniscus mECM preparations for meniscus tissue engineering.

4.2 REGION-SPECIFIC BIOACTIVITY OF SOLUBLE INNER AND OUTER MENISCAL-DERIVED EXTRACELLULAR MATRICES IN PHOTOCURABLE METHACRYLATED GELATIN (GELMA) HYDROGELS

4.2.1 Introduction

The menisci of the knee, crescent-shaped fibrocartilaginous tissues interposed between the articular surfaces of the femur and tibia, must resist compressive, tensile, and shear forces in order to efficiently distribute tibiofemoral contact stresses and maintain joint health.[51,275] As with other musculoskeletal tissues, the complex structure of the meniscus imparts a unique function, allowing the meniscus to facilitate efficient articulation of the tibiofemoral joint. A gradient of decreasing collagen type II and proteoglycan content exists when moving from inner meniscal regions towards the periphery, while the outer region is principally composed of aligned type I collagen fibers capable of resisting hoop stresses arising from joint loading.[53-55,276] The region-specific differences in ultrastructure and biochemical composition correspond to differences in cell phenotype; inner meniscal cells possess a round morphology reminiscent of articular chondrocytes while cells of the outer meniscus are found between aligned collagen fibers, similar to fibroblasts of tendon or ligament.[51,275] Similarly, cells of the inner region express higher levels of collagen type II and aggrecan while cells of the outer region express greater collagen type I.[56]

Given the rapid onset of joint degeneration experienced with the loss of meniscal function,[57,277] coupled with the limited availability and narrow inclusion criteria associated with meniscal allograft transplantation, tissue engineers have sought to develop novel biomaterials to serve as a meniscus substitute.[278] Decellularized menisci derived from animal sources have been explored, as the removal of cellular material could mitigate any adverse immune response while preservation of tissue ultrastructure and biochemical composition could maintain meniscal function and promote region-specific differentiation of infiltrating host cells. However, the dense collagenous extracellular matrix of native menisci necessitates relatively harsh decellularization protocols with resulting losses in proteoglycan content and the associated compressive moduli of inner meniscal regions.[94,279] Despite these alternations in ultrastructural and biochemical properties, infiltration of seeded cells is still limited.[86,93]

Enzymatic digestion (e.g., pepsin) of decellularized meniscus extracellular matrix can produce a thermoresponsive hydrogel capable of delivering exogenous cells to a meniscal lesion while theoretically retaining meniscus-specific bioactive motifs capable of directing fibrocartilaginous neotissue formation.[109] However, Lin et al.[114] reported that pepsin digestion of extracellular matrices offered negligible advantage over collagen type I in terms of promoting proliferation, migration, and multilineage differentiation of mesenchymal stem cells (MSCs). Conversely, a urea-soluble fraction of ECM has been demonstrated in several studies to promote differentiation of MSCs towards tissue-specific (i.e., homologous) phenotypes.[113-115] Most recently, we demonstrated that urea-soluble extracts of the inner and outer meniscus ECM could promote region-specific gene expression of MSCs seeded in a photocrosslinked polyethylene glycol diacrylate (PEGDA) hydrogel (**Section 4.1**). Expanding on these findings, this study explores the effect of urea-soluble extracts of the inner and outer meniscus ECM in promoting

fibrochondrogenic differentiation of MSCs seeded in a visible light (VL) photoinducible methacrylated gelatin (GelMA) hydrogel. GelMA hydrogels have been shown to support robust chondrogenesis of encapsulated MSCs[134] while the use of a VL-activated photoinitiator obviates concerns of UV light-induced mutagenesis or cytotoxicity.[280] We hypothesized that the ECM extracts would promote region-specific cell phenotypes, with the inner and outer ECM extracts respectively enhancing chondrogenic and fibrochondrogenic differentiation of MSCs seeded in GelMA hydrogels.

4.2.2 Methods

4.2.2.1 Overview of experimental design Urea-soluble extracts from the decellularized ECM of inner and outer regions of juvenile bovine menisci were isolated and characterized. The biological effects of ECM extracts on human bone marrow MSCs were evaluated in both 2D and 3D in vitro cultures. MSCs were cultured on 2D plastic in the presence of ECM-supplemented media; assays for cell morphology, metabolism, and gene expression were performed up to 7 days. Additionally, MSCs were cultured in ECM-enhanced GelMA hydrogels for up to 42 days to determine the region-specific bioactivity of the ECM extracts, as evaluated by measures of gene expression, histology, immunohistochemistry, biochemical composition, and mechanical properties.

4.2.2.2 ECM decellularization Menisci were procured from hindlimbs of 6-8 week old cows (Research 87, Boylston, MA) and stored in a protease inhibitor solution (phosphate-buffered saline, 1X PBS; 5 mM ethylenediaminetetraacetic acid, EDTA; 0.5 mM phenylmethylsulfonyl fluoride, PMSF) at -20°C until use. Once thawed, menisci were halved,

coarsely minced (**Figure 25A-C**), and decellularized by adapting a previously established method.[115] Briefly, 4 g of minced tissue was agitated for 24 hours at 4°C in 40 ml of protease inhibitor solution containing 1% Triton X-100 (Sigma-Aldrich, St. Louis, MO, USA), followed by 3 washes (30 minutes each at 4°C) in 1X PBS. Subsequently, 40 ml of Hanks Buffered Salt Solution (HBSS, Thermo Fisher Scientific, Pittsburgh, PA, USA) supplemented with 200 U/ml DNase and 50 U/ml RNase (Worthington, Lakewood, NJ, USA) was added to the tissue, with continuous agitation for 12 hours at room temperature. The tissue was washed six times in 1X PBS, as above, before freezing and subsequent lyophilization. Native and decellularized tissues were evaluated for histological appearance, cellular content, and biochemical composition, including total collagen and sulfated glycosaminoglycan (sGAG) content, as described below.

4.2.2.3 Histology of native and decellularized ECM Native and decellularized tissues were fixed in 10% phosphate-buffered formalin, serially dehydrated, embedded in paraffin, and then sectioned (6 μm thickness) with a microtome (Leica RM2255, Leica Biosystems, Buffalo Grove, IL, USA). Samples were rehydrated and stained with haematoxylin & eosin (H&E, Sigma-Aldrich) or 4',6-diamidino-2-phenylindole, dilactate (DAPI, Life Technologies, Carlsbad, CA, USA). H&E-stained samples were photographed using an Olympus SZX16 stereo microscope while DAPI-stained sections were visualized with an Olympus CKX41 inverted microscope using fluorescent excitation at 405 nm.

4.2.2.4 Biochemical composition of native and decellularized ECM To determine the biochemical composition of native and decellularized tissues, dry samples were digested overnight at 65°C at a concentration of 10 mg/ml in a digestion buffer (pH 6.0) containing 2%

papain (v/v, from Papaya latex, Sigma-Aldrich), 0.1 M sodium acetate, 0.01 M cysteine HCl, and 0.05 M EDTA. The pH was then adjusted to 7.0 through addition of concentrated NaOH. sGAG content was quantified with a Blyscan Assay according to the manufacturer's instructions (Biocolor, Carrickfergus, United Kingdom). dsDNA content was determined using the Quant-iT Picogreen dsDNA assay (Life Technologies). Total collagen was determined using a modified hydroxyproline assay. Briefly, 200 μL of each sample was hydrolyzed with an equal volume of 4 N NaOH at 121°C for 75 min, neutralized with an equal volume of 4 N HCl, and then titrated to an approximate pH of 7.0. The resulting solution was combined with 1.2 mL chloramine-T (14.1 g/L) in buffer (50 g/L citric acid, 120 g/L sodium acetate trihydrate, 34 g/L NaOH, and 12.5 g/L acetic acid) and allowed to stand at room temperature for 30 min. The solution was then combined with 1.2 mL of 1.17 mM p-dimethylaminobenzaldehyde in perchloric acid and placed in a 65°C water bath for 20 minutes. 200 μL of each sample was added to a clear 96-well plate, in duplicate, and absorbance at 550 nm was read. PureCol bovine collagen (3.2 mg/ml, Advanced Biomatrix, Carlsbad, CA, USA) was serially diluted to provide a standard curve ranging from 0 to 1000 μg/ml.

4.2.2.5 Solubilization of decellularized ECM Decellularized tissues were cryomilled into a fine powder (Spex Freezer Mill 8670, Metuchen, NJ, USA) and urea-soluble extracts of the decellularized ECM of inner and outer meniscal regions were obtained using a previously described method (**Figure 25D-F**).[115] Briefly, 4 g of wet decellularized ECM powder was agitated for 3 days at 4°C in 40 mL of 3 M urea dissolved in water. The suspension was centrifuged for 20 minutes at 1500g and the supernatant was transferred to benzoylated tubing (Sigma-Aldrich) and dialyzed against ddH_2O for 2 days at 4°C, changing the water every 8

hours. The dialyzed ECM extract was transferred to centrifugal filter tubes (3000 MWCO; EMD Millipore, Billerica, MA, USA) and spin-concentrated approximately 10-fold at 1500g for 60 minutes. The final ECM extract was filter-sterilized through a PVDF syringe filter unit (0.22 μm; EMD Millipore). Protein concentration was determined by BCA assay (Thermo Fisher Scientific) and aliquots of 1000 μg/ml were stored at -80°C until further use. Before use in experimental studies, aliquots prepared from three different batches were pooled.

In preliminary studies, decellularized ECM was alternatively solubilized by pepsin digestion using an established protocol.[104,150] In particular, ECM powders were enzymatically digested in a solution of 1 mg/mL porcine pepsin (Sigma-Aldrich) in 0.01 N HCl for 48 hours at room temperature under continuous stirring. The resulting ECM slurries (**Figure 25F**) were neutralized by addition of one-tenth digest volume of 0.1 N NaOH and one-ninth digest volume of 10X PBS, then further diluted by addition of 1X PBS. These pepsin-solubilized ECM hydrogels (i.e., imAP, omAP) were principally composed of collagen (**Figure 25G,H**) and were inferior to urea-soluble extracts in promoting cell proliferation and fibrochondrogenic differentiation (data not shown); they were therefore excluded from additional experiments.

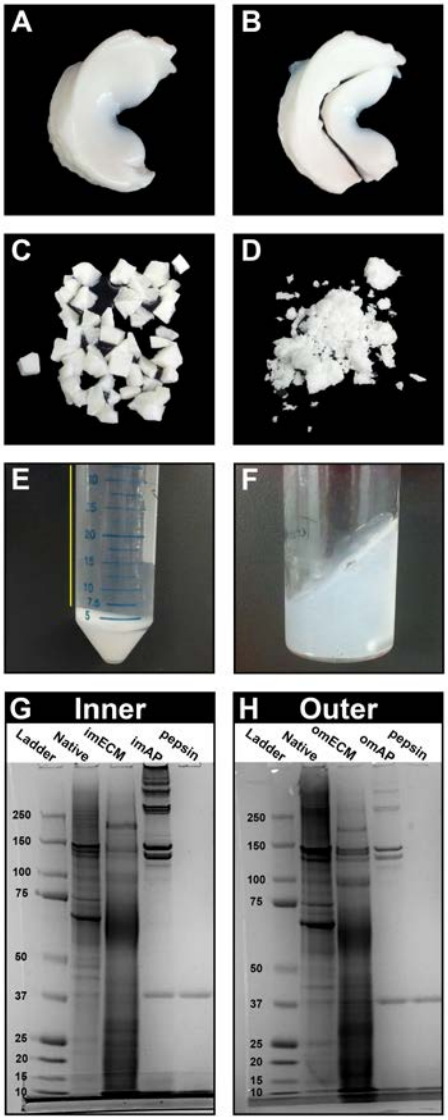

Figure 25. Solubilization of ECM from inner and outer meniscus. (A) Whole menisci were obtained from 6-8 week old cow hindlimbs, (B) halved, and (C) manually minced (8-27 mm^3). Following decellularization, (D) tissues were cryomilled and soluble fractions were obtained either by (E) urea-extraction (supernatant was retained, yellow line) or (F) acid-pepsin digestion. SDS-PAGE of (G) inner meniscus and (H) outer meniscus tissues and soluble preparations demonstrate that urea extraction retained low- and moderate-weight proteins while pepsin digestion yielded mostly collagen.

4.2.2.6 SDS-PAGE and growth factory analysis of ECM Dry samples of native inner and outer meniscus ECM, and their corresponding urea-soluble and pepsin-digested extracts were suspended in TM buffer (Total Protein Extraction Kit, EMD Millipore). 30 μg total protein was mixed with LDS loading buffer and reducing agent (NuPAGE; Life Technologies, Carlsbad, CA, USA) and heated for 10 minutes at 70°C. Protein was loaded into a pre-cast 10-well NuPAGE 4-12% Bis-tris Minigel (Life Technologies) and separated by electrophoresis in MOPS running buffer for 50 minute at constant 200V. The gel was washed several times in water and photographed using a CCD camera gel imaging system (FOTODYNE, Hartland, WI, USA).

Additionally, the growth factor contents of the urea-soluble extracts of the inner meniscus (imECM) and outer meniscus (omECM) were measured using a Human Growth Factor Array (RayBiotech, Norcross, GA), according to the manufacturer's instructions.

4.2.2.7 Bioactivity of meniscus ECM extract in 2D culture Human bone marrow MSCs were obtained as previously described.[114] All experiments were performed with passage 3 (P3) MSCs pooled from 3 patients (31 year old female, 42 year old male, 44 year old male) undergoing total hip arthroplasty with Institutional Review Board approval (University of Washington and University of Pittsburgh). To determine the effect of ECM extracts on MSC morphology and metabolism, cells were suspended in growth medium (DMEM, 10% FBS, 1% Anti-Anti; Life Technologies) and plated in 6-well culture plates at a density of 1 x 10^3 cells/cm^2. One day following cell seeding, growth medium was replaced with serum-free medium (DMEM, 1% Anti-Anti, 1% Insulin-transferrin-selenium [ITS]; Life Technologies) with or without ECM extract supplementation. There were three media conditions – (1) serum-free control, (2) supplementation with 50 μg/ml imECM, and

(3) supplementation with 50 μg/ml omECM. Media were changed every 2 days. On days 1, 3, and 7, an MTS assay (CellTiter 96® AQ_{ueous} Non-Radioactive Cell Proliferation Assay; Promega, Madison, WI) was performed according to manufacturer's instructions.

To determine the effects of ECM extracts on gene expression, 2 x 10^4 cells/cm^2 were plated in 6-well culture plates and cultured up to 7 days, as described above. On days 1, 3, and 7, total RNA was isolated from cells using an RNeasy Plus Mini Kit (Qiagen, Valencia, CA, USA) and reverse transcribed into cDNA through use of SuperScript III first-strand synthesis kit (ThermoFisher Scientific, Pittsburgh, PA, USA). Quantitative real-time polymerase chain reaction (qPCR) was performed using SYBR® Green master mix (Applied Biosystems, Foster City, CA) on a StepOnePlus Real-Time PCR system (Applied Biosystems). Relative expression of each target was calculated using the $\Delta\Delta C_T$ method with the arithmetic average of GAPDH and r18S expression used as the endogenous reference. For 2D cultures, expression of Sox9, collagen type 2 (Col2), collagen type 1 (Col1), aggrecan (Acan), and Runx2, was analyzed. Additional targets were included for 3D cultures, as described below. Primer sequences are listed in **Supplemental Table 4**. As significant differences across treatment groups were only seen at day 3, expression levels were normalized against day 3 controls.

4.2.2.8 Bioactivity of meniscus ECM extract in 3D GelMA hydrogels Methacrylated gelatin (GelMA) was synthesized as previously described.[134] ECM-enhanced GelMA contained 500 μg/mL of imECM or omECM, whereas controls were supplemented with an equal volume of 1X PBS. MSCs were suspended in the liquid GelMA (8% w/v suspended in HBSS with 0.2% v/v of visible light-sensitive photoinitiator lithium phenyl-2,4,6-trimethylbenzoylphosphinate, LAP) at 15 x 10^6 cells/ml. 50 μL of the cell suspension was distributed to silicone molds measuring 5 mm

diameter x 2 mm depth and exposed to high intensity visible light (450-490 nm) for 2 minutes to induce photogelation. MSC-encapsulated hydrogels were transferred to 6-well plates previously coated with silicone (Sigmacote, Sigma-Aldrich) to prevent cell migration and adhesion onto the plastic surface, and cultured for up to 42 days in full chondrogenic medium (DMEM, 1% Anti-Anti, 10 μg/ml ITS, 0.1 μM dexamethasone, 40 μg/mL proline, 50 μg/mL ascorbate-2-phopshate, 10 ng/mL Transforming Growth Factor β3 [TGF-β3; Peprotech, Rocky Hill, NJ, USA]). Medium was changed every 2-3 days. The MSC-encapsulated hydrogels were collected at various time points and analyses for gene expression, biochemical composition, histology and immunohistochemistry, and compressive mechanical properties.

4.2.2.9 Gene expression and biochemical composition analyses On days 1, 7, 21, and 42, total RNA was isolated from constructs through sequential use of Trizol (Thermo Fisher Scientific) and RNeasy Plus Mini Kit (Qiagen), according to manufacturers' protocols. Reverse transcription and qPCR was performed as described above. Expression of the following gene targets was determined for the 3D constructs – Sox9, Col2, Col1, Acan, Collagen type 6 (Col6), Runx2, cartilage oligomeric matrix protein (COMP), platelet-derived growth factor receptor (PDGFR), tissue inhibitor of metalloproteinase 2 (TIMP2), scleraxis (Scx), tenascin C (Tnc), and fibromodulin (Fmod). Primer sequences are listed in **Supplemental Table 4**. On days 21 and 42, constructs were digested overnight in papain using the protocol described in **Section 4.2.3.4**. Total sGAG and dsDNA contents were determined, allowing subsequent normalization of sGAG by dsDNA.

4.2.2.10 Histological and immunohistochemical analysis Histological sections were prepared on days 21 and 42 using a similar protocol as performed when characterizing the

appearance of native and decellularized meniscal tissues described in Section 4.2.3.3. Following rehydration, samples were stained with Safranin O/Fast Green (Electron Microscopy Sciences, Hatfield, PA USA); nuclei were counterstained with Haemotoxylin. For immunohistochemical staining of collagens type 2 and type 1, antigen retrieval was achieved by incubation of slides for 30 minutes at 37°C in Chondroitinase ABC (100mU/ml, Sigma) and Hyaluronidase (250 U/ml, Sigma) suspended in 0.02% bovine serum albumin (BSA). Endogenous peroxidases were blocked with 3% H_2O_2 (in methanol). Non-specific binding was blocked with 1% horse serum. Samples were then exposed to rabbit anti-human collagen II primary antibody (ab34712; Abcam, Cambridge, MA, USA) diluted 1:400 or rabbit anti-human collagen I primary antibody (ab34710; Abcam) diluted 1:100 in 1% horse serum overnight at 4°C. Equine biotinylated secondary antibody binding, signal amplification, and visualization, were achieved through the use of VectaStain Universal Elite ABC Kit (Vector Laboratories, Burlingame, CA, USA) in accordance with the manufacturer's instructions. Nuclei were counterstained with Haematoxylin QS (Vector).

4.2.2.11 Compressive mechanical testing On day 42 the cylindrical specimens were tested in uniaxial unconfined compression with a Bose Electroforce 3200 series II (resolution 1nm, load cell 1000g) while kept moist in 1X PBS. After a preload of 0.1% strain, samples were compressed at a 0.01mm/s rate reaching a strain of 20% The elastic modulus E was extracted by linear fitting of the final part of the stress-strain curve near the maximum load, as previously described.

4.2.2.12 Statistical analyses Comparisons across multiple conditions or time points were made using a one-way or two-way analysis of variance (ANOVA) with Tukey post-hoc

testing for multiple comparisons. When comparing two conditions, a Student's t-test was performed. Data are presented as mean ± standard deviation. Sample sizes are indicated in figure legends. Statistical significance was considered $p < 0.05$.

4.2.3 Results

4.2.3.1 Characterization of inner and outer meniscal ECM Histological staining confirmed the absence of cell nuclei in both inner and outer meniscal ECM following the decellularization protocol (**Figure 26A-H**), with a corresponding reduction in dsDNA content (**Figure 26I**; Native vs. Decellularized – Inner: 555.1 ± 62.5 ng/mg vs. 7.7 ± 6.2 ng/mg, $p < 0.001$; Outer: 616.3 ± 52.1 ng/mg vs. 11.7 ± 9.4 ng/mg, $p < 0.001$). Decellularized ECM from both inner and outer regions possessed a lower sGAG content than native tissues ($p < 0.001$). However, native and decellularized inner meniscal ECM possessed higher sGAG content (31.7 ± 6.8 μg/mg and 9.7 ± 5.9 μg/mg, respectively) than outer meniscal ECM (10.0 ± 1.7 μg/mg and 1.6 ± 1.0 μg/mg, respectively) at the corresponding step (**Figure 26J**). Conversely, the total collagen content was equivalent between meniscal regions and remained constant following decellularization (**Figure 26K**). As compared to native inner and outer meniscus, imECM and omECM possessed a reduced concentration of high molecular weight proteins, including collagen, but abundant low and moderate weight proteins and/or fragments (**Figure 25G,H**). The growth factor array revealed differences in several proteins when comparing imECM with omECM; notably, basic fibroblast group factor (bFGF) was found only in omECM while TGF-β concentrations were higher in imECM (**Table 2**).

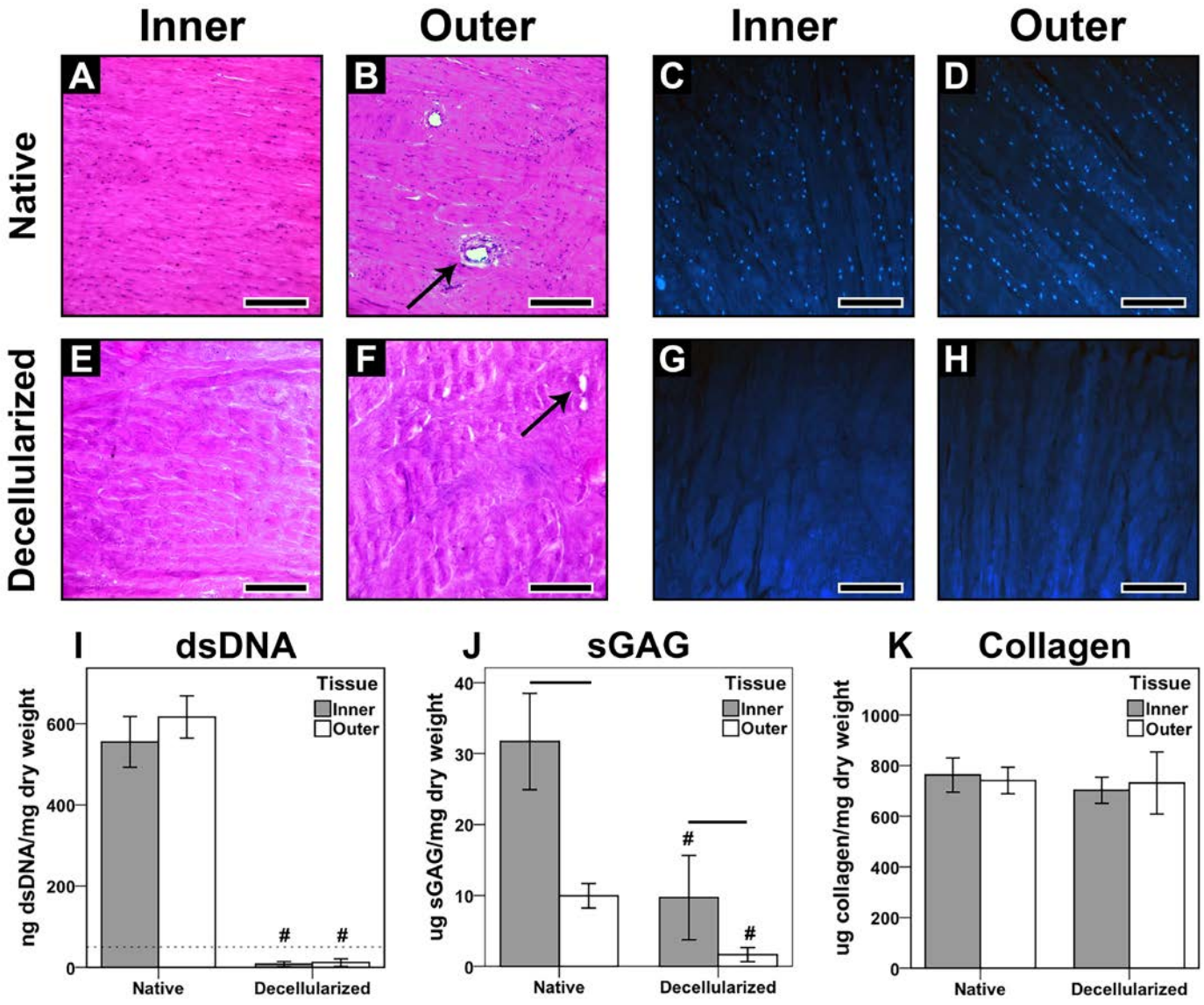

Figure 26. Characterization of native and decellularized meniscus tissue. (A, B) H&E and (C, D) DAPI staining of native inner and outer meniscus, respectively. (E, F) H&E and (G, H) DAPI staining of decellularized tissues. Arrows indicate blood vessels found in outer meniscus (B, F); Scale bar = 500 μm. (I) dsDNA content of native and decellularized meniscus; dotted line at 50 ng/mg is established threshold for sufficient decellularization. (J) sGAG content. (K) Total collagen content. For biochemistry assays, n = 8-10 per condition. # $p < 0.001$, significant difference between native and decellularized tissue from a given region. Lines over bars indicate significant difference between regions for a given step, $p < 0.05$.

Table 2. Growth factor concentrations (pg/mL) in imECM and omECM extracts

Protein	imECM	omECM
bFGF	0.0	362.6
EGF R	3.1	0.0
EG-VEGF	0.1	0.0
IGFBP-4	3.6	0.0
Insulin	0.0	36.6
NT-3	3.4	3.2
OPG	59.0	54.7
SCF	1.8	1.1
SCF R	16.3	0.0
TGFb1	241.7	140.9
TGFb3	29.3	0.0

4.2.3.2 ECM-induced proliferation and differentiation in 2D culture Over a 7 day culture, imECM and omECM enhanced cell proliferation of MSCs as shown through phase contrast microscopy (**Figure 27A-C**) and MTS assay. imECM and omECM supplementation increased cell proliferation equivalently at all time points (**Figure 27D**). On day 3, both imECM and omECM increased expression of Sox9, Col2, and Col1, although statistically significant increases were only achieved with imECM supplementation ($p < 0.05$). Acan and Runx2 expression did not significantly differ across conditions (**Figure 27E**).

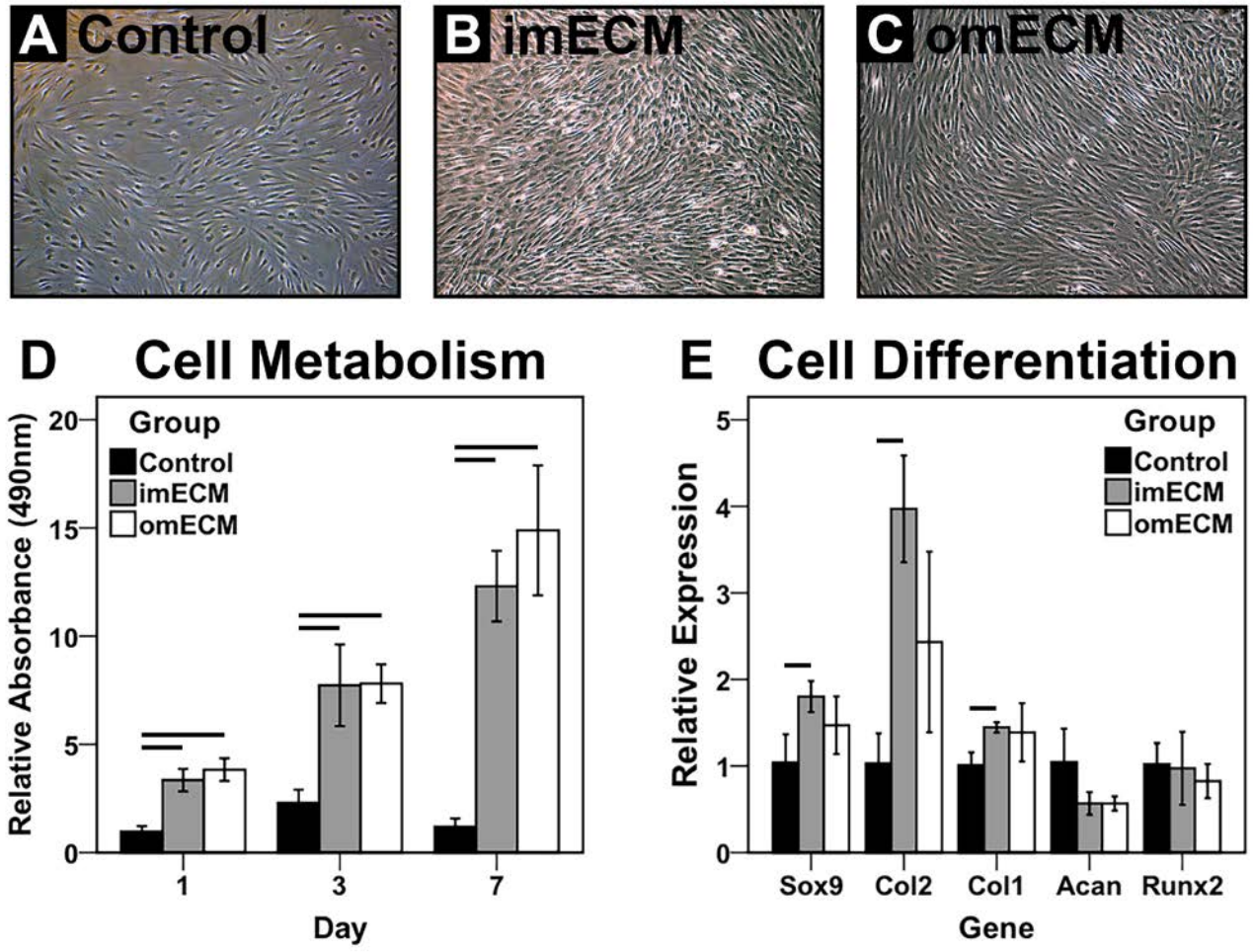

Figure 27. Bioactivity of soluble ECM extracts on MSCs in 2D culture. (A-C) phase contrast microscopy. (D) MTS assay measuring cell metabolism; n = 6-8 per condition; Lines indicate significant difference between groups on given day, $p < 0.05$. (E) Gene expression analysis on day 3; n=3 independent trials, each performed in biological triplicate; Lines indicate significant difference between groups, $p < 0.05$.

4.2.3.3 Gene expression of MSC-seeded hydrogels enhanced with ECM MSC-seeded GelMA hydrogels supported robust upregulation of chondrogenic proteins Col2 and Acan over a 42 day culture, with modest increases in Col1 and Runx2 expression in all groups on days 7 and 21, before returning to baseline on day 42 (**Figure 28**). imECM upregulated Sox9 over controls and omECM on day 1, while both ECM groups were slightly inferior to controls on day 7 before demonstrating equivalency across groups at later time points. Both ECM groups strongly upregulated Col2 expression on day 7, while only imECM supplementation maintained enhanced expression over controls on day 21. Conversely, omECM upregulated Col1 expression on day 1, while both imECM and omECM had significantly reduced Col1 expression on day 21 compared to controls. imECM and omECM increased Acan expression on day 21, but differences were not statistically significant. Col6 expression across all groups was downregulated after day 1, with further reductions induced by omECM on days 7 and 21. Runx2 expression was decreased in omECM and imECM constructs on days 7 and 42, respectively, as compared with controls. Expression of additional genes associated with the fibrochondrocyte and fibroblast phenotype were measured (**Supplemental Figure 8**). ECM supplementation had either a negligible or inhibitory effect on gene expression as compared against controls.

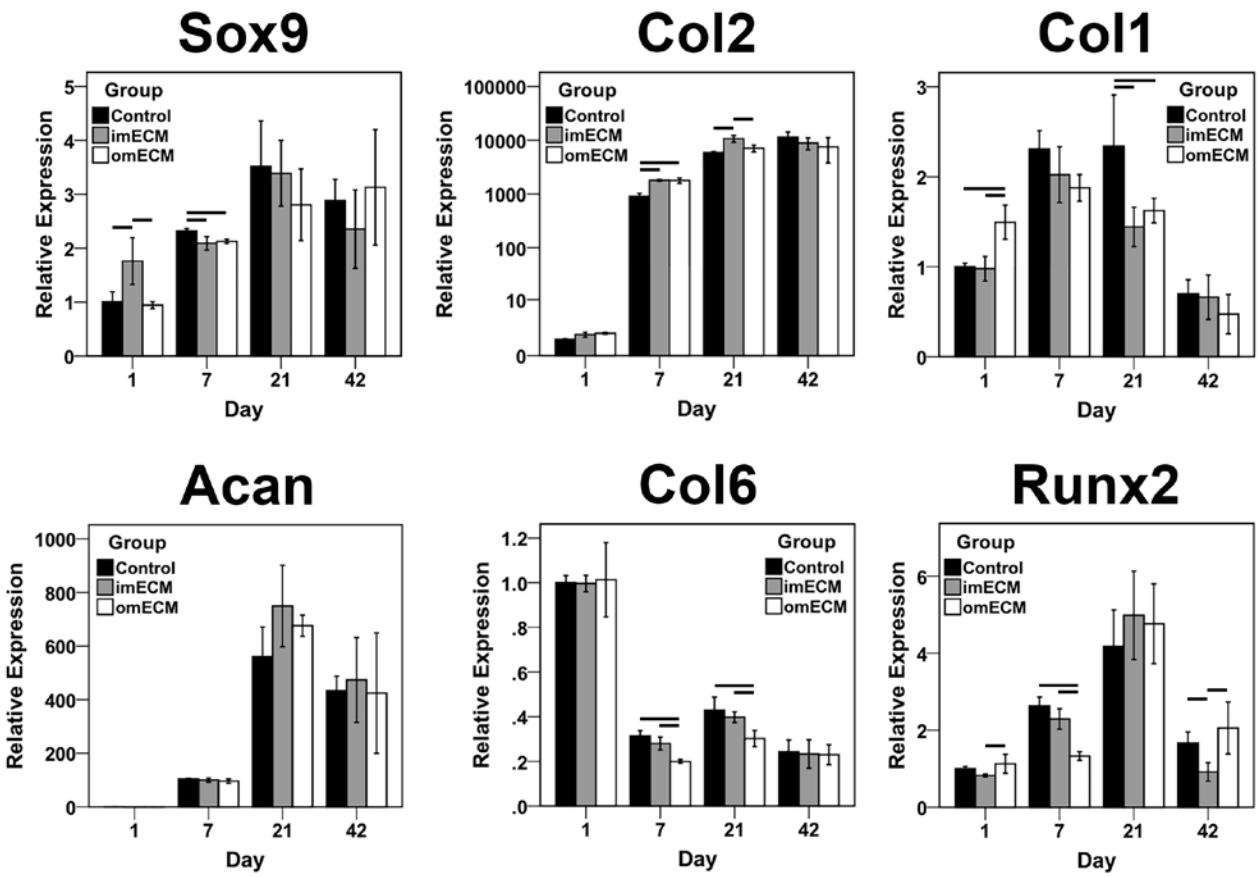

Figure 28. Gene expression in MSC-GelMA constructs. n=3 independent trials, each performed in biological triplicate; Lines indicate significant differences between groups, $p < 0.05$.

4.2.3.4 Immunohistochemical and histological staining of hydrogels At day 21, positive staining for collagen type 2 was found in the pericellular region, with cells near the construct perimeter demonstrating more intense staining (**Figure 29A-F**). ECM-supplemented constructs exhibited greater Col2 deposition, with imECM constructs superior to omECM constructs. By day 42, all groups demonstrated robust Col2 staining distributed throughout the entire construct area (**Figure 29G-L**). Nevertheless, regions of reduced intensity were found between intensely

staining clusters only in Controls, while imECM and omEMC constructs exhibited a more homogenous distribution of intense Col2 staining.

Proteoglycan deposition, as visualized through Safranin O staining, paralleled Col2 staining (**Figure 30**). imECM and omECM constructs showed greater staining on day 21, as compared to Controls, with imECM producing the greatest effect (**Figure 30A-F**). However, by day 42, all constructs showed intense proteoglycan deposition and differences among groups could not be qualitatively appreciated (**Figure 30G-L**). Supplementation of the culture medium with TGF-β3 was essential for such robust anabolic effects. When constructs were cultured in the absence of TGF-β3, no proteoglycan deposition was noted in Controls by day 42 (**Supplemental Figure 9A,F**). Inclusion of imECM and omECM within hydrogels produced a small degree of proteoglycan deposition surrounding the cells (**Supplemental Figure 9B-C, G-H**), but staining intensity was much less that of constructs cultured in full chondrogenic medium (**Figure 30**). Acellular constructs, even with ECM supplementation, were negative for proteoglycan deposition (data not shown), suggesting that imECM and omECM promoting proteoglycan deposition through cell-mediated synthesis.

Immunohistochemical staining for Col1 produced a pattern opposite to that seen for Col2 and proteoglycan (**Figure 31**). In particular, imECM constructs showed the least Col1 deposition on days 21 and 42. Controls and omECM constructs showed comparable Col1 deposition on day 21 (**Figure 31A-F**), but by day 42, Col1 staining intensity was most profound in Controls (**Figure 31G-L**).

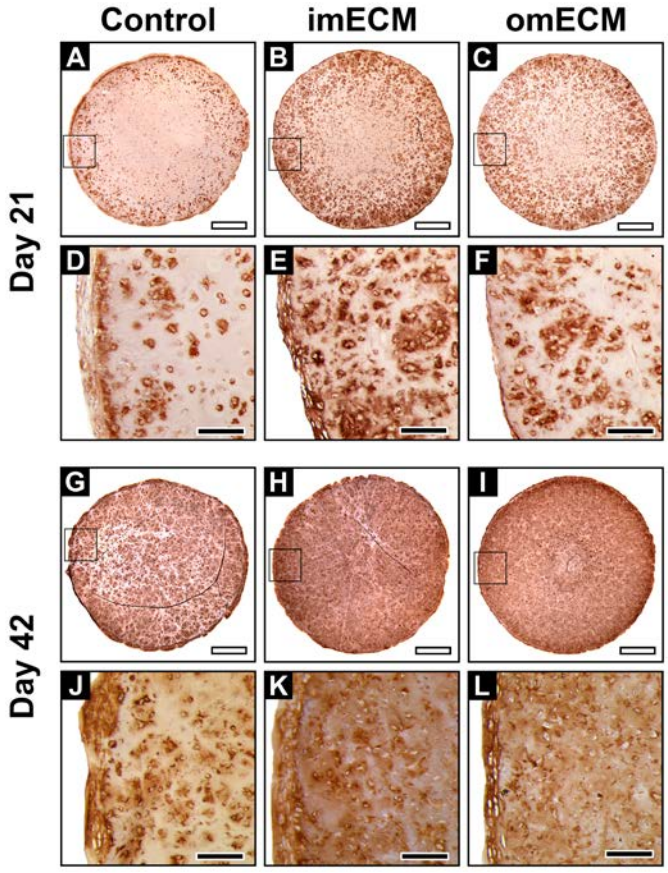

Figure 29. Immunohistochemical staining of collagen type 2. (A-F) Constructs on day 21; (A-C) Low magnification, scale bar = 1 mm; Area of magnification shown by black box; (D-F) High magnification, scale bar = 200 μm. (G-L) Constructs on day 42; (G-I) Low magnification, scale bar = 1 mm; Area of magnification shown by black box; (J-L) High magnification, scale bar = 200 μm.

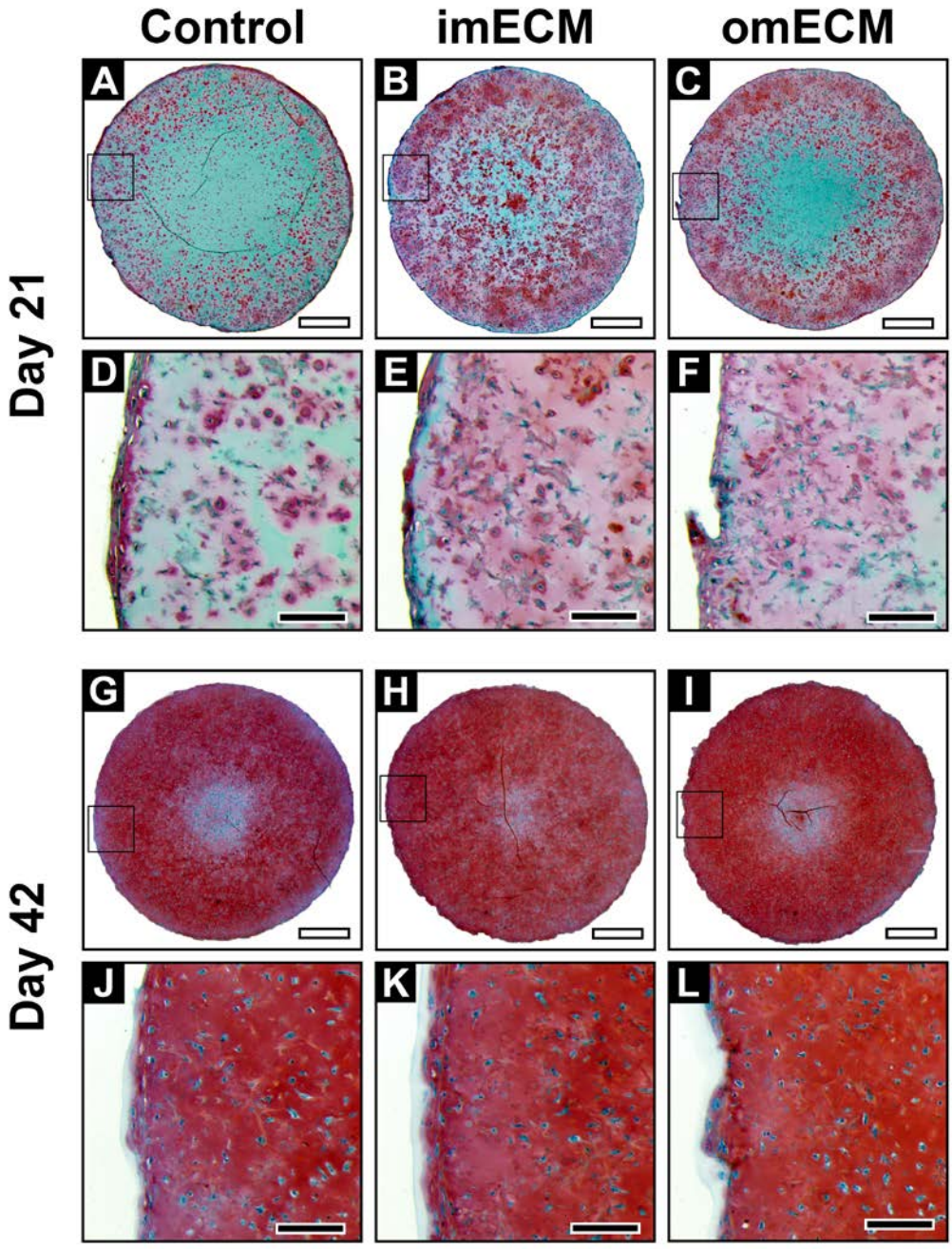

Figure 30. Safranin O staining. (A-F) Constructs on day 21; (A-C) Low magnification, scale bar = 1 mm; Area of magnification shown by black box; (D-F) High magnification, scale bar = 200 μm. (G-L) Constructs on day 42; (G-I) Low magnification, scale bar = 1 mm; Area of magnification shown by black box; (J-L) High magnification, scale bar = 200 μm.

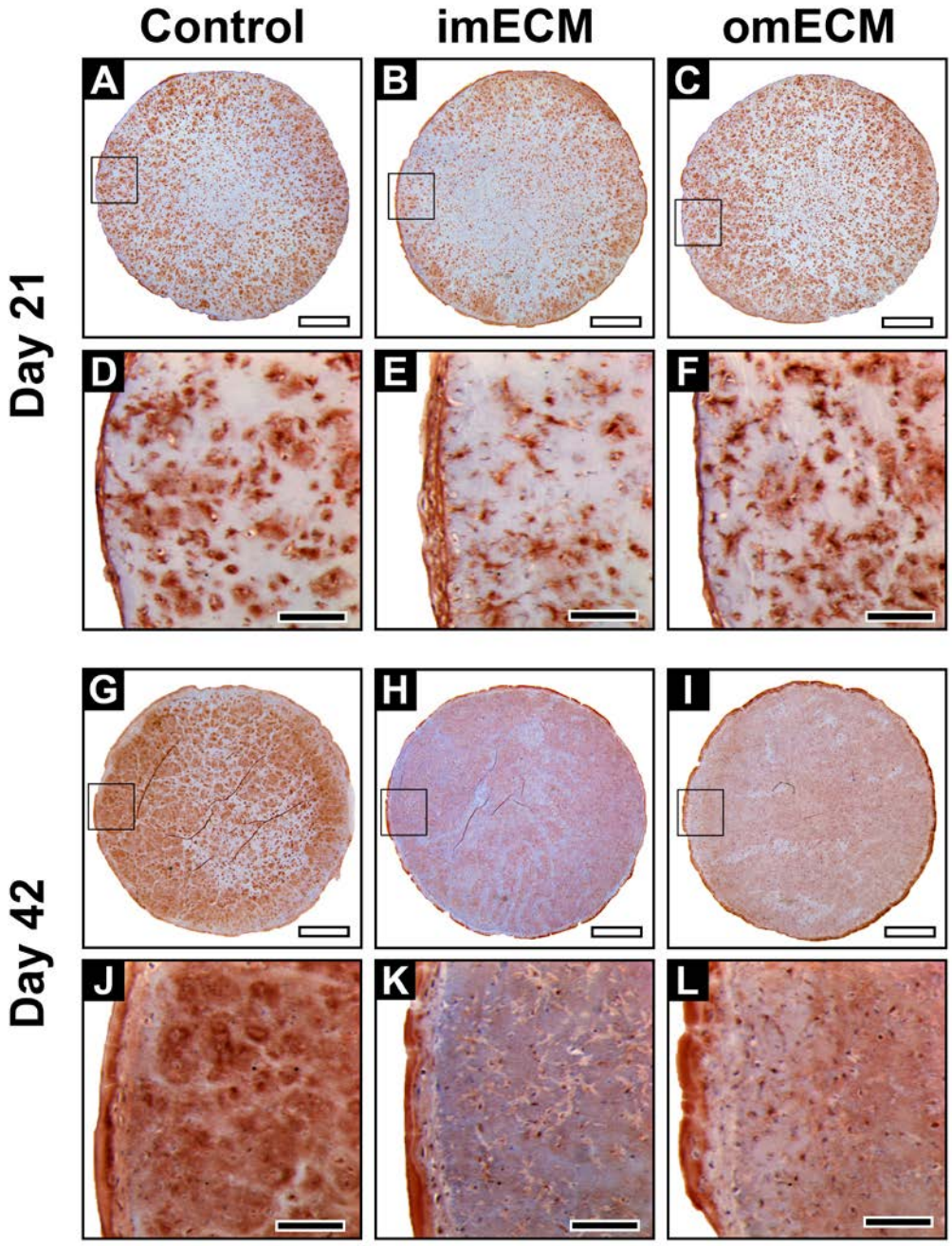

Figure 31. Immunohistochemical staining of collagen type 1. (A-F) Constructs on day 21; (A-C) Low magnification, scale bar = 1 mm; Area of magnification shown by black box; (D-F) High magnification, scale bar = 200 μm. (G-L) Constructs on day 42; (G-I) Low magnification, scale bar = 1 mm; Area of magnification shown by black box; (J-L) High magnification, scale bar = 200 μm.

4.2.3.5 Biochemical composition and compressive moduli of hydrogels The biochemical composition of constructs mirrored the histological findings. Total sGAG content was significantly increased in imECM and omECM constructs on days 21 and 42 (**Figure 32A**), while no significant difference in dsDNA content was found over time or among groups (**Figure 32B**). Nevertheless, when sGAG content was normalized to cellular content, only imECM constructs were significantly elevated over Controls on day 21, while both ECM-supplemented groups were significantly increased by day 42 (**Figure 32C**). Similar to histological findings, acellular constructs possessed negligible sGAG content, even when supplemented with imECM or omECM (data not shown). imECM and omECM constructs trended towards higher compressive moduli than Controls, but these differences were not statistically significant (**Figure 32D**).

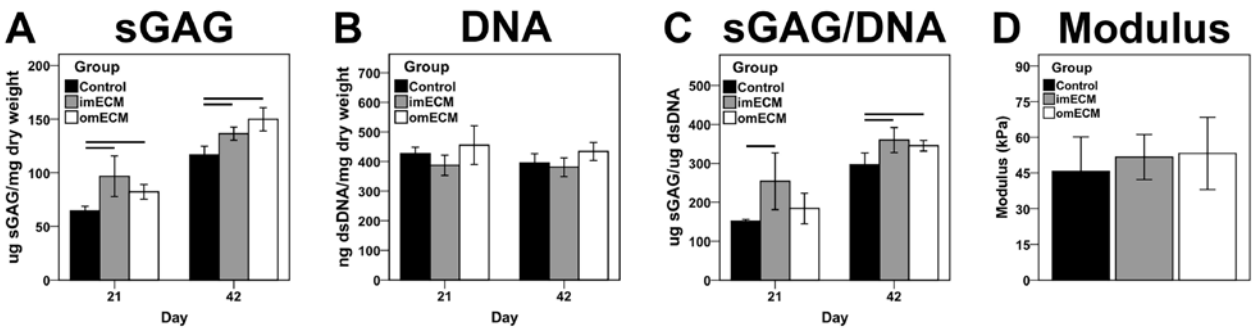

Figure 32. Biochemical composition and compressive modulus of MSC-GelMA constructs. (A) Total sGAG content. (B) Total dsDNA content. (C) sGAG normalized by DNA. (D) Compressive modulus on day 42. n=8-10 samples per condition; Lines indicate significant difference between groups, $p < 0.05$.

4.2.4 Discussion

Expanding on recent work (**Section 4.1**), this study investigated the region-specific bioactivity of urea-extracted decellularized meniscal ECM when presented to human bone marrow MSCs in both 2D and 3D cultures. In preliminary studies, pepsin-digested hydrogels derived from decellularized inner and outer meniscal ECM did not affect fibrochondrogenic differentiation of MSCs when added as a medium supplement in 2D culture or when seeded with MSCs as a 3D scaffold. The absence of fibrochondroinductivity of pepsin-digested hydrogels agrees with recent work by Visser et al.[111] in which supplementation of GelMA hydrogels with pepsin-soluble meniscal ECM did not alter gene expression or protein deposition. As seen both grossly and by SDS-PAGE, pepsin digestion yields a slurry that contains predominantly collagen. Conversely, urea-extracted fractions are enriched for low- to moderate-weight proteins, the combination of which has been previously demonstrated to promote tissue- or region-specific differentiation of MSCs.[113-115] Similarly, in this study, imECM and omECM were found to promote MSC proliferation and upregulation of fibrochondrogenic markers Sox9, Col2, and Col1, when added as a supplement in 2D culture. Based upon these findings, the bioactivities of imECM and omECM were further explored when mixed with GelMA hydrogels.

GelMA is a versatile biomaterial capable of supporting robust chondrogenic differentiation of MSCs after rapid light-activated gelation.[133,134] Additionally, the inclusion of a water-soluble, visible light-responsive photoinitiatior (i.e., LAP) obviates concerns of possible cellular damage caused by UV light exposure, as required by most photoinitiators (e.g., Irgacure).[280] While the effect of meniscal ECM supplementation on MSC-seeded GelMA hydrogels was previously unexplored, functionalization of GelMA with particulated (hyaline) cartilage ECM has been reported to enhance chondrogenesis of encapsulated MSCs.[101,281]

Although the particulated ECM was presumably chondroinductive due to retention of intrinsic chondrogenic cues, robust chondrogenesis required stimulation with exogenous TGF-β3. A similar result was found in this study. Namely, imECM and omECM supplementation of MSC-GelMA constructs produced faint but discernible deposition of proteoglycan in the pericellular regions when cultured in medium without TGF-β3. In contrast, the addition of TGF-β3 to culture medium produced robust chondrogenic differentiation of MSCs, as determined by multiple assays. Supplementation with ECM, especially imECM, enhanced chondrogenic gene expression at earlier time points (i.e., days 7 and 21), translating into sustained increases in collagen type II and sGAG deposition at days 21 and 42. In accordance with the chondrocytic phenotype of inner meniscal cells, these results suggest that imECM is capable of supporting region-specific differentiation of MSCs. While omECM supplementation significantly upregulated Col1 expression on day 1, the effect was not sustained over the culture period. Rather, constructs supplemented with either imECM or omECM demonstrated repressed Col1 expression at day 21, as compared against Controls. Similarly, ECM-mediated decrements in collagen type I deposition were seen on day 42 by immunohistochemistry. In our previous study (**Section 4.1**), in which PEGDA hydrogels were supplemented with meniscal ECM, omECM constructs showed sustained upregulation of Col1 expression for at least 7 days, although longer time points were not examined nor was immunohistochemistry performed. Although the mechanistic basis underlying these discrepancies was beyond the scope of this study, differences in hydrogel composition (i.e., GelMA vs. PEGDA), meniscal ECM-hydrogel interactions, cell adhesion/morphology, and duration of TGF-β3 exposure, may have contributed to the inability of omECM to maintain an increased Col1 expression.

imECM transiently upregulated expression of chondrogenic regulator Sox9 on day 1, with negligible differences across groups at later time points. Interestingly, cells isolated from the inner and outer regions of native menisci were reported to express equivalent levels of Sox9, suggesting minimal influence of Sox9 in distinguishing region-specific phenotypes.[56] Conversely, Vanderploeg et al.[53] showed collagen type VI to be concentrated in inner meniscal regions and localized to the pericellular matrix; in this study, omECM supplementation downregulated Col6 expression, as compared with Controls and imECM constructs. In examining additional putative meniscal cell markers,[65] ECM supplementation tended to have a negligible or inhibitory effect at early time points, with broad equivalency across groups by day 42. To the extent that these transcriptional changes are meaningful for tissue engineering application remains uncertain, given the paucity of studies characterizing the phenotypes of cells across various meniscus regions.

On the other hand, the homogenous distribution of MSCs within GelMA hydrogels clearly does not recapitulate the complex fibrous architecture of native menisci.[51,275] In particular, tie fibers are known to extend radially from the central meniscus to the periphery, binding aligned circumferential fibers and allowing efficient transformation of compressive loads into hoop stresses.[275] In an *in vitro* model, Puetzer and Bonassar[138] demonstrated that simulated tibiofemoral loading of an engineered meniscus composed of high density collagen seeded with meniscal fibrochondrocytes began to recapitulate the fibrous ultrastructure and resulting mechanical anisotropy of native menisci. Whether mechanical loading could orchestrate similar structural organization of MSC-GelMA constructs is unknown. Alternatively, ECM-supplemented hydrogels may be combined with electrospun nanofibers to better reconstitute the structural and biochemical properties of the meniscus.[282,283] Baek et al.[284] fabricated multilayered

scaffolds with alternating layers of electrospun nanofibers and MSC-seeded alginate hydrogels, which allowed tunable tensile anisotropy depending on fiber orientation. However, compressive mechanical properties were not measured. In this study, compressive moduli of constructs (~ 40-50 kPa) did not differ across groups, but were congruent with reported values for GelMA hydrogels.[134,285] Unlike other studies, in which values of compressive modulus correlated with glycosaminoglycan content,[137,285] the greater total and normalized sGAG content of ECM-supplemented constructs did not significantly enhance compressive moduli, suggesting that the differences in sGAG content or the resulting hydrogel architecture were insufficient to produce discernible changes in mechanical properties. As with fiber architecture, mechanical loading has been found to further increase sGAG deposition, with concurrent improvements in compressive mechanical properties.[138,286] Controlled mechanical loading as part of post-surgical rehabilitation may serve as a viable strategy to further enhance the compressive moduli of the remodeling hydrogels, as the GelMA constructs are presently weaker than native menisci (~ 100-500 kPa).[51,256,287] Additional improvements in initial material properties of GelMA constructs may also be realized by adding exogenous hyaluronic acid and/or modifying the decellularization process so as to retain a higher endogenous sGAG content within the resulting ECM extracts.[288] As demonstrated by Levett et al.,[285] supplementation of GelMA hydrogels with exogenous hyaluronic acid, rather than endogenous production by encapsulated cells, produced the greatest improvements in compressive mechanical properties.

While preservation of the biophysical and biochemical motifs of the native ECM is presumed to most faithfully reconstitute tissue-specific cell phenotypes, limitations in whole meniscus decellularization, as described in the introduction, necessitate further processing to improve cell infiltration.[6] To that end, one must balance the disruption of native motifs with

technical and biological utility gained by further ECM processing. Retention of higher sGAG content within ECM extracts may not only improve mechanical properties of constructs but may also enhance chondrogenic differentiation of seeded cells. For instance, hyaluronan of native ECM, through binding to the CD44 receptor of the cell surface, can upregulate chondrogenesis.[143,289] Alternatively, exogenous hyaluronan/sGAG could be added to the present formulation of ECM-supplemented GelMA for possible benefit. Nevertheless, future investigations elucidating the essential elements of the meniscus ECM governing cell phenotype are essential to further guide tissue engineering applications aimed at restoring the structure and function of the meniscus, in turn preserving joint integrity.

4.2.5 Conclusions

In this study, urea-extracted fractions of decellularized inner and outer meniscal ECM enhanced proliferation and fibrochondrogenic differentiation of human bone marrow MSCs cultured on plastic. GelMA hydrogels supplemented with soluble ECM fractions accelerated chondrogenic differentiation of seeded MSCs as determined by analyses of gene expression, protein deposition, and biochemical composition of the constructs. Upregulation of chondrogenesis was most pronounced with inclusion of imECM. While ECM supplementation alone enhanced chondrogenic differentiation, robust effects required supplementation of media with exogenous TGF-β3. Given these findings, photocrosslinkable hydrogels enhanced with imECM, TGF-β3, and MSCs, may offer a potential therapeutic strategy to promote region-specific neotissue formation when combined with surgical repair of tears in the avascular meniscal region.

5.0 DISCUSSION

5.1 SUMMARY

Through a series of studies, we demonstrated that urea-extracted ECM derived from decellularized tendon and cartilage could promote homologous (i.e., tissue-specific) differentiation of MSCs when cultured on 2D surfaces and as 3D pellets, which mimic aggregating mesenchymal cells of the developing limb. Endogenous TGF-β is necessary, but not sufficient, to promote ECM-mediated tissue-specific differentiation. When added to tissue-appropriate biomimetic scaffolds – aligned nanofibrous scaffolds and photocurable GelMA hydrogels – tECM and cECM enhanced tissue-specific differentiation of MSCs and interacted synergistically with exogenous TGF-β. Applying these findings to a single tissue with noted regional variation, we found that urea-extracted ECM derived the inner and outer meniscus was capable of promoting region-specific differentiation of MSCs seeded in PEGDA hydrogels. When combined with MSC-GelMA constructs, both imECM and omECM promoted chondrogenesis, an effect more strongly promoted by imECM. The discrepancy between GelMA and PEGDA may be attributable to the presence or absence of bioactive motifs with the polymer backbone of gelatin and PEG, respectively. Taken together, these studies begin to clarify the mechanisms by which ECM may exert tissue-specific bioactivity while also supporting the use

of urea-extracted fractions of soluble ECM to promote homologous cell phenotypes in adult stem cells seeded in biomimetic scaffolds.

In addition to the immediate challenges and future directions articulated within the discussion of each specific aim, broader considerations about the future direction of tissue engineering are expanded upon below.

5.2 FUTURE PERSPECTIVES

This following section contains material from the publication:

Yang G, Lin H, **Rothrauff BB**, Yu S, Tuan RS. (2016) Multilayered polycaprolactone/gelatin fiber-hydrogel composite for tendon tissue engineering. *Acta Biomaterialia*. [Epub ahead of print] PMID: 26945631

5.2.1 ECM-Enhanced Biomaterials – Getting Closer to Native Structure & Function

The results contained herein suggest that urea-extracted ECMs can further enhance tissue-specific differentiation in MSCs seeded in biomimetic scaffolds by ostensibly recapitulating the biophysical and biochemical cues of native ECM to a greater degree than the scaffolds or soluble ECMs alone. However, the fold-changes in gene expression induced by soluble ECMs were, depending on the experiment, often far lower than those induced by exogenous TGF-β. While this likely suggests the necessity of including exogenous growth factors to induce robust neotissue formation for tissue engineering application, this interpretation must be tempered by the fact that in vitro assays do not necessarily predict in vivo responses, especially when

considering the complexity of tissue regeneration. Nevertheless, the synergism consistently found between soluble ECMs and exogenous TGF-β support their combined use with biomimetic scaffolds, as the ECM component may accelerate tissue-specific differentiation and/or diminish the heterologous bioactivity that is possible when applying pleotropic growth factors such as TGF-β.

Assuming an intention of perfectly matching the many properties of native tissues, the engineered constructs developed in these studies fall short on several parameters. In particular, the mechanical properties of both electrospun nanofibers and photocrosslinked GelMA hydrogels are inferior to native tendon/ligament and cartilage/meniscus, respectively. Incorporation of textile patterns (e.g., weaving, braiding, etc.)[290,291] or the use of novel polymers[292] could enhance initial mechanical properties, although the effect of these alternative strategies on cell behavior would require further investigation. At the same time, the application of mechanical stimulation in a bioreactor could accelerate ECM synthesis by seeded cells, augmenting the initial strength of the biomaterials.[128,138] Mechanical stimulation mimicking physiological loading parameters has also been found to independently promote homologous differentiation. Interestingly, compressive mechanical loading was shown to prevent hypertrophy of MSCs seeded in biomimetic hydrogels, perhaps serving as a strategy to mitigate the upregulation of hypertrophic and osteogenic markers seen above with cECM supplementation.[286,293] These considerations, while important for iterative improvements in tissue engineering applications as presently practiced, belie broader questions that must be answered if we seek to bring the promise of tissue engineering to fruition. I've attempted to identify some of these issues in the following discussion.

5.2.2 Top-Down vs. Bottom-Up Tissue Engineering

5.2.2.1 Top-down tissue engineering (reverse engineering) Tissue engineering has largely confronted its task through a top-down approach; that is, the deconstruction of a tissue into individual elements, which can be mimicked through engineering methods or procured from simpler biological systems (e.g., recombinant proteins), then reassembled under the intention of rebuilding the system. The work performed herein is very much a part of this paradigm. The biophysical elements of a tissue were mimicked through engineered scaffolds (i.e., electrospun nanofibers and porous hydrogels) and the biochemical components were extracted from decellularized xenogeneic tissues (obviating an adverse immune response) then combined with biomimetic scaffolds with the intention of more faithfully reconstituting tissue structure and function than what might be possible with the use of a single or combined growth factor. The results suggest that the urea-extracted fraction of decellularized tissues does indeed promote tissue-specific differentiation of adult MSCs across multiple 3D microenvironments, supporting the hypothesis. Although still preliminary, experiments further suggest that the provision of tissue-specific ECM may direct the bioactivity of a pleotropic growth factor (e.g., TGF-β) towards homologous effects. Thus a synergistic effect occurs. However, the combination of urea-extracted ECM with a homologous biomimetic scaffold did not always suppress heterologous gene express. To the extent that these non-specific effects compromise the ultimate cell phenotype is unknown. At the same time, it is also unclear to what degree an engineered construct must recapitulate all elements of the native tissue to provide in vivo benefit.[294]

Advances in biomaterial fabrication methods continue to expand the elements of the native tissue that can be mimicked.[116,295] For instance, there have been numerous reports of composite scaffolds that combine electrospun fibers with hydrogels, thereby replicating the

viscoelastic properties several musculoskeletal soft tissues.[296] In fact, our lab recently developed a composite scaffold of aligned electrospun nanofibers coupled with visible light-responsive GelMA hydrogel (**Figure 33**).[297] GelMA provides cell-binding motifs otherwise absent on polyester nanofibers. Additionally, the ability of the hydrogel component to undergo photogelation allows for rapid cell encapsulation that would be required in single-stage point-of-care procedures. As we recently showed, not only are these composite scaffolds cytocompatible, but the cells elongate in the direction of the fibers and are subsequently responsive to exogenous tenogenic cues (e.g., TGF-β) (**Figure 34**).[297] Equally promising are hydrogels with reversible chemistries that can more precisely regulate cell spreading, ligand presentation, and matrix mechanics.[298] At the same time, advances in 3D printing technologies facilitate the production of human-scale tissue constructs with structural integrity.[299] Nevertheless, it is increasingly appreciated that cell morphogenesis and differentiation can require stringent spatial arrangements of ECM motifs,[300] and our understanding of cell-matrix interactions on a single cell level is still limited.

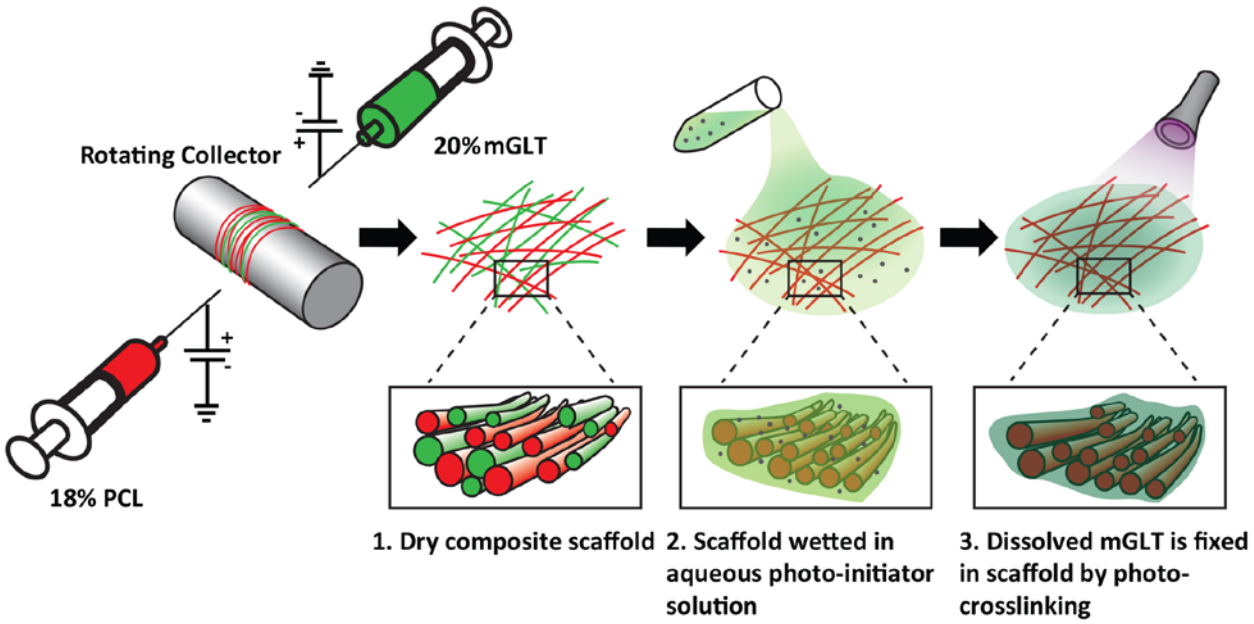

Figure 33. Composite fiber-hydrogel scaffold fabrication. Dual electrospinning was employed to fabricate a scaffold containing PCL and mGLT fibers (Insert 1). Dry scaffold was wetted with aqueous photo-initiator solution (Insert 2) and then photocrosslinked by visible light (VL) to retain the gelatin (Insert 3).

Fortunately, tissue matrix arrays and other approaches for engineering nanoscale microenvironmental cues are growing in sophistication.[301,302] In combining these 3D tissue arrays with systems-level analyses, it may be possible to gain greater insight into the mechanistic basis by which biophysical cues modulate cell signaling pathways.[302,303] However, in order to understand the multifactorial complexities inherent in cell-matrix interactions, the prevailing reductionistic paradigm, which has provided innumerable insights regarding the function of individual elements of the system, must be expanded. Namely, systems biology could provide newfound sophistication in top-down tissue engineering approaches. Systems biology seeks to

reveal how interactions among elements of a system (i.e., signaling network → cell → tissue → organ → organism) can give rise to emergent properties of the system.[304,305] To do so, computational models are compared with experimental findings through an iterative process of testing, validation, and retesting, with experimental findings guided an increasingly predictive model. Thus far, systems biology has been almost exclusively applied to signaling networks with cell lines grown in 2D culture. With exponential increases in complexity with every step in scale, the application of systems biology to tissue engineering is highly challenging but greatly needed.[306,307]

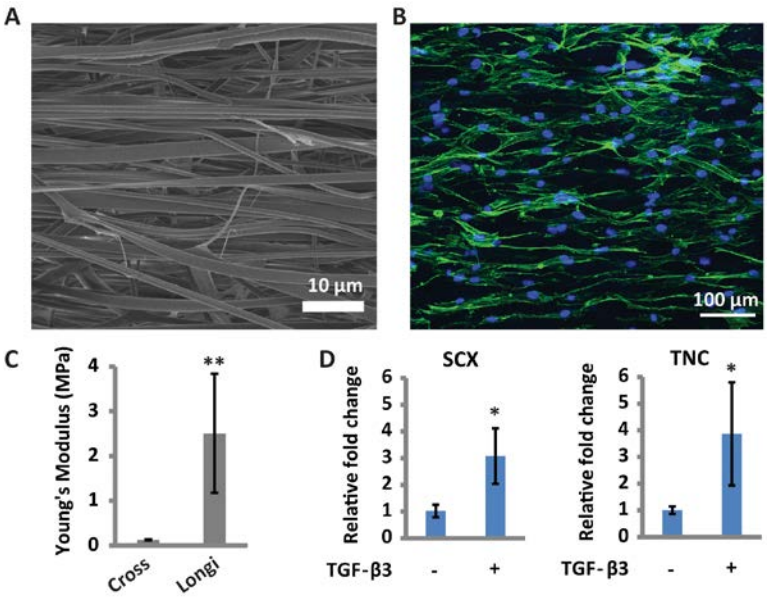

Figure 34. Tendon-like features of MSCs encapsulated in composite scaffold. (A) Fiber alignment observed by SEM. (B) Elongated morphology of human adipose stem cells (hASCs) aligned in the direction of fibers (green, F-actin; blue, nuclei). (C) Anisotropy based on tensile strength properties measured by mechanical testing along two directions (Longi. vs. Cross). (D) Significant upregulation of tendon markers scleraxis (SCX) and tenascin C (TNC) upon treatment with exogenous tenogenic factor TGF-β3, measured by real-time PCR analysis.

5.2.2.2 Bottom-up tissue engineering (developmental engineering) The confluence of advancing engineering technologies with greater computational sophistication will, in theory, ultimately permit the fabrication of biomaterials possessing nano- through meso-scale microenvironmental cues capable of fully reconstituting the complex structure and function of native tissues. However, the timescale on which such promise becomes reality is presently unknown. An alternative to the top-down approach to tissue engineering is a bottom-up approach, perhaps more simply referred to as developmental engineering. Developmental engineering approaches tissue engineering by trying to recapitulate the ***elements and sequences*** of embryogenesis.[308,309] Importantly, recapitulation of development requires more than merely the provision of individual elements known to play a role in tissue formation. Rather, it necessitates nascent cells and a minimum set of conditions from which a robust, semi-autonomous process emerges, with the cells and their evolving ECM culminating in an engineered tissue indistinguishable from the native tissue. In so far as the molecular mechanisms governing differentiation of progenitor cells are known (and can be replicated in vitro), it may be possible to recapitulate tissue formation in vitro.[30] As an example, the steps governing the specification and maturation of chondrocytes starting from mesodermal progenitors are moderately well established.[310-312] When replicated, large, stratified, and mechanically functional human cartilage has been grown in vitro and successfully transplanted (and integrated) into a focal chondral defect.[313,314] While the molecular mechanisms regulated tendon cell fate are less well known, increasing knowledge of the subject may allow similar applications to tendon tissue engineering in the near future.[315,316]

At the same time, there is growing understanding of the role of mechanical loading in both developmental processes and tissue engineering.[317] While it is has been known for decades

that the recovery of tissue structure and function is best achieved by progressively increasing the loading demands on a healing tissue, [318] the systematic application of physical therapy to improve the integration and maturation of tissue engineered constructs remains in the nascent stages. Termed "regenerative rehabilitation", this evolving paradigm seeks to use the body as a bioreactor, through the prescriptions of a physical therapist, to provide controlled mechanical loads to the healing tissue. [319,320] As the field is still in the earliest stages, future studies should seek not only to elucidate the in vivo dynamics experienced by musculoskeletal tissues, but also how these in situ stresses and strains affect ex vivo engineered constructs. In theory, this would allow a range of 'physical therapy' protocols to be tested ex vivo in microphysiological systems, with experimental results informing the predictive models of in vivo responses.

5.2.3 *In Situ* Tissue Engineering

As highlighted above, in vitro recapitulation of the molecular events guiding cell differentiation during development may provide us with engineered constructs that more faithfully match the structure and function of native tissues, while in vivo mechanical loading (the parameters of which could one day be guided by ex vivo modeling in microphysiological systems) could mimic the mechanical environment guiding tissue formation during organogenesis. However, the diseased microenvironment can drastically differ from that of the developing embryo. Therefore, the direct application of knowledge concerning the molecular mechanisms of development may not prove fruitful in promoting tissue regeneration in a diseased state. While musculoskeletal soft tissues do not possess a strong intrinsic healing capacity, increases in progenitor cells at the time of injury have been found for many of these tissues, including tendon,[321] meniscus,[64] and cartilage.[36,38] Taken together, the restoration of tissue integrity following injury or disease may

be better served by mitigating the factors that actively inhibit tissue healing rather than seeking to stimulate repair in the face of these unabated impediments.

Although not the focus of this work, biological scaffolds composed of tissue-derived ECM promote constructive remodeling (i.e., improved healing) in part by altering the characteristics of the default inflammatory response following injury.[322] In particular, the proportion of a particular macrophage phenotype appears to dictate the quality of healing, with M2 macrophages serving a more anti-inflammatory role while M1 macrophages are pro-inflammatory and seem to promote generic scarring.[173] ECM scaffolds, when sufficiently decellularized, have been shown to promote a stronger M2 macrophage polarization,[168,323] with macrophage phenotype actually predicting the quality of healing.[172] Immunomodulation of the injured microenvironment, either through ECM-based scaffolds, pharmaceuticals, or engineered biomaterials, may be necessary in order to create a more permissive microenvironment in which conventional tissue engineering approaches can then achieve maximum benefit.[324-326]

Should such strategies prove feasible, the injury-mediated increase in local progenitor cells may be sufficient for intrinsic healing to proceed. However, numerous strategies are currently being explored that can enhance the recruitment of reparative cells to the wound site, including partial digestion of the dense collagen ECM or chemokine-guided localization.[327-330] Novel biomaterials capable of sequential release of chemotactic and differentiation factors could theoretically attract progenitor cells to the wound site and subsequently direct tissue-specific cell differentiation and neotissue formation.[331-333] What role urea-extracted ECM could play in these processes is the subject of future investigations.

5.2.4 Conclusions

The field of tissue engineering continues to expand at an exponential pace, filling both patients and providers alike with hope for medical breakthroughs. But at present, the treatment options for orthopaedic soft tissues are starkly limited. Ever evolving engineering techniques allow greater and greater fidelity in mimicking the structure and function of musculoskeletal tissues, but no effort thus far has yielded an engineered construct matching that of native tissues. In bridging that gap, the combination of solubilized ECM with biomimetic scaffolds may allow closer replication of the biophysical and biochemical cues of the native ECM while permitting the flexibility and tunability of synthetic materials. However, the precision to which engineered constructs must match the structure of native tissues in order to promote in vivo regeneration remains a vexing question. Furthermore, it is increasingly apparent that the complex microenvironment of the diseased state, coupled with the immune response to engineered constructs, will have tremendous bearing on bringing the promise of tissue engineering to fruition. To that end, continued efforts to elucidate the molecular bases of musculoskeletal development and disease are of the utmost importance, in turn guiding the development of therapeutics that seek to alleviate suffering and improve function. It is a challenge most worthy of my decades to come.

SUPPLEMENTAL FIGURES

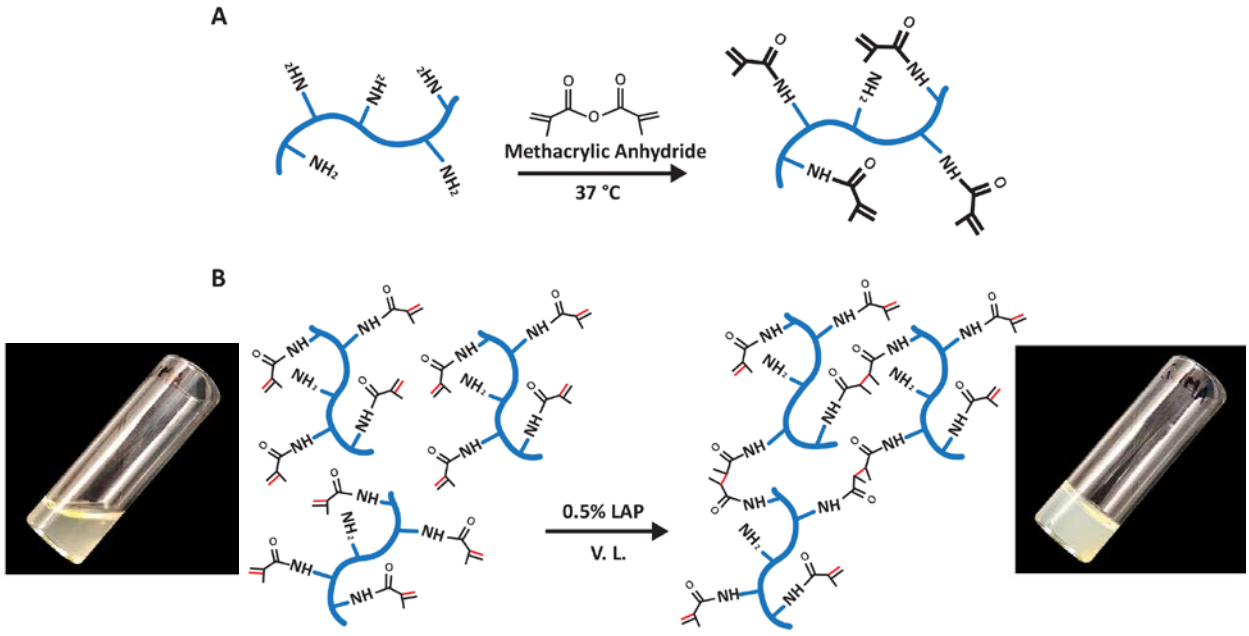

Supplemental Figure 1. (A) Schematic depicting the functionalization of primary amines of gelatin with methacrylate pendant. (B) Exposure of liquid GelMA to visible light, in the presence of a water-soluble photoinitiator (0.5% LAP) causes rapid photocrosslinking to form hydrogel.

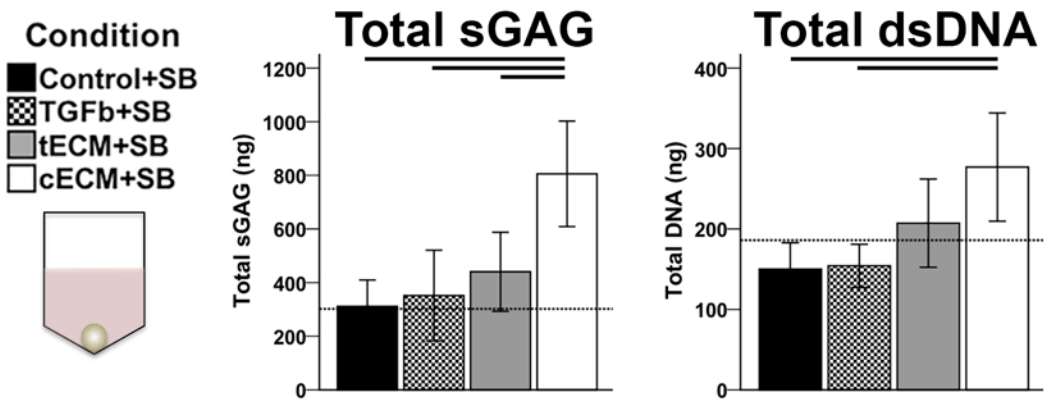

Supplemental Figure 2. The effect of TGF-β inhibition on biochemical content of MSC pellets. Medium conditions for pellet cultures were further supplemented with 10 μM SB-431542. Pellets supplemented with cECM exhibited elevated (albeit blunted) total sGAG and dsDNA content compared to other medium conditions ($p < 0.05$, n=9); dotted line indicates sGAG and dsDNA contents of control medium (without SB-431542).

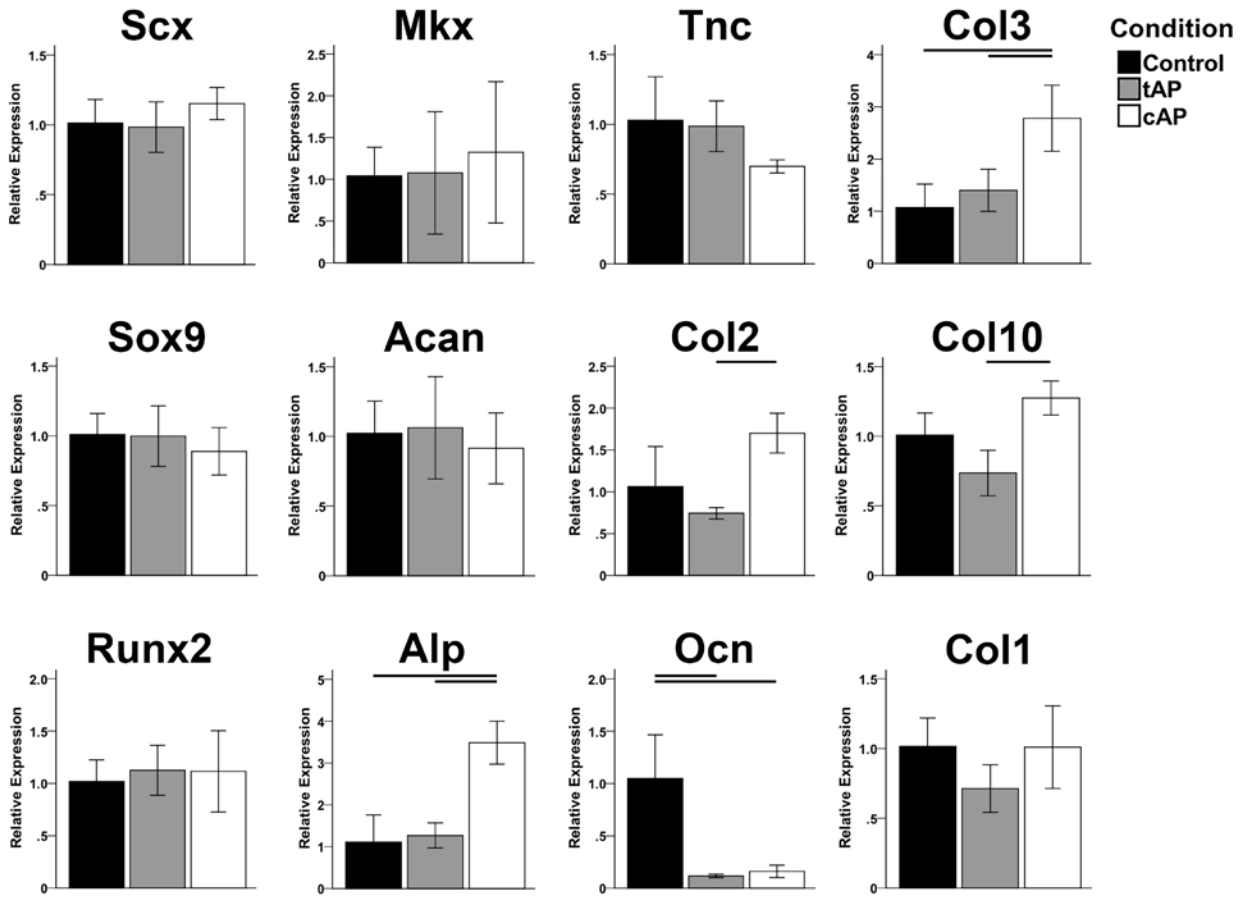

Supplemental Figure 3. MSC-seeded hydrogels derived from pepsin-digested ECM. MSCs were seeded in 5 mg/mL hydrogels of Collagen 1 (Control), tAP, and cAP. ECM-derived hydrogels showed negligible tissue-specificity compared to collagen controls ($p < 0.05$, $n = 9$)

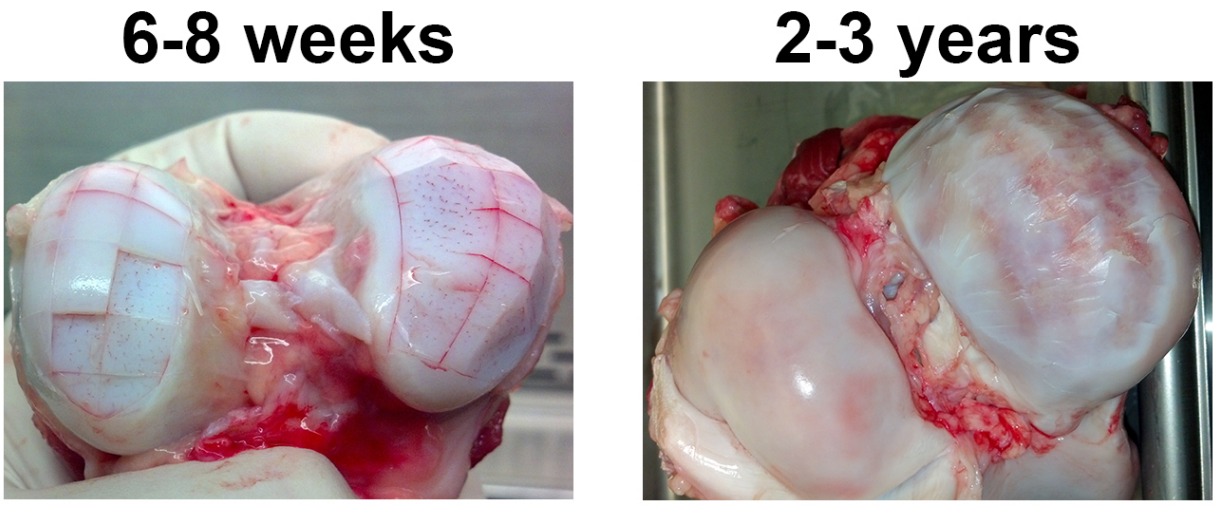

Supplemental Figure 4. Macroscopic image of femoral condyles from young (6-8 weeks) and mature (2-3 years) cows. The osteochondral interface is distinct in adult animals but indistinct in young animals, with clear vasculature seen in dissected cartilage pieces.

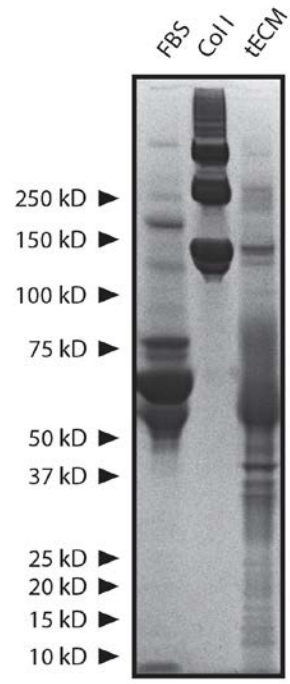

Supplemental Figure 5. Characterization of tECM and other medium supplements by SDS-PAGE. tECM contains abundant low molecular weight proteins (<50 KD) that are absent in collagen type I solution (Col I) and FBS.

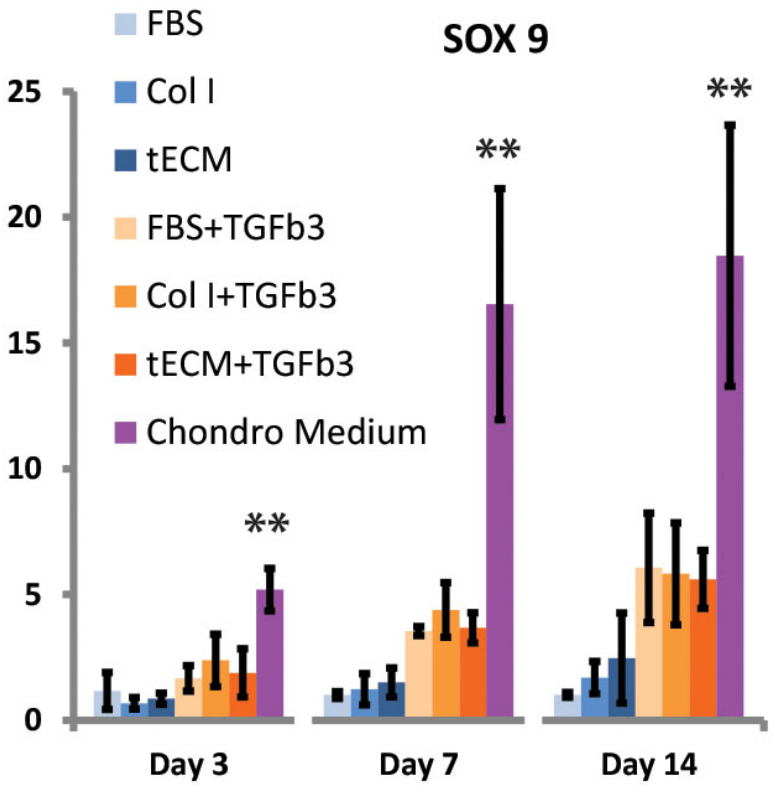

Supplementary Figure 6. Real-time PCR analysis of SOX9 expression revealed that tECM alone possessed little inductive effect on chondrogenesis of ASCs in 2D culture compared to other treatment groups with TGF-β3. The expression level of SOX9 was significantly higher in cell pellets cultured in standard chondrogenic medium (Chondro Medium) than in all other groups. **, $p<0.01$; N=3.

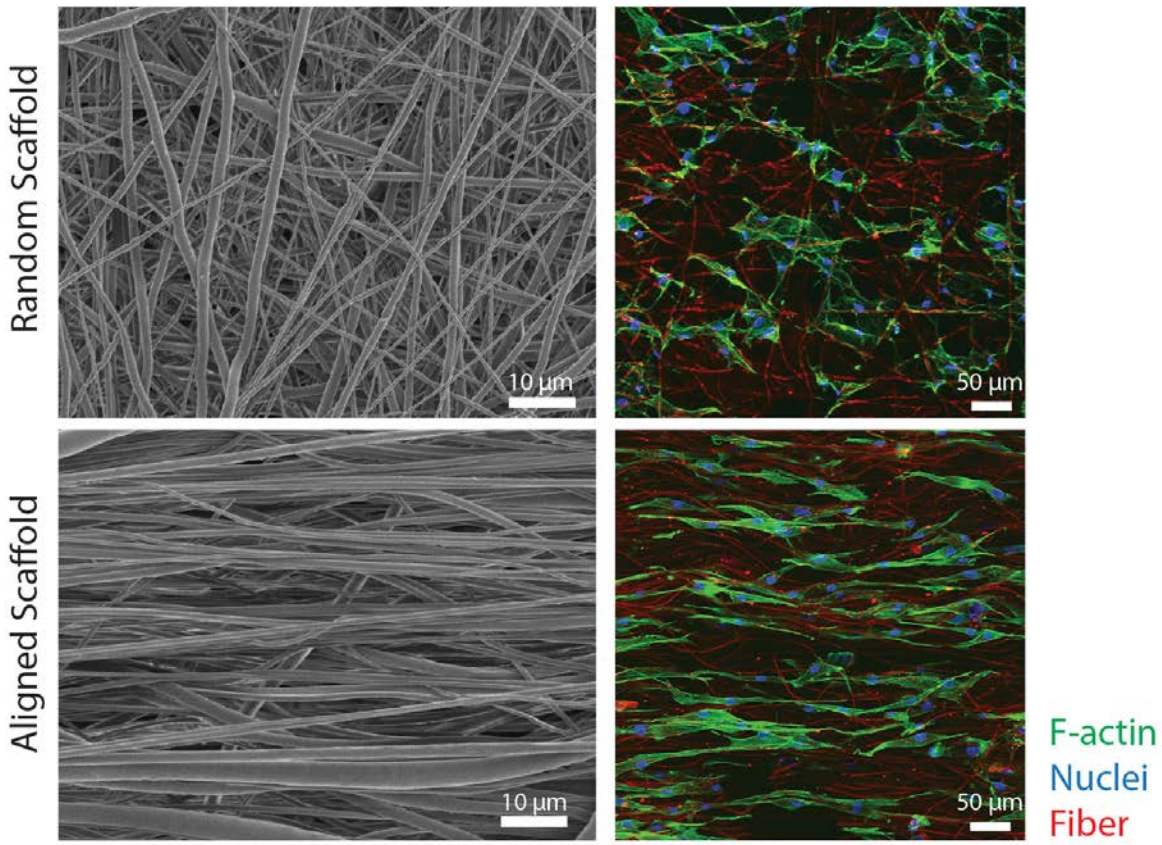

Supplemental Figure 7. Morphology of ASCs cultured on scaffolds. hASCs seeded on random scaffolds (upper left, SEM) exhibited polygonal shape without uniformity in orientation (upper right, confocal microscopy). In contrast, hASCs seeded on aligned scaffolds (lower left, SEM) adopted an elongated morphology and were orientated in the direction of the fibers (lower right, confocal microscopy; F-actin, green; nuclei, blue; microfiber, red).

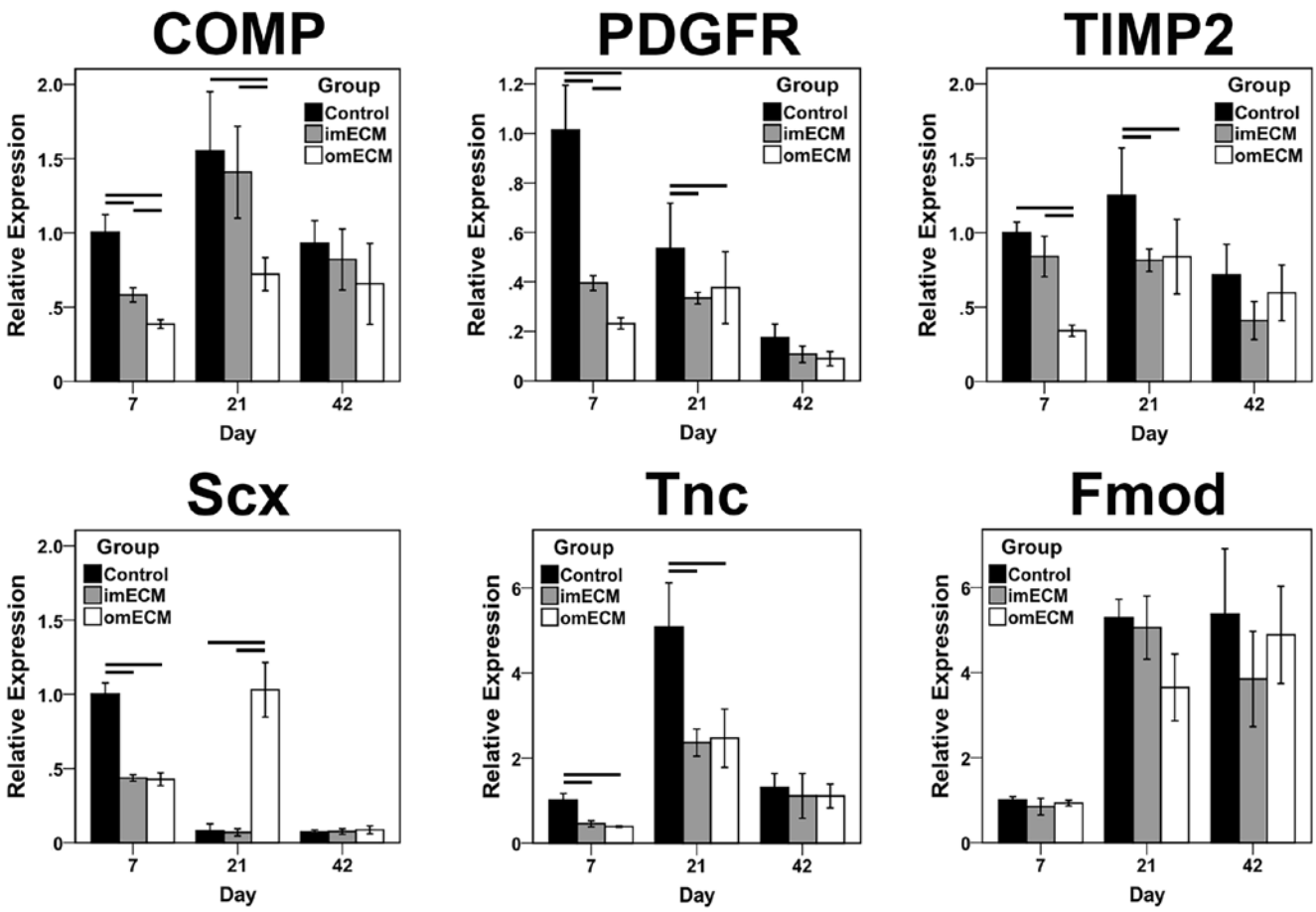

Supplemental Figure 8. Gene expression analysis of MSC-GelMA constructs. n=3 independent trials, each performed in triplicate; Lines indicate significant difference between groups, $p < 0.05$.

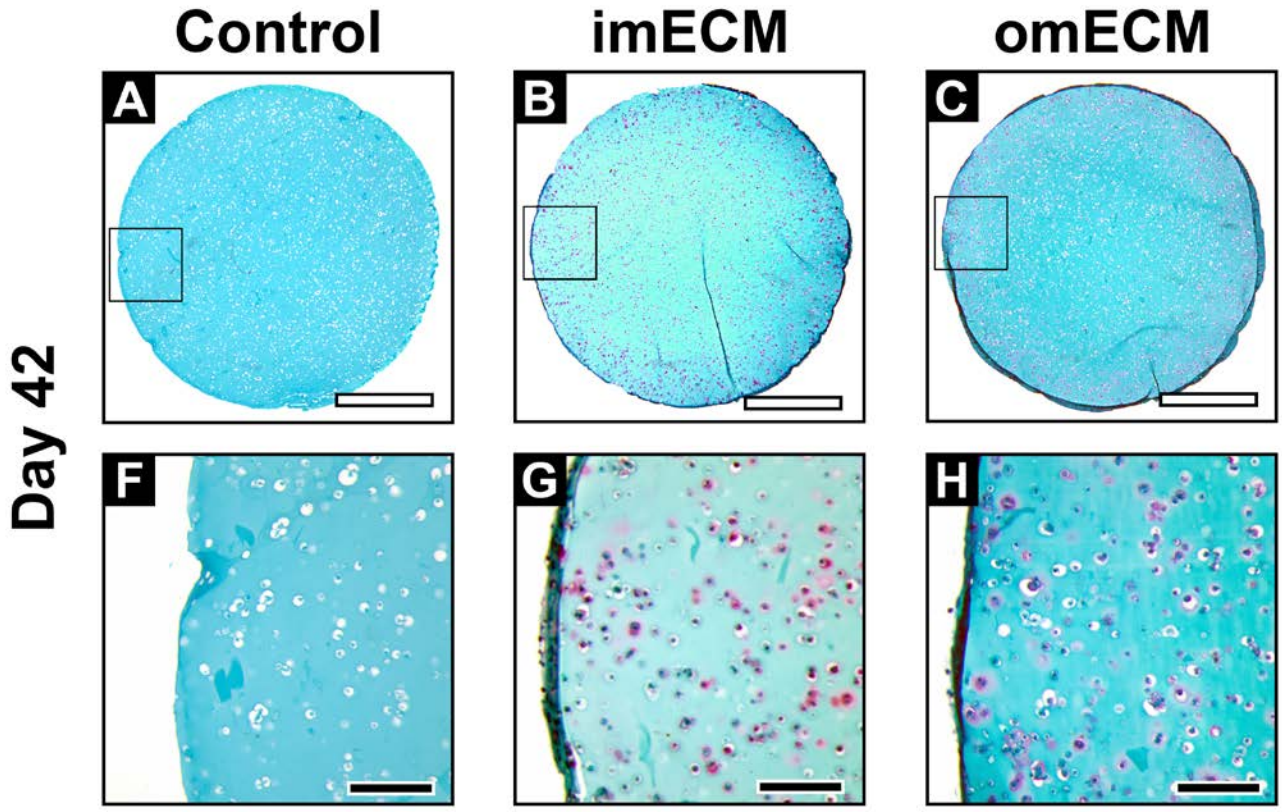

Supplemental Figure 9. Safranin O staining of constructs cultured in TGF-β3-free medium on day 42. (A-C) Low magnification, scale bar = 1 mm; Area of magnification shown by black box; (F-H) High magnification, scale bar = 200 μm.

SUPPLEMENTAL TABLES

Supplemental Table 1. Primer sequences for qPCR.

Gene		Primer sequence (5'→3')	Product size (bp)
Gapdh	Forward	CAAGGCTGAGAACGGGAAGC	194
	Reverse	AGGGGGCAGAGATGATGACC	
r18S	Forward	GTAACCCGTTGAACCCCATT	151
	Reverse	CCATCCAATCGGTAGTAGCG	
Scx	Forward	TGCGAATCGCTGTCTTTC	91
	Reverse	GAGAACACCCAGCCCAAA	
Mkx	Forward	GCAGCCACAGAAGCCGA	502
	Reverse	AAATCTGGCTGTCGAACGGT	
Tnc	Forward	TTCACTGGAGCTGACTGTGG	223
	Reverse	TAGGGCAGCTCATGTCACTG	
Col3a1	Forward	CAGCGGTTCTCCAGGCAAGG	179
	Reverse	CTCCAGTGATCCCAGCAATCC	
Sox9	Forward	CTGAGCAGCGACGTCATCTC	72
	Reverse	GTTGGGCGGCAGGTACTG	
Acan	Forward	GCTACACTGGCGAGCACTGTAACAT	287
	Reverse	GCGCCAGTTCTCAAATTGCATGGG	
Col2a1	Forward	GGATGGCTGCACGAAACATACCGG	157
	Reverse	CAAGAAGCAGACCGGCCCTATG	
Col10a1	Forward	GTGTTTTACGCTGAACGATACCAA	273
	Reverse	ACCTGGTTTCCCTACAGCTGATG	
Runx2	Forward	CAACCACAGAACCACAAGTGCG	196
	Reverse	TGTTTGATGCCATAGTCCCTCC	
Alp	Forward	TGGAGCTTCAGAAGCTCAACACCA	413
	Reverse	ATCTCGTTGTCTGAGTACCAGTCC	
Ocn	Forward	ATGAGAGCCCTCACACTCCTC	294
	Reverse	GCCGTAGAAGCGCCGATAGGC	
Col1a1	Forward	TAAAGGGTCACCGTGGCT	355
	Reverse	CGAACCACATTGGCATCA	

Supplemental Table 2. Growth factor concentrations (pg/mL) in 500 μg/mL of soluble ECM extracts

				6-8 weeks	2-3 years
Protein	**tAP**	**tECM**	**cAP**	**cECM**	**cECM**
AR	0.0	0.0	0.0	**1.7**	0.0
BDNF	0.0	0.0	0.0	**2.0**	0.0
bFGF	0	**469.4**	0.0	**17,314.6**	**4,330.6**
BMP-4	0.0	0.0	0.0	0.0	0.0
BMP-5	0.0	0.0	0.0	**906.2**	0.0
BMP-7	0.0	0.0	0.0	**170.7**	**57.1**
b-NGF	0.0	**0.1**	0.0	0.0	0.0
EGF	0.0	**0.1**	0.0	0.0	0.0
EGF R	**3.1**	0.0	**1.3**	0.0	0.0
EG-VEGF	0.0	0.0	0.0	**11.9**	**2.9**
FGF-4	**114.9**	**137.3**	0.0	**276.1**	**79.3**
FGF-7	0.0	0.0	0.0	0.0	0.0
GDF-15	0.0	0.0	0.0	0.0	0.0
GDNF	0.0	0.0	0.0	0.0	0.0
GH	0.0	0.0	0.0	**31.4**	0.0
HB-EGF	0.0	0.0	0.0	0.0	0.0
HGF	**5.7**	0.0	0.0	0.0	**0.5**
IGFBP-1	0.0	0.0	0.0	**24.8**	0.0
IGFBP-2	0.0	0.0	0.0	**1,952.7**	**114.0**
IGFBP-3	0.0	**162.8**	0.0	**260.3**	**233.7**
IGFBP-4	0.0	0.0	0.0	**58.7**	**0.1**
IGFBP-6	0.0	0.0	0.0	**80.1**	0.0
IGF-1	0.0	0.0	0.0	0.0	0.0
Insulin	**18.4**	0.0	**70.7**	**425.8**	**149.6**
MCSF R	0.0	0.0	0.0	0.0	0.0
NGF R	0.0	0.0	0.0	**11.7**	0.0
NT-3	**1.3**	**4.9**	**0.6**	**47.8**	**22.0**
NT-4	0.0	**2.2**	0.0	**22.3**	0.0
OPG	0.0	**0.1**	0.0	**2.9**	**153.3**
PDGF-AA	0.0	0.0	0.0	0.0	0.0
PIGF	0.0	0.0	0.0	0.0	0.0
SCF	**1.4**	**1.9**	0.0	**1.4**	**1.3**
SCF R	0.0	**15.7**	0.0	**16.5**	**10.0**
TGFa	0.0	0.0	0.0	0.0	0.0
TGFb1	**83.2**	**872.2**	**942.7**	**2,789.5**	**758.0**
TGFb3	0.0	**34.6**	0.0	**154.7**	0.0
VEGF	0.0	0.0	0.0	0.0	0.0
VEGF R2	0.0	0.0	0.0	0.0	0.0
VEGF R3	0.0	0.0	0.0	**8.0**	0.0
VEGF-D	0.0	0.0	0.0	0.0	0.0

Supplemental Table 3. Primer sequences for qPCR.

Gene		Primer sequence (5'-3')	Product size (bp)
18S rRNA	Forward	GTAACCCGTTGAACCCCATT	151
	Reverse	CCATCCAATCGGTAGTAGCG	
SCX	Forward	ACACCCAGCCCAAACAGA	65
	Reverse	GCGGTCCTTGCTCAACTTTC	
TNC	Forward	GGTGGATGGATTGTGTTCCTGAGA	328
	Reverse	CTGTGTCCTTGTCAAAGGTGGAGA	
SOX9	Forward	CTGTAGGCGATCTGTTGGGG	85
	Reverse	AGCGAACGCACATCAAGA	
COL II	Forward	GGATGGCTGCACGAAACATACCGG	157
	Reverse	CAAGAAGCAGACCGGCCCTAT	

Supplemental Table 4. Primer sequences for qPCR.

Gene		Primer sequence (5'→3')	Product size (bp)
Gapdh	Forward	CAAGGCTGAGAACGGGAAGC	194
	Reverse	AGGGGGCAGAGATGATGACC	
r18S	Forward	GTAACCCGTTGAACCCCATT	151
	Reverse	CCATCCAATCGGTAGTAGCG	
Sox9	Forward	CTGAGCAGCGACGTCATCTC	72
	Reverse	GTTGGGCGGCAGGTACTG	
Col2a1	Forward	GGATGGCTGCACGAAACATACCGG	157
	Reverse	CAAGAAGCAGACCGGCCCTATG	
Col1a1	Forward	TAAAGGGTCACCGTGGCT	355
	Reverse	CGAACCACATTGGCATCA	
Acan	Forward	GCTACACTGGCGAGCACTGTAACAT	401
	Reverse	GCGCCAGTTCTCAAATTGCATGGG	
Col6a1	Forward	ACAGTGACGAGGTGGAGATCA	122
	Reverse	GATAGCGCAGTCGGTGTAGG	
Runx2	Forward	CAACCACAGAACCACAAGTGCG	196
	Reverse	TGTTTGATGCCATAGTCCCTCC	
COMP	Forward	GATCACGTTCCTGAAAAACACG	148
	Reverse	GCTCTCCGTCTGGATGCAG	
PDGFRB	Forward	AGCACCTTCGTTCTGACCTG	152
	Reverse	TATTCTCCCGTGTCTAGCCCA	
TIMP2	Forward	AAGCGGTCAGTGAGAAGGAAG	136
	Reverse	GGGGCCGTGTAGATAAACTCTAT	
Scx	Forward	TGCGAATCGCTGTCTTTC	91
	Reverse	GAGAACACCCAGCCCAAA	
Tnc	Forward	TTCACTGGAGCTGACTGTGG	223
	Reverse	TAGGGCAGCTCATGTCACTG	
Fmod	Forward	ATTGGTGGTTCCACTACCTCC	87
	Reverse	GGTAAGGCTCGTAGGTCTCATA	

BIBLIOGRAPHY

1. Palmer M, Stanford E, Murray MM. 2011. The Effect of Synovial Fluid Enzymes on the Biodegradability of Collagen and Fibrin Clots. Materials 4: 1469-1482.

2. Langer R, Vacanti JP. 1993. Tissue Engineering. Science 14: 920-926.

3. Somoza RA, Welter JF, Correa D, et al. 2014. Chondrogenic Differentiation of Mesenchymal Stem Cells: Challenges and Unfulfilled Expectations. Tissue Eng Part B 20: 596-608.

4. Caplan AI. 2007. Adult mesenchymal stem cells for tissue engineering versus regenerative medicine. Journal of Cellular Physiology 213: 341-347.

5. Meirelles LDS, Chagastelles PC, Nardi NB. 2006. Mesenchymal stem cells reside in virtually all post-natal organs and tissues. J Cell Sci 119: 2204-2213.

6. Crapo PM, Gilbert TW, Badylak SF. 2011. An overview of tissue and whole organ decellularization processes. Biomaterials 32: 3233-3243.

7. Badylak SF, Freytes DO, Gilbert TW. 2009. Extracellular matrix as a biological scaffold material: Structure and function. Acta Biomater 5: 1-13.

8. Schwarz S, Elsaesser AF, Koerber L, et al. 2015. Processed xenogenic cartilage as innovative biomatrix for cartilage tissue engineering: effects on chondrocyte differentiation and function. J Tissue Eng Regen Med 9: 239-251.

9. Ozasa Y, Amadio PC, Thoreson AR, et al. 2014. Repopulation of Intrasynovial Flexor Tendon Allograft with Bone Marrow Stromal Cells: An Ex Vivo Model. Tissue Eng Part A 20: 566-574.

10. Rothrauff BB, Yang G, Tuan RS. 2015. Tendon Resident Cells - Functions and Features in Section I - Developmental Biology and Physiology of Tendons. In: Gomes ME, Reis RL, Rodrigues MT editors. Tendon Regeneration - Understanding Tissue Physiology and Development to Engineer Functional Substitutes. London, UK: Elsevier; pp. 41-77.

11. Schweitzer R, Chyung JH, Murtaugh LC, et al. 2001. Analysis of the tendon cell fate using Scleraxis, a specific marker for tendons and ligaments. Development 128: 3855-3866.

12. Shukunami C, Takimoto A, Oro M, et al. 2006. Scleraxis positively regulates the expression of tenomodulin, a differentiation marker of tenocytes. Dev Biol 298: 234-247.

13. Docheva D, Hunziker EB, Fassler R, et al. 2005. Tenomodulin is necessary for tenocyte proliferation and tendon maturation. Mol Cell Biol 25: 699-705.

14. Jelinsky SA, Archambault J, Li L, et al. 2010. Tendon-selective genes identified from rat and human musculoskeletal tissues. J Orthop Res 28: 289-297.

15. O'Brien M. 1997. Structure and metabolism of tendons. Scand J Med Sci Sports 7: 55-61.

16. Komi PV, Fukashiro S, Jarvinen M. 1992. Biomechanical Loading of Achilles Tendon During Normal Locomotion. Clinics in Sports Medicine 11: 521-531.

17. Wang JHC. 2006. Mechanobiology of tendon. J Biomech 39: 1563-1582.

18. Butler DL, Juncosa N, Dressler MR. 2004. Functional efficacy of tendon repair processes. Annu Rev Biomed Eng 6: 303-329.

19. Sun L, Zhou XH, Wu B, et al. 2012. Inhibitory Effect of Synovial Fluid on Tendon-to-Bone Healing: An Experimental Study in Rabbits. Arthroscopy 28: 1297-1305.

20. Cimino F, Volk BS, Setter D. 2010. Anterior Cruciate Ligament Injury: Diagnosis, Management, and Prevention. Am Fam Physician 82: 917-922.

21. Aurora A, McCarron J, Iannotti JP, et al. 2007. Commercially available extracellular matrix materials for rotator cuff repairs: State of the art and future trends. J Shoulder Elbow Surg 16: 171S-178S.

22. Sharma P, Maffulli N. 2006. Biology of tendon injury: healing, modeling and remodeling. J Musculoskelet Neuron Interact 6: 181-190.

23. Molloy T, Wang Y, Murrell GAC. 2003. The Roles of Growth Factors in Tendon and Ligament Healing. Sports Med 33: 381-394.

24. Galatz LM, Gerstenfeld L, Heber-Katz E, et al. 2015. Tendon Regeneration and Scar Formation: The Concept of Scarless Healing. J Orthop Res 33: 823-831.

25. Abramowitch SD, Yagi M, Tsuda E, et al. 2003. The healing medial collateral ligament following a combined anterior cruciate and medial collateral ligament injury - a biomechanical study in a goat model. J Orthop Res 21: 1124-1130.

26. Barber FA, Burns JP, Deutsch A, et al. 2012. A Prospective, Randomized Evaluation of Acellular Human Dermal Matrix Augmentation for Arthroscopic Rotator Cuff Repair. Arthroscopy 28: 8-15.

27. Iannotti JP, Codsi MJ, Kwon YW, et al. 2006. Porcine small intestine submucosa augmentation of surgical repair of chronic two-tendon rotator cuff tears - A randomized, controlled trial. J Bone Jt Surg (Am) 88A: 1238-1244.

28. Surgeons AAoO. 2010. American Academy of Orthopaedic Surgeons Clinical Practice Guideline on Optimizing the Management of Rotator Cuff Problems - Guidelines and Evidence Report. Rosemont, IL: American Academy of Orthopaedic Surgeons.

29. Hernigou P, Lachaniette CHF, Delambre J, et al. 2014. Biologic augmentation of rotator cuff repair with mesenchymal stem cells during arthroscopy improves healing and prevents further tears: a case-controlled study. International Orthopaedics 38: 1811-1818.

30. Gadjanski I, Vunjak-Novakovic G. 2015. Challenges in engineering osteochondral tissue grafts with hierarchical structures. Expert Opinion on Biological Therapy 15: 1583-1599.

31. Buckwalter JA, Mankin HJ. 1997. Articular cartilage .1. Tissue design and chondrocyte-matrix interactions. J Bone Jt Surg (Am) 79A: 600-611.

32. Ludwig TE, Hunter MM, Schmidt TA. 2015. Cartilage boundary lubrication synergism is mediated by hyaluronan concentration and PRG4 concentration and structure. BMC Musculoskel Disord 16.

33. Li S, Oreffo ROC, Sengers BG, et al. 2014. The Effect of Oxygen Tension on Human Articular Chondrocyte Matrix Synthesis: Integration of Experimental and Computational Approaches. Biotechnol Bioeng 111: 1876-1885.

34. Lawrence RC, Felson DT, Helmick CG, et al. 2008. Estimates of the prevalence of arthritis and other rheumatic conditions in the United States. Arthritis and Rheumatism 58: 26-35.

35. Brown TD, Johnston RC, Saltzman CL, et al. 2006. Posttraumatic osteoarthritis: A first estimate of incidence, prevalence, and burden of disease. Journal of Orthopaedic Trauma 20: 739-744.

36. Sekiya I, Ojima M, Suzuki S, et al. 2012. Human mesenchymal stem cells in synovial fluid increase in the knee with degenerated cartilage and osteoarthritis. J Orthop Res 30: 943-949.

37. Jiang Y, Cai Y, Zhang W, et al. 2016. Human Cartilage-Derived Progenitor Cells From Committed Chondrocytes for Efficient Cartilage Repair and Regeneration. Stem Cells Translational Medicine 5: 733-744.

38. Jiang Y, Tuan RS. 2015. Origin and function of cartilage stem/progenitor cells in osteoarthritis. Nat Rev Rheumatol 11: 206-212.

39. Makris EA, Gomoll AH, Malizos KN, et al. 2015. Repair and tissue engineering techniques for articular cartilage. Nat Rev Rheumatol 11: 21-34.

40. Brittberg M, Lindahl A, Nilsson A, et al. 1994. Treatment of Deep Cartilage Defects in the Knee with Autologous Chondrocyte Transplantation. New Engl J Med 331: 889-895.

41. Kozhemyakina E, Lassar AB, Zelzer E. 2015. A pathway to bone: signaling molecules and transcription factors involved in chondrocyte development and maturation. Development 142: 817-831.

42. Pitsillides AA, Ashhurst DE. 2008. A critical evaluation of specific aspects of joint development. Dev Dyn 237: 2284-2294.

43. Quintana L, Nieden NIZ, Semino CE. 2009. Morphogenetic and Regulatory Mechanisms During Developmental Chondrogenesis: New Paradigms for Cartilage Tissue Engineering. Tissue Eng Part B 15: 29-41.

44. Huang BJ, Hu JC, Athanasiou KA. 2016. Cell-based tissue engineering strategies used in the clinical repair of articular cartilage. Biomaterials 98: 1-22.

45. Zlotnicki JP, Geeslin AG, Murray IR, et al. 2016. Biologic Treatments for Sports Injuries II Think TankCurrent Concepts, Future Research, and Barriers to Advancement, Part 3: Articular Cartilage. Orthop J Sports Med 4.

46. Lozito TP, Alexander PG, Lin H, et al. 2013. Three-dimensional osteochondral microtissue to model pathogenesis of osteoarthritis. Stem Cell Res Ther 4.

47. Cheng HW, Luk KDK, Cheung KMC, et al. 2011. In vitro generation of an osteochondral interface from mesenchymal stem cell-collagen microspheres. Biomaterials 32: 1526-1535.

48. Zhang W, Lian Q, Li D, et al. 2014. Cartilage Repair and Subchondral Bone Migration Using 3D Printing Osteochondral Composites: A One-Year-Period Study in Rabbit Trochlea. Biomed Research International.

49. Chevrier A, Nelea M, Hurtig MB, et al. 2009. Meniscus Structure in Human, Sheep, and Rabbit for Animal Models of Meniscus Repair. J Orthop Res 27: 1197-1203.

50. Fox AJS, Bedi A, Rodeo S. 2012. The basic science of human knee menisci: structure, composition, and function. Sports Health: A Multidisciplinary Approach 4: 340-351.

51. Makris EA, Hadidi P, Athanasiou KA. 2011. The knee meniscus: Structure-function, pathophysiology, current repair techniques, and prospects for regeneration. Biomaterials 32: 7411-7431.

52. Andrews SHJ, Rattner JB, Abusara Z, et al. 2014. Tie-fibre structure and organization in the knee menisci. J Anat 224: 531-537.

53. Vanderploeg EJ, Wilson CG, Imler SM, et al. 2012. Regional variations in the distribution and colocalization of extracellular matrix proteins in the juvenile bovine meniscus. J Anat 221: 174-186.

54. Nakano T, Dodd CM, Scott PG. 1997. Glycosaminoglycans and proteoglycans from different zones of the porcine knee meniscus. J Orthop Res 15: 213-220.

55. Zhang X, Aoyama T, Ito A, et al. 2014. Regional comparisons of porcine menisci. J Orthop Res 32: 1602-1611.

56. Upton ML, Chen J, Setton LA. 2006. Region-specific constitutive gene expression in the adult porcine meniscus. J Orthop Res 24: 1562-1570.

57. Fairbank TJ. 1948. Knee joint changes after meniscectomy. J Bone Jt Surg (Br) 30: 664-670.

58. Krause WR, Pope MH, Johnson RJ, et al. 1976. Mechanical changes in the knee after meniscectomy. J Bone Jt Surg (Am) 58: 599-604.

59. Bedi A, Kelly NH, Baad M, et al. 2010. Dynamic Contact Mechanics of the Medial Meniscus as a Function of Radial Tear, Repair, and Partial Meniscectomy. J Bone Jt Surg (Am) 92A: 1398-1408.

60. Bedi A, Kelly N, Baad M, et al. 2012. Dynamic Contact Mechanics of Radial Tears of the Lateral Meniscus: Implications for Treatment. Arthroscopy 28: 372-381.

61. Hutchinson ID, Moran CJ, Potter HG, et al. 2014. Restoration of the Meniscus Form and Function. Am J Sports Med 42: 987-998.

62. Arnoczky SP, Warren RF. 1983. The microvasculature of the meniscus and its response to injury - an experimental study in the dog. Am J Sports Med 11: 131-141.

63. Mauck RL, Martinez-Diaz GJ, Yuan X, et al. 2007. Regional multilineage differentiation potential of meniscal fibrochondrocytes: Implications for meniscus repair. Anatomical Record-Advances in Integrative Anatomy and Evolutionary Biology 290: 48-58.

64. Matsukura Y, Muneta T, Tsuji K, et al. 2014. Mesenchymal Stem Cells in Synovial Fluid Increase After Meniscus Injury. Clin Orthop Relat Res 472: 1357-1364.

65. Muhammad H, Schminke B, Bode C, et al. 2014. Human Migratory Meniscus Progenitor Cells Are Controlled via the TGF-beta Pathway. Stem Cell Reports 3: 789-803.

66. Abrams GD, Frank RM, Gupta AK, et al. 2013. Trends in Meniscus Repair and Meniscectomy in the United States, 2005-2011. Am J Sports Med 41: 2333-2339.

67. Beamer BS, Masoudi A, Walley KC, et al. 2015. Analysis of a New All-Inside Versus Inside-Out Technique for Repairing Radial Meniscal Tears. Arthroscopy 31: 293-298.

68. Matsubara H, Okazaki K, Izawa T, et al. 2012. New Suture Method for Radial Tears of the Meniscus Biomechanical Analysis of Cross-Suture and Double Horizontal Suture Techniques Using Cyclic Load Testing. Am J Sports Med 40: 414-418.

69. Bhatia S, Civitarese DM, Turnbull TL, et al. 2015. A Novel Repair Method for Radial Tears of the Medial Meniscus: Biomechanical Comparison of Transtibial 2-Tunnel and Double Horizontal Mattress Suture Techniques Under Cyclic Loading. Am J Sports Med 44: 639-645.

70. James EW, LaPrade CM, Feagin JA, et al. 2015. Repair of a complete radial tear in the midbody of the medial meniscus using a novel crisscross suture transtibial tunnel surgical technique: a case report. Knee Surg Sports Traumatol Arthrosc 23: 2750-2755.

71. Choi N-H, Kim T-H, Son K-M, et al. 2010. Meniscal Repair for Radial Tears of the Midbody of the Lateral Meniscus. Am J Sports Med 38: 2472-2476.

72. Arnoczky SP, Warren RF, Spivak JM. 1988. Meniscal Repair Using an Exogenous Fibrin Clot - An Experimental Study in Dogs. J Bone Jt Surg (Am) 70A: 1209-1216.

73. Zhang ZN, Arnold JA, Williams T, et al. 1995. Repairs by Trephination and Suturing of Longitudinal Injuries in the Avascular Area of the Meniscus in Goats. Am J Sports Med 23: 35-41.

74. Cook JL, Fox DB. 2007. A novel bioabsorbable conduit augments healing of avascular meniscal tears in a dog model. Am J Sports Med 35: 1877-1887.

75. Taylor SA, Rodeo SA. 2013. Augmentation techniques for isolated meniscal tears. Curr Rev Musculoskelet Med 6: 95-101.

76. Yu H, Adesida AB, Jomha NM. 2015. Meniscus repair using mesenchymal stem cells - a comprehensive review. Stem Cell Res Ther 6.

77. Angele P, Kujat R, Koch M, et al. 2014. Role of mesenchymal stem cells in meniscal repair. J Exp Orthop 1: 12-12.

78. Vangsness CT, Jr., Farr J, II, Boyd J, et al. 2014. Adult Human Mesenchymal Stem Cells Delivered via Intra-Articular Injection to the Knee Following Partial Medial Meniscectomy A Randomized, Double-Blind, Controlled Study. J Bone Jt Surg (Am) 96A: 90-98.

79. Moran CJ, Busilacchi A, Lee CA, et al. 2015. Biological Augmentation and Tissue Engineering Approaches in Meniscus Surgery. Arthroscopy 31: 944-955.

80. Londono R, Badylak SF. 2015. Biologic Scaffolds for Regenerative Medicine: Mechanisms of In vivo Remodeling. Ann Biomed Eng 43: 577-592.

81. Ott HC, Matthiesen TS, Goh S-K, et al. 2008. Perfusion-decellularized matrix: using nature's platform to engineer a bioartificial heart. Nat Med 14: 213-221.

82. Uygun BE, Soto-Gutierrez A, Yagi H, et al. 2010. Organ reengineering through development of a transplantable recellularized liver graft using decellularized liver matrix. Nat Med 16: 814-U120.

83. Petersen TH, Calle EA, Zhao L, et al. 2010. Tissue-Engineered Lungs for in Vivo Implantation. Science 329: 538-541.

84. Benders KEM, van Weeren PR, Badylak SF, et al. 2013. Extracellular matrix scaffolds for cartilage and bone regeneration. Trends Biotechnol 31: 169-176.

85. Youngstrom DW, Barrett JG, Jose RR, et al. 2013. Functional characterization of detergent-decellularized equine tendon extracellular matrix for tissue engineering applications. PloS one 8: e64151.

86. Stapleton TW, Ingram J, Fisher J, et al. 2011. Investigation of the Regenerative Capacity of an Acellular Porcine Medial Meniscus for Tissue Engineering Applications. Tissue Eng Part A 17: 231-242.

87. Deeken CR, White AK, Bachman SL, et al. 2011. Method of preparing a decellularized porcine tendon using tributyl phosphate. J Biomed Mater Res B Appl Biomater 96B: 199-206.

88. Ning LJ, Zhang Y, Chen XH, et al. 2012. Preparation and characterization of decellularized tendon slices for tendon tissue engineering. Journal of Biomedical Materials Research Part A 100A: 1448-1456.

89. Ning LJ, Zhang YJ, Zhang Y, et al. 2015. The utilization of decellularized tendon slices to provide an inductive microenvironment for the proliferation and tenogenic differentiation of stem cells. Biomaterials 52: 539-550.

90. Yin Z, Chen X, Zhu T, et al. 2013. The effect of decellularized matrices on human tendon stem/progenitor cell differentiation and tendon repair. Acta Biomater 9: 9317-9329.

91. Baker AR, McCarron JA, Tan CD, et al. 2012. Does Augmentation with a Reinforced Fascia Patch Improve Rotator Cuff Repair Outcomes? Clin Orthop Relat Res 470: 2513-2521.

92. Aurora A, McCarron JA, van den Bogert AJ, et al. 2012. The biomechanical role of scaffolds in augmented rotator cuff tendon repairs. J Shoulder Elbow Surg 21: 1064-1071.

93. Schwarz S, Koerber L, Elsaesser AF, et al. 2012. Decellularized Cartilage Matrix as a Novel Biomatrix for Cartilage Tissue-Engineering Applications. Tissue Eng Part A 18: 2195-2209.

94. Chen Y-C, Chen R-N, Jhan H-J, et al. 2015. Development and Characterization of Acellular Extracellular Matrix Scaffolds from Porcine Menisci for Use in Cartilage Tissue Engineering. Tissue Eng Part C 21: 971-986.

95. Farr J, Graciteli GC, Shah N, et al. 2016. High Failure Rate of a Decellularized Osteochondral Allograft for the Treatment of Cartilage Lesions. Am J Sports Med 44: 2015-2022.

96. Rowland CR, Lennon DP, Caplan AI, et al. 2013. The effects of crosslinking of scaffolds engineered from cartilage ECM Cross Mark on the chondrogenic differentiation of MSCs. Biomaterials 34: 5802-5812.

97. Cheng NC, Estes BT, Young TH, et al. 2013. Genipin-Crosslinked Cartilage-Derived Matrix as a Scaffold for Human Adipose-Derived Stem Cell Chondrogenesis. Tissue Eng Part A 19: 484-496.

98. Rowland CR, Colucci LA, Guilak F. 2016. Fabrication of anatomically-shaped cartilage constructs using decellularized cartilage-derived matrix scaffolds. Biomaterials 91: 57-72.

99. Almeida HV, Liu Y, Cunniffe GM, et al. 2014. Controlled release of transforming growth factor-beta 3 from cartilage-extra-cellular-matrix-derived scaffolds to promote chondrogenesis of human-joint-tissue-derived stem cells. Acta Biomater 10: 4400-4409.

100. Almeida HV, Cunniffe GM, Vinardell T, et al. 2015. Coupling Freshly Isolated CD44(+) Infrapatellar Fat Pad-Derived Stromal Cells with a TGF-3 Eluting Cartilage ECM-Derived Scaffold as a Single-Stage Strategy for Promoting Chondrogenesis. Adv Healthc Mater 4: 1043-1053.

101. Almeida HV, Eswaramoorthy R, Cunniffe GM, et al. 2016. Fibrin hydrogels functionalized with cartilage extracellular matrix and incorporating freshly isolated stromal cells as an injectable for cartilage regeneration. Acta Biomater 36: 55-62.

102. Little D, Guilak F, Ruch DS. 2010. Ligament-Derived Matrix Stimulates a Ligamentous Phenotype in Human Adipose-Derived Stem Cells. Tissue Eng Part A 16: 2307-2319.

103. Chainani A, Hippensteel KJ, Kishan A, et al. 2013. Multilayered Electrospun Scaffolds for Tendon Tissue Engineering. Tissue Eng Part A 19: 2594-2604.

104. Wolf MT, Daly KA, Brennan-Pierce EP, et al. 2012. A hydrogel derived from decellularized dermal extracellular matrix. Biomaterials 33: 7028-7038.

105. Kim MY, Farnebo S, Woon CYL, et al. 2014. Augmentation of Tendon Healing with an Injectable Tendon Hydrogel in a Rat Achilles Tendon Model. Plast Reconstr Surg 133: 645E-653E.

106. Farnebo S, Woon CYL, Schmitt T, et al. 2014. Design and Characterization of an Injectable Tendon Hydrogel: A Novel Scaffold for Guided Tissue Regeneration in the Musculoskeletal System. Tissue Eng Part A 20: 1550-1561.

107. Pati F, Jang J, Ha D-H, et al. 2014. Printing three-dimensional tissue analogues with decellularized extracellular matrix bioink. Nature Communications 5.

108. Kwon JS, Yoon SM, Shim SW, et al. 2013. Injectable extracellular matrix hydrogel developed using porcine articular cartilage. Int J Pharm 454: 183-191.

109. Wu J, Ding Q, Dutta A, et al. 2015. An injectable extracellular matrix derived hydrogel for meniscus repair and regeneration. Acta Biomater 16: 49-59.

110. Beck EC, Barragan M, Tadros MH, et al. 2016. Chondroinductive Hydrogel Pastes Composed of Naturally Derived Devitalized Cartilage. Ann Biomed Eng 44: 1863-1880.

111. Visser J, Levett PA, te Moller NCR, et al. 2015. Crosslinkable Hydrogels Derived from Cartilage, Meniscus, and Tendon Tissue. Tissue Eng Part A 21: 1195-1206.

112. DeQuach JA, Mezzano V, Miglani A, et al. 2010. Simple and High Yielding Method for Preparing Tissue Specific Extracellular Matrix Coatings for Cell Culture. Plos One 5.

113. Zhang YY, He YJ, Bharadwaj S, et al. 2009. Tissue-specific extracellular matrix coatings for the promotion of cell proliferation and maintenance of cell phenotype. Biomaterials 30: 4021-4028.

114. Lin H, Yang G, Tan J, et al. 2012. Influence of decellularized matrix derived from human mesenchymal stem cells on their proliferation, migration and multi-lineage differentiation potential. Biomaterials 33: 4480-4489.

115. Yang G, Rothrauff BB, Lin H, et al. 2013. Enhancement of tenogenic differentiation of human adipose stem cells by tendon-derived extracellular matrix. Biomaterials 34: 9295-9306.

116. Kim TG, Shin H, Lim DW. 2012. Biomimetic Scaffolds for Tissue Engineering. Adv Funct Mater 22: 2446-2468.

117. Murphy WL, McDevitt TC, Engler AJ. 2014. Materials as stem cell regulators. Nature Materials 13: 547-557.

118. Rim NG, Shin CS, Shin H. 2013. Current approaches to electrospun nanofibers for tissue engineering. Biomed Mater 8.

119. Li W-J, Mauck RL, Cooper JA, et al. 2007. Engineering controllable anisotropy in electrospun biodegradable nanofibrous scaffolds for musculoskeletal tissue engineering. J Biomech 40: 1686-1693.

120. Spanoudes K, Gaspar D, Pandit A, et al. 2014. The biophysical, biochemical, and biological toolbox for tenogenic phenotype maintenance in vitro. Trends Biotechnol 32: 474-482.

121. Chen JL, Zhang W, Liu ZY, et al. 2015. Physical regulation of stem cells differentiation into teno-lineage: current strategies and future direction. Cell Tissue Res 360: 195-207.

122. Cardwell RD, Dahlgren LA, Goldstein AS. 2014. Electrospun fibre diameter, not alignment, affects mesenchymal stem cell differentiation into the tendon/ligament lineage. J Tissue Eng Regen Med 8: 937-945.

123. Erisken C, Zhang X, Moffat KL, et al. 2013. Scaffold Fiber Diameter Regulates Human Tendon Fibroblast Growth and Differentiation. Tissue Eng Pt A 19: 519-528.

124. Moffat KL, Kwei ASP, Spalazzi JP, et al. 2009. Novel Nanofiber-Based Scaffold for Rotator Cuff Repair and Augmentation. Tissue Eng Part A 15: 115-126.

125. Zhang C, Yuan HH, Liu HH, et al. 2015. Well-aligned chitosan-based ultrafine fibers committed teno-lineage differentiation of human induced pluripotent stem cells for Achilles tendon regeneration. Biomaterials 53: 716-730.

126. James R, Kumbar SG, Laurencin CT, et al. 2011. Tendon tissue engineering: adipose-derived stem cell and GDF-5 mediated regeneration using electrospun matrix systems. Biomed Mater 6: 13.

127. Leung M, Jana S, Tsao CT, et al. 2013. Tenogenic differentiation of human bone marrow stem cells via a combinatory effect of aligned chitosan-polycaprolactone nanofibers and TGF-beta 3. J Mater Chem B 1: 6516-6524.

128. Subramony SD, Dargis BR, Castillo M, et al. 2013. The guidance of stem cell differentiation by substrate alignment and mechanical stimulation. Biomaterials 34: 1942-1953.

129. Kishore V, Bullock W, Sun XH, et al. 2012. Tenogenic differentiation of human MSCs induced by the topography of electrochemically aligned collagen threads. Biomaterials 33: 2137-2144.

130. Gilchrist CL, Ruch DS, Little D, et al. 2014. Micro-scale and meso-scale architectural cues cooperate and compete to direct aligned tissue formation. Biomaterials 35: 10015-10024.

131. Madry H, Rey-Rico A, Venkatesan JK, et al. 2014. Transforming Growth Factor Beta-Releasing Scaffolds for Cartilage Tissue Engineering. Tissue Eng Part B 20: 106-125.

132. Lai JH, Kajiyama G, Smith RL, et al. 2013. Stem cells catalyze cartilage formation by neonatal articular chondrocytes in 3D biomimetic hydrogels. Scientific Reports 3.

133. Nichol JW, Koshy ST, Bae H, et al. 2010. Cell-laden microengineered gelatin methacrylate hydrogels. Biomaterials 31: 5536-5544.

134. Lin H, Cheng AW-M, Alexander PG, et al. 2014. Cartilage tissue engineering application of injectable gelatin hydrogel with in situ visible-light-activated gelation capability in both air and aqueous solution. Tissue Eng Part A 20: 2402-2411.

135. Levett PA, Melchels FPW, Schrobback K, et al. 2014. A biomimetic extracellular matrix for cartilage tissue engineering centered on photocurable gelatin, hyaluronic acid and chondroitin sulfate. Acta Biomater 10: 214-223.

136. Kelly BT, Robertson W, Potter HG, et al. 2007. Hydrogel meniscal replacement in the sheep knee - Preliminary evaluation of chondroprotective effects. Am J Sports Med 35: 43-52.

137. Puetzer JL, Bonassar LJ. 2013. High density type I collagen gels for tissue engineering of whole menisci. Acta Biomater 9: 7787-7795.

138. Puetzer JL, Bonassar LJ. 2016. Physiologically Distributed Loading Patterns Drive the Formation of Zonally Organized Collagen Structures in Tissue Engineered Meniscus. Tissue Eng Part A 22: 907-916.

139. Jülke H, Mainil-Varlet P, Jakob RP, et al. 2015. The Role of Cells in Meniscal Guided Tissue Regeneration: A Proof of Concept Study in a Goat Model. Cartilage 6: 20-29.

140. Lomas AJ, Ryan CNM, Sorushanova A, et al. 2015. The past, present and future in scaffold-based tendon treatments. Adv Drug Del Rev 84: 257-277.

141. Yang G, Rothrauff BB, Tuan RS. 2013. Tendon and Ligament Regeneration and Repair: Clinical Relevance and Developmental Paradigm. Birth Defects Res C Embryo Today 99: 203-222.

142. Mollon B, Kandel R, Chahal J, et al. 2013. The clinical status of cartilage tissue regeneration in humans. Osteoarthritis Cartilage 21: 1824-1833.

143. Bian L, Guvendiren M, Mauck RL, et al. 2013. Hydrogels that mimic developmentally relevant matrix and N-cadherin interactions enhance MSC chondrogenesis. Proc Natl Acad Sci 110: 10117-10122.

144. Lai JH, Rogan H, Kajiyama G, et al. 2015. Interaction Between Osteoarthritic Chondrocytes and Adipose-Derived Stem Cells Is Dependent on Cell Distribution in Three-Dimension and Transforming Growth Factor-beta 3 Induction. Tissue Eng Part A 21: 992-1002.

145. Havis E, Bonnin MA, Olivera-Martinez I, et al. 2014. Transcriptomic analysis of mouse limb tendon cells during development. Development 141: 3683-3696.

146. Wang W, Rigueur D, Lyons KM. 2014. TGF beta signaling in cartilage development and maintenance. Birth Defects Res C Embryo Today 102: 37-51.

147. Lorda-Diez CI, Montero JA, Garcia-Porrero JA, et al. 2014. Divergent Differentiation of Skeletal Progenitors into Cartilage and Tendon: Lessons from the Embryonic Limb. ACS Chem Biol 9: 72-79.

148. Schulze-Tanzil G, Al-Sadi O, Ertel W, et al. 2012. Decellularized tendon extracellular matrix-a valuable approach for tendon reconstruction? Cells 1: 1010-1028.

149. Pati F, Jang J, Ha DH, et al. 2014. Printing three-dimensional tissue analogues with decellularized extracellular matrix bioink. Nat Commun 5: 11.

150. Keane TJ, DeWard A, Londono R, et al. 2015. Tissue-Specific Effects of Esophageal Extracellular Matrix. Tissue Eng Part A 21: 2293-2300.

151. Inman GJ, Nicolas FJ, Callahan JF, et al. 2002. SB-431542 is a potent and specific inhibitor of transforming growth factor-beta superfamily type I activin receptor-like kinase (ALK) receptors ALK4, ALK5, and ALK7. Mol Pharmacol 62: 65-74.

152. Valentin JE, Badylak JS, McCabe GP, et al. 2006. Extracellular matrix bioscaffolds for orthopaedic applications - A comparative histologic study. J Bone Jt Surg (Am) 88A: 2673-2686.

153. Keane TJ, Londono R, Turner NJ, et al. 2012. Consequences of ineffective decellularization of biologic scaffolds on the host response. Biomaterials 33: 1771-1781.

154. Wolf MT, Daly KA, Reing JE, et al. 2012. Biologic scaffold composed of skeletal muscle extracellular matrix. Biomaterials 33: 2916-2925.

155. Tuli R, Tuli S, Nandi S, et al. 2003. Transforming growth factor-beta-mediated chondrogenesis of human mesenchymal progenitor cells involves N-cadherin and mitogenactivated protein kinase and Wnt signaling cross-talk. J Biol Chem 278: 41227-41236.

156. Lorda-Diez CI, Montero JA, Diaz-Mendoza MJ, et al. 2013. beta ig-h3 Potentiates the Profibrogenic Effect of TGF beta Signaling on Connective Tissue Progenitor Cells Through the Negative Regulation of Master Chondrogenic Genes. Tissue Eng Part A 19: 448-457.

157. Lorda-Diez CI, Montero JA, Martinez-Cue C, et al. 2009. Transforming Growth Factors beta Coordinate Cartilage and Tendon Differentiation in the Developing Limb Mesenchyme. J Biol Chem 284: 29988-29996.

158. Lorda-Diez CI, Montero JA, Choe S, et al. 2014. Ligand- and Stage-Dependent Divergent Functions of BMP Signaling in the Differentiation of Embryonic Skeletogenic Progenitors In Vitro. J Bone Miner Res 29: 735-748.

159. Sutherland AJ, Beck EC, Dennis SC, et al. 2015. Decellularized Cartilage May Be a Chondroinductive Material for Osteochondral Tissue Engineering. Plos One 10.

160. Visser J, Gawlitta D, Benders KEM, et al. 2015. Endochondral bone formation in gelatin methacrylamide hydrogel with embedded cartilage-derived matrix particles. Biomaterials 37: 174-182.

161. Li WJ, Laurencin CT, Caterson EJ, et al. 2002. Electrospun nanofibrous structure: A novel scaffold for tissue engineering. J Biomed Mater Res 60: 613-621.

162. Furumatsu T, Shukunami C, Amemiya-Kudo M, et al. 2010. Scleraxis and E47 cooperatively regulate the Sox9-dependent transcription. Int J Biochem Cell Biol 42: 148-156.

163. Smeriglio P, Dhulipala L, Lai JH, et al. 2015. Collagen VI Enhances Cartilage Tissue Generation by Stimulating Chondrocyte Proliferation. Tissue Eng Part A 21: 840-849.

164. Grogan SP, Chen X, Sovani S, et al. 2014. Influence of Cartilage Extracellular Matrix Molecules on Cell Phenotype and Neocartilage Formation. Tissue Eng Part A 20: 264-274.

165. Wang T, Lai JH, Han L-H, et al. 2014. Chondrogenic Differentiation of Adipose-Derived Stromal Cells in Combinatorial Hydrogels Containing Cartilage Matrix Proteins with Decoupled Mechanical Stiffness. Tissue Eng Part A 20: 2131-2139.

166. Sun Y, Jiang Y, Liu QJ, et al. 2013. Biomimetic Engineering of Nanofibrous Gelatin Scaffolds with Noncollagenous Proteins for Enhanced Bone Regeneration. Tissue Eng Part A 19: 1754-1763.

167. Crapo PM, Tottey S, Slivka PF, et al. 2014. Effects of Biologic Scaffolds on Human Stem Cells and Implications for CNS Tissue Engineering. Tissue Eng Part A 20: 313-323.

168. Sicari BM, Dziki JL, Siu BF, et al. 2014. The promotion of a constructive macrophage phenotype by solubilized extracellular matrix. Biomaterials 35: 8605-8612.

169. Meng FW, Sliyka PF, Dearth CL, et al. 2015. Solubilized extracellular matrix from brain and urinary bladder elicits distinct functional and phenotypic responses in macrophages. Biomaterials 46: 131-140.

170. Tottey S, Johnson SA, Crapo PM, et al. 2011. The effect of source animal age upon extracellular matrix scaffold properties. Biomaterials 32: 128-136.

171. Slivka PF, Dearth CL, Keane TJ, et al. 2014. Fractionation of an ECM hydrogel into structural and soluble components reveals distinctive roles in regulating macrophage behavior. Biomater Sci 2: 1521-1534.

172. Brown BN, Londono R, Tottey S, et al. 2012. Macrophage phenotype as a predictor of constructive remodeling following the implantation of biologically derived surgical mesh materials. Acta Biomater 8: 978-987.

173. Brown BN, Ratner BD, Goodman SB, et al. 2012. Macrophage polarization: An opportunity for improved outcomes in and regenerative medicine. Biomaterials 33: 3792-3802.

174. Sutherland AJ, Converse GL, Hopkins RA, et al. 2015. The Bioactivity of Cartilage Extracellular Matrix in Articular Cartilage Regeneration. Adv Healthc Mater 4: 29-39.

175. Nourissat G, Berenbaum F, Duprez D. 2015. Tendon injury: from biology to tendon repair. Nat Rev Rheumatol 11: 223-233.

176. Bach BRJ, Tradonsky S, Bojchuk J, et al. 1998. Arthroscopically assisted anterior cruciate ligament reconstruction using patellar tendon autograft. Five- to nine-year follow-up evaluation. Am J Sports Med 26: 20-29.

177. Duquin TR, Buyea C, Bisson LJ. 2010. Which method of rotator cuff repair leads to the highest rate of structural healing? A systematic review. Am J Sports Med 38: 835-841.

178. Liu CF, Aschbacher-Smith L, Barthelery NJ, et al. 2011. What we should know before using tissue engineering techniques to repair injured tendons: a developmental biology perspective. Tissue Eng Part B Rev 17: 165-176.

179. Violini S, Ramelli P, Pisani LF, et al. 2009. Horse bone marrow mesenchymal stem cells express embryo stem cell markers and show the ability for tenogenic differentiation by in vitro exposure to BMP-12. BMC Cell Biol 10: 29.

180. Dai L, Hu X, Zhang X, et al. 2015. Different tenogenic differentiation capacities of different mesenchymal stem cells in the presence of BMP-12. Journal of translational medicine 13: 200.

181. Schon LC, Gill N, Thorpe M, et al. 2014. Efficacy of a mesenchymal stem cell loaded surgical mesh for tendon repair in rats. Journal of translational medicine 12: 110.

182. Konno M, Hamabe A, Hasegawa S, et al. 2013. Adipose-derived mesenchymal stem cells and regenerative medicine. Dev Growth Differ 55: 309-318.

183. Mizuno H, Tobita M, Uysal AC. 2012. Concise review: Adipose-derived stem cells as a novel tool for future regenerative medicine. Stem Cells 30: 804-810.

184. Park A, Hogan MV, Kesturu GS, et al. 2010. Adipose-derived mesenchymal stem cells treated with growth differentiation factor-5 express tendon-specific markers. Tissue engineering Part A 16: 2941-2951.

185. Shen H, Gelberman RH, Silva MJ, et al. 2013. BMP12 induces tenogenic differentiation of adipose-derived stromal cells. PloS one 8: e77613.

186. Zeng Q, Li X, Beck G, et al. 2007. Growth and differentiation factor-5 (GDF-5) stimulates osteogenic differentiation and increases vascular endothelial growth factor (VEGF) levels in fat-derived stromal cells in vitro. Bone 40: 374-381.

187. Shen FH, Zeng Q, Lv Q, et al. 2006. Osteogenic differentiation of adipose-derived stromal cells treated with GDF-5 cultured on a novel three-dimensional sintered microsphere matrix. The spine journal : official journal of the North American Spine Society 6: 615-623.

188. Feng G, Wan Y, Balian G, et al. 2008. Adenovirus-mediated expression of growth and differentiation factor-5 promotes chondrogenesis of adipose stem cells. Growth Factors 26: 132-142.

189. Goncalves AI, Rodrigues MT, Lee SJ, et al. 2013. Understanding the role of growth factors in modulating stem cell tenogenesis. PloS one 8: e83734.

190. Erickson GR, Gimble JM, Franklin DM, et al. 2002. Chondrogenic potential of adipose tissue-derived stromal cells in vitro and in vivo. Biochem Biophys Res Commun 290: 763-769.

191. Munger JS, Sheppard D. 2011. Cross Talk among TGF-beta Signaling Pathways, Integrins, and the Extracellular Matrix. Cold Spring Harbor Perspectives in Biology 3.

192. Bi YM, Stuelten CH, Kilts T, et al. 2005. Extracellular matrix proteoglycans control the fate of bone marrow stromal cells. J Biol Chem 280: 30481-30489.

193. Discher DE, Mooney DJ, Zandstra PW. 2009. Growth Factors, Matrices, and Forces Combine and Control Stem Cells. Science 324: 1673-1677.

194. Liu CF, Aschbacher-Smith L, Barthelery NJ, et al. 2012. Spatial and temporal expression of molecular markers and cell signals during normal development of the mouse patellar tendon. Tissue Eng Part A 18: 598-608.

195. Lorda-Diez CI, Montero JA, Martinez-Cue C, et al. 2009. Transforming growth factors beta coordinate cartilage and tendon differentiation in the developing limb mesenchyme. J Biol Chem 284: 29988-29996.

196. Pryce BA, Watson SS, Murchison ND, et al. 2009. Recruitment and maintenance of tendon progenitors by TGFbeta signaling are essential for tendon formation. Development 136: 1351-1361.

197. Natsu-ume T, Nakamura N, Shino K, et al. 1997. Temporal and spatial expression of transforming growth factor-beta in the healing patellar ligament of the rat. J Orthop Res 15: 837-843.

198. Chen CH, Cao Y, Wu YF, et al. 2008. Tendon healing in vivo: gene expression and production of multiple growth factors in early tendon healing period. J Hand Surg Am 33: 1834-1842.

199. Juneja SC, Schwarz EM, O'Keefe RJ, et al. 2013. Cellular and molecular factors in flexor tendon repair and adhesions: a histological and gene expression analysis. Connect Tissue Res 54: 218-226.

200. Marturano JE, Arena JD, Schiller ZA, et al. 2013. Characterization of mechanical and biochemical properties of developing embryonic tendon. Proc Natl Acad Sci U S A 110: 6370-6375.

201. Bi Y, Ehirchiou D, Kilts TM, et al. 2007. Identification of tendon stem/progenitor cells and the role of the extracellular matrix in their niche. Nat Med 13: 1219-1227.

202. Watt FM, Huck WT. 2013. Role of the extracellular matrix in regulating stem cell fate. Nat Rev Mol Cell Biol 14: 467-473.

203. Faulk DM, Johnson SA, Zhang L, et al. 2014. Role of the extracellular matrix in whole organ engineering. J Cell Physiol 229: 984-989.

204. Bi YM, Ehirchiou D, Kilts TM, et al. 2007. Identification of tendon stem/progenitor cells and the role of the extracellular matrix in their niche. Nat Med 13: 1219-1227.

205. Zhang GY, Ezura Y, Chervoneva I, et al. 2006. Decorin regulates assembly of collagen fibrils and acquisition of biomechanical properties during tendon development. J Cell Biochem 98: 1436-1449.

206. Yang G, Rothrauff BB, Lin H, et al. 2013. Enhancement of tenogenic differentiation of human adipose stem cells by tendon-derived extracellular matrix. Biomaterials 34: 9295-9306.

207. Yin Z, Chen X, Zhu T, et al. 2013. The effect of decellularized matrices on human tendon stem/progenitor cell differentiation and tendon repair. Acta Biomater 9: 9317-9329.

208. Tuli R, Tuli S, Nandi S, et al. 2003. Characterization of multipotential mesenchymal progenitor cells derived from human trabecular bone. Stem Cells 21: 681-693.

209. Hennig T, Lorenz H, Thiel A, et al. 2007. Reduced chondrogenic potential of adipose tissue derived stromal cells correlates with an altered TGFbeta receptor and BMP profile and is overcome by BMP-6. Journal of cellular physiology 211: 682-691.

210. Lin G, Garcia M, Ning H, et al. 2008. Defining stem and progenitor cells within adipose tissue. Stem Cells Dev 17: 1053-1063.

211. Zhang J, Li B, Wang JH. 2011. The role of engineered tendon matrix in the stemness of tendon stem cells in vitro and the promotion of tendon-like tissue formation in vivo. Biomaterials 32: 6972-6981.

212. Thibault MM, Hoemann CD, Buschmann MD. 2007. Fibronectin, vitronectin, and collagen I induce chemotaxis and haptotaxis of human and rabbit mesenchymal stem cells in a standardized transmembrane assay. Stem Cells Dev 16: 489-502.

213. Singh P, Schwarzbauer JE. 2012. Fibronectin and stem cell differentiation - lessons from chondrogenesis. J Cell Sci 125: 3703-3712.

214. Bi Y, Stuelten CH, Kilts T, et al. 2005. Extracellular matrix proteoglycans control the fate of bone marrow stromal cells. J Biol Chem 280: 30481-30489.

215. Zheng Z, Jian J, Zhang X, et al. 2012. Reprogramming of human fibroblasts into multipotent cells with a single ECM proteoglycan, fibromodulin. Biomaterials 33: 5821-5831.

216. Ning LJ, Zhang Y, Chen XH, et al. 2012. Preparation and characterization of decellularized tendon slices for tendon tissue engineering. Journal of biomedical materials research Part A 100: 1448-1456.

217. Raghavan SS, Woon CY, Kraus A, et al. 2012. Optimization of human tendon tissue engineering: synergistic effects of growth factors for use in tendon scaffold repopulation. Plast Reconstr Surg 129: 479-489.

218. Schmitt T, Fox PM, Woon CY, et al. 2013. Human flexor tendon tissue engineering: in vivo effects of stem cell reseeding. Plast Reconstr Surg 132: 567e-576e.

219. Vindigni V, Tonello C, Lancerotto L, et al. 2013. Preliminary report of in vitro reconstruction of a vascularized tendonlike structure: a novel application for adipose-derived stem cells. Ann Plast Surg 71: 664-670.

220. Martinello T, Bronzini I, Volpin A, et al. 2014. Successful recellularization of human tendon scaffolds using adipose-derived mesenchymal stem cells and collagen gel. J Tissue Eng Regen Med 8: 612-619.

221. Raabe O, Shell K, Fietz D, et al. 2013. Tenogenic differentiation of equine adipose-tissue-derived stem cells under the influence of tensile strain, growth differentiation factors and various oxygen tensions. Cell Tissue Res 352: 509-521.

222. Eagan MJ, Zuk PA, Zhao KW, et al. 2011. The suitability of human adipose-derived stem cells for the engineering of ligament tissue. J Tissue Eng Regen Med.

223. Stanco D, Vigano M, Perucca Orfei C, et al. 2015. Multidifferentiation potential of human mesenchymal stem cells from adipose tissue and hamstring tendons for musculoskeletal cell-based therapy. Regen Med: 1-15.

224. Liu HH, Zhang C, Zhu SA, et al. 2015. Mohawk Promotes the Tenogenesis of Mesenchymal Stem Cells Through Activation of the TGF beta Signaling Pathway. Stem Cells 33: 443-455.

225. Silver FH, Kato YP, Ohno M, et al. 1992. Analysis of mammalian connective tissue: relationship between hierarchical structures and mechanical properties. J Long Term Eff Med Implants 2: 165-198.

226. Erisken C, Zhang X, Moffat KL, et al. 2013. Scaffold fiber diameter regulates human tendon fibroblast growth and differentiation. Tissue Eng Part A 19: 519-528.

227. Cardwell RD, Dahlgren LA, Goldstein AS. 2014. Electrospun fibre diameter, not alignment, affects mesenchymal stem cell differentiation into the tendon/ligament lineage. J Tissue Eng Regen Med 8: 937-945.

228. Kuo CK, Tuan RS. 2008. Mechanoactive Tenogenic Differentiation of Human Mesenchymal Stem Cells. Tissue Eng Pt A 14: 1615-1627.

229. Louis-Ugbo J, Leeson B, Hutton WC. 2004. Tensile properties of fresh human calcaneal (Achilles) tendons. Clin Anat 17: 30-35.

230. Zhu YB, Gao CY, Liu XY, et al. 2002. Surface modification of polycaprolactone membrane via aminolysis and biomacromolecule immobilization for promoting cytocompatibility of human endothelial cells. Biomacromolecules 3: 1312-1319.

231. Baker BM, Shah RP, Silverstein AM, et al. 2012. Sacrificial nanofibrous composites provide instruction without impediment and enable functional tissue formation. Proc Natl Acad Sci U S A 109: 14176-14181.

232. Zhang G, Ezura Y, Chervoneva I, et al. 2006. Decorin regulates assembly of collagen fibrils and acquisition of biomechanical properties during tendon development. J Cell Biochem 98: 1436-1449.

233. Kilts T, Ameye L, Syed-Picard F, et al. 2009. Potential roles for the small leucine-rich proteoglycans biglycan and fibromodulin in ectopic ossification of tendon induced by exercise and in modulating rotarod performance. Scand J Med Sci Sports 19: 536-546.

234. Chakravarti S. 2002. Functions of lumican and fibromodulin: lessons from knockout mice. Glycoconj J 19: 287-293.

235. Halasz K, Kassner A, Morgelin M, et al. 2007. COMP acts as a catalyst in collagen fibrillogenesis. J Biol Chem 282: 31166-31173.

236. McDermott ID, Amis AA. 2006. The consequences of meniscectomy. J Bone Joint Surg Br 88: 1549-1556.

237. Beaupre A, Choukroun R, Guidouin R, et al. 1986. Knee menisci. Correlation between microstructure and biomechanics. Clin Orthop Relat Res: 72-75.

238. Krause WR, Pope MH, Johnson RJ, et al. 1976. Mechanical changes in the knee after meniscectomy. J Bone Joint Surg Am 58: 599-604.

239. Walker PS, Erkman MJ. 1975. The role of the menisci in force transmission across the knee. Clin Orthop Relat Res: 184-192.

240. Makris EA, Hadidi P, Athanasiou KA. 2011. The knee meniscus: structure-function, pathophysiology, current repair techniques, and prospects for regeneration. Biomaterials 32: 7411-7431.

241. Mitchell J, Graham W, Best TM, et al. 2016. Epidemiology of meniscal injuries in US high school athletes between 2007 and 2013. Knee Surg Sports Traumatol Arthrosc 24: 715-722.

242. El Ghazaly SA, Rahman AA, Yusry AH, et al. 2015. Arthroscopic partial meniscectomy is superior to physical rehabilitation in the management of symptomatic unstable meniscal tears. International orthopaedics 39: 769-775.

243. Takeda H, Nakagawa T, Nakamura K, et al. 2011. Prevention and management of knee osteoarthritis and knee cartilage injury in sports. British journal of sports medicine 45: 304-309.

244. Arnoczky SP, Warren RF. 1982. Microvasculature of the human meniscus. Am J Sports Med 10: 90-95.

245. Fauno P, Nielsen AB. 1992. Arthroscopic partial meniscectomy: a long-term follow-up. Arthroscopy 8: 345-349.

246. Fairbank TJ. 1948. Knee joint changes after meniscectomy. J Bone Joint Surg Br 30B: 664-670.

247. Nawabi DH, Cro S, Hamid IP, et al. 2014. Return to play after lateral meniscectomy compared with medial meniscectomy in elite professional soccer players. Am J Sports Med 42: 2193-2198.

248. Stein T, Mehling AP, Welsch F, et al. 2010. Long-term outcome after arthroscopic meniscal repair versus arthroscopic partial meniscectomy for traumatic meniscal tears. Am J Sports Med 38: 1542-1548.

249. Matteo BD, Perdisa F, Gostynska N, et al. 2015. Meniscal Scaffolds - Preclinical Evidence to Support their Use: A Systematic Review. Open Orthop J 9: 143-156.

250. Moran CJ, Busilacchi A, Lee CA, et al. 2015. Biological augmentation and tissue engineering approaches in meniscus surgery. Arthroscopy 31: 944-955.

251. Shimomura K, Bean AC, Lin H, et al. 2015. In Vitro Repair of Meniscal Radial Tear Using Aligned Electrospun Nanofibrous Scaffold. Tissue Eng Part A 21: 2066-2075.

252. Freytes DO, Martin J, Velankar SS, et al. 2008. Preparation and rheological characterization of a gel form of the porcine urinary bladder matrix. Biomaterials 29: 1630-1637.

253. Mauck RL, Martinez-Diaz GJ, Yuan X, et al. 2007. Regional multilineage differentiation potential of meniscal fibrochondrocytes: implications for meniscus repair. Anatomical record (Hoboken, NJ : 2007) 290: 48-58.

254. Furumatsu T, Kanazawa T, Yokoyama Y, et al. 2011. Inner meniscus cells maintain higher chondrogenic phenotype compared with outer meniscus cells. Connect Tissue Res 52: 459-465.

255. Chevrier A, Nelea M, Hurtig MB, et al. 2009. Meniscus structure in human, sheep, and rabbit for animal models of meniscus repair. J Orthop Res 27: 1197-1203.

256. Proctor CS, Schmidt MB, Whipple RR, et al. 1989. Material properties of the normal medial bovine meniscus. J Orthop Res 7: 771-782.

257. Proffen BL, McElfresh M, Fleming BC, et al. 2012. A comparative anatomical study of the human knee and six animal species. Knee 19: 493-499.

258. Lin H, Zhang D, Alexander PG, et al. 2013. Application of visible light-based projection stereolithography for live cell-scaffold fabrication with designed architecture. Biomaterials 34: 331-339.

259. Fox AJ, Bedi A, Rodeo SA. 2012. The basic science of human knee menisci: structure, composition, and function. Sports health 4: 340-351.

260. Mezhov V, Teichtahl AJ, Strasser R, et al. 2014. Meniscal pathology - the evidence for treatment. Arthritis Res Ther 16: 206.

261. Edd SN, Netravali NA, Favre J, et al. 2015. Alterations in knee kinematics after partial medial meniscectomy are activity dependent. Am J Sports Med 43: 1399-1407.

262. Petersen W, Tillmann B. 1998. Collagenous fibril texture of the human knee joint menisci. Anat Embryol (Berl) 197: 317-324.

263. Bulgheroni E, Grassi A, Bulgheroni P, et al. 2014. Long-term outcomes of medial CMI implant versus partial medial meniscectomy in patients with concomitant ACL reconstruction. Knee Surg Sports Traumatol Arthrosc.

264. Bouyarmane H, Beaufils P, Pujol N, et al. 2014. Polyurethane scaffold in lateral meniscus segmental defects: clinical outcomes at 24 months follow-up. Orthopaedics & traumatology, surgery & research : OTSR 100: 153-157.

265. Monllau JC, Gelber PE, Abat F, et al. 2011. Outcome after partial medial meniscus substitution with the collagen meniscal implant at a minimum of 10 years' follow-up. Arthroscopy 27: 933-943.

266. Zaffagnini S, Marcheggiani Muccioli GM, Lopomo N, et al. 2011. Prospective long-term outcomes of the medial collagen meniscus implant versus partial medial meniscectomy: a minimum 10-year follow-up study. Am J Sports Med 39: 977-985.

267. Rodkey WG, DeHaven KE, Montgomery WH, 3rd, et al. 2008. Comparison of the collagen meniscus implant with partial meniscectomy. A prospective randomized trial. J Bone Joint Surg Am 90: 1413-1426.

268. Gilbert TW, Wognum S, Joyce EM, et al. 2008. Collagen fiber alignment and biaxial mechanical behavior of porcine urinary bladder derived extracellular matrix. Biomaterials 29: 4775-4782.

269. Petersen TH, Calle EA, Zhao L, et al. 2010. Tissue-engineered lungs for in vivo implantation. Science 329: 538-541.

270. Lehr EJ, Rayat GR, Chiu B, et al. 2011. Decellularization reduces immunogenicity of sheep pulmonary artery vascular patches. The Journal of thoracic and cardiovascular surgery 141: 1056-1062.

271. Gao G, Cui X. 2015. Three-dimensional bioprinting in tissue engineering and regenerative medicine. Biotechnology letters.

272. Sicari BM, Johnson SA, Siu BF, et al. 2012. The effect of source animal age upon the in vivo remodeling characteristics of an extracellular matrix scaffold. Biomaterials 33: 5524-5533.

273. Pauli C, Grogan SP, Patil S, et al. 2011. Macroscopic and histopathologic analysis of human knee menisci in aging and osteoarthritis. Osteoarthritis Cartilage 19: 1132-1141.

274. Melrose J, Smith S, Cake M, et al. 2005. Comparative spatial and temporal localisation of perlecan, aggrecan and type I, II and IV collagen in the ovine meniscus: an ageing study. Histochemistry and cell biology 124: 225-235.

275. Fox AJS, Wanivenhaus F, Burge AJ, et al. 2015. The Human Meniscus: A Review of Anatomy, Function, Injury, and Advances in Treatment. Clin Anat 28: 269-287.

276. Di Giancamillo A, Deponti D, Addis A, et al. 2014. Meniscus maturation in the swine model: changes occurring along with anterior to posterior and medial to lateral aspect during growth. J Cell Mol Med 18: 1964-1974.

277. Rao AJ, Erickson BJ, Cvetanovich GL, et al. 2015. The Meniscus-Deficient Knee Biomechanics, Evaluation, and Treatment Options. Orthop J Sports Med 3: 2325967115611386.

278. Rongen JJ, van Tienen TG, van Bochove B, et al. 2014. Biomaterials in search of a meniscus substitute. Biomaterials 35: 3527-3540.

279. Lakes EH, Matuska AM, McFetridge PS, et al. 2016. Mechanical Integrity of a Decellularized and Laser Drilled Medial Meniscus. J Biomech Eng 138: 4032381.

280. Lin H, Zhang DN, Alexander PG, et al. 2013. Application of visible light-based projection stereolithography for live cell-scaffold fabrication with designed architecture. Biomaterials 34: 331-339.

281. Almeida HV, Liu YR, Cunniffe GM, et al. 2014. Controlled release of transforming growth factor-beta 3 from cartilage-extra-cellular-matrix-derived scaffolds to promote chondrogenesis of human-joint-tissue-derived stem cells. Acta Biomater 10: 4400-4409.

282. Nerurkar NL, Han WJ, Mauck RL, et al. 2011. Homologous structure-function relationships between native fibrocartilage and tissue engineered from MSC-seeded nanofibrous scaffolds. Biomaterials 32: 461-468.

283. Fisher MB, Henning EA, Soeegaard N, et al. 2015. Engineering meniscus structure and function via multi-layered mesenchymal stem cell-seeded nanofibrous scaffolds. J Biomech 48: 1412-1419.

284. Baek J, Chen X, Sovani S, et al. 2015. Meniscus Tissue Engineering Using a Novel Combination of Electrospun Scaffolds and Human Meniscus Cells Embedded Within an Extracellular Matrix Hydrogel. J Orthop Res 33: 572-583.

285. Levett PA, Hutmacher DW, Malda J, et al. 2014. Hyaluronic Acid Enhances the Mechanical Properties of Tissue-Engineered Cartilage Constructs. Plos One 9: e113216.

286. Bian L, Zhai DY, Zhang EC, et al. 2012. Dynamic Compressive Loading Enhances Cartilage Matrix Synthesis and Distribution and Suppresses Hypertrophy in hMSC-Laden Hyaluronic Acid Hydrogels. Tissue Eng Part A 18: 715-724.

287. Fithian DC, Kelly MA, Mow VC. 1990. Material properties and structure-function relationships in the menisci. Clin Orthop Relat Res 252: 19-31.

288. Elder BD, Eleswarapu SV, Athanasiou KA. 2009. Extraction techniques for the decellularization of tissue engineered articular cartilage constructs. Biomaterials 30: 3749-3756.

289. Carrion B, Souzanchi MF, Wang VT, et al. 2016. The Synergistic Effects of Matrix Stiffness and Composition on the Response of Chondroprogenitor Cells in a 3D Precondensation Microenvironment. Adv Healthc Mater 5: 1192-1202.

290. Hakimi O, Mouthuy PA, Zargar N, et al. 2015. A layered electrospun and woven surgical scaffold to enhance endogenous tendon repair. Acta Biomater 26: 124-135.

291. Czaplewski SK, Tsai T-L, Duenwald-Kuehl SE, et al. 2014. Tenogenic differentiation of human induced pluripotent stem cell-derived mesenchymal stem cells dictated by properties of braided submicron fibrous scaffolds. Biomaterials 35: 6907-6917.

292. Sun AX, Lin H, Beck AM, et al. 2015. Projection Stereolithographic Fabrication of Human Adipose Stem Cell-Incorporated Biodegradable Scaffolds for Cartilage Tissue Engineering. Frontiers in bioengineering and biotechnology 3: 115-115.

293. Aisenbrey EA, Bryant SJ. 2016. Mechanical loading inhibits hypertrophy in chondrogenically differentiating hMSCs within a biomimetic hydrogel. J Mater Chem B 4: 3562-3574.

294. Kyburz KA, Anseth KS. 2015. Synthetic Mimics of the Extracellular Matrix: How Simple is Complex Enough? Ann Biomed Eng 43: 489-500.

295. Lee S-H, Shin H. 2007. Matrices and scaffolds for delivery of bioactive molecules in bone and cartilage tissue engineering. Adv Drug Del Rev 59: 339-359.

296. Bosworth LA, Turner LA, Cartmell SH. 2013. State of the art composites comprising electrospun fibres coupled with hydrogels: a review. Nanomedicine-Nanotechnology Biology and Medicine 9: 322-335.

297. Yang G, Lin H, Rothrauff BB, et al. 2016. Multilayered polycaprolactone/gelatin fiber-hydrogel composite for tendon tissue engineering. Acta Biomater 35: 68-76.

298. Rosales AM, Anseth KS. 2016. The design of reversible hydrogels to capture extracellular matrix dynamics. Nature Reviews Materials 1: 15012.

299. Kang H-W, Lee SJ, Ko IK, et al. 2016. A 3D bioprinting system to produce human-scale tissue constructs with structural integrity. Nat Biotechnol 34: 312-319.

300. Tang SW, Tong WY, Shen W, et al. 2014. Stringent requirement for spatial arrangement of extracellular matrix in supporting cell morphogenesis and differentiation. BMC Cell Biol 15.

301. Han YL, Wang S, Zhang X, et al. 2014. Engineering physical microenvironement for stem cell based regenerative medicine. Drug Discov Today 19: 763-773.

302. Beachley VZ, Wolf MT, Sadtler K, et al. 2015. Tissue matrix arrays for high-throughput screening and systems analysis of cell function. Nat Methods 12: 1197-1204.

303. Ranga A, Gobaa S, Okawa Y, et al. 2014. 3D niche microarrays for systems-level analyses of cell fate. Nat Commun 5.

304. Hood L. 2003. Systems biology: integrating technology, biology, and computation. Mechanisms of Ageing and Development 124: 9-16.

305. Ideker T, Galitski T, Hood L. 2001. A new approach to decoding life: Systems biology. Annual Review of Genomics and Human Genetics 2: 343-372.

306. Cosgrove BD, Griffith LG, Lauffenburger DA. 2008. Fusing Tissue Engineering and Systems Biology Toward Fulfilling Their Promise. Cellular and Molecular Bioengineering 1: 33-41.

307. Eddy JA, Funk CC, Price ND. 2015. Fostering synergy between cell biology and systems biology. Trends Cell Biol 25: 440-445.

308. Lenas P, Moos M, Jr., Luyten FP. 2009. Developmental Engineering: A New Paradigm for the Design and Manufacturing of Cell-Based Products. Part I: From Three-Dimensional Cell Growth to Biomimetics of In Vivo Development. Tissue Eng Part B 15: 381-394.

309. Lenas P, Moos M, Jr., Luyten FP. 2009. Developmental Engineering: A New Paradigm for the Design and Manufacturing of Cell-Based Products. Part II. From Genes to Networks: Tissue Engineering from the Viewpoint of Systems Biology and Network Science. Tissue Eng Part B 15: 395-422.

310. Craft AM, Ahmed N, Rockel JS, et al. 2013. Specification of chondrocytes and cartilage tissues from embryonic stem cells. Development 140: 2597-2610.

311. Craft AM, Rockel JS, Nartiss Y, et al. 2015. Generation of articular chondrocytes from human pluripotent stem cells. Nat Biotechnol 33: 638-645.

312. Lorda-Diez CI, Montero JA, Diaz-Mendoza MJ, et al. 2011. Defining the Earliest Transcriptional Steps of Chondrogenic Progenitor Specification during the Formation of the Digits in the Embryonic Limb. Plos One 6.

313. Bhumiratana S, Eton RE, Oungoulian SR, et al. 2014. Large, stratified, and mechanically functional human cartilage grown in vitro by mesenchymal condensation. Proc Natl Acad Sci 111: 6940-6945.

314. Yamashita A, Morioka M, Yahara Y, et al. 2015. Generation of Scaffoldless Hyaline Cartilaginous Tissue from Human iPSCs. Stem Cell Reports 4: 404-418.

315. Huang AH, Lu HH, Schweitzer R. 2015. Molecular Regulation of Tendon Cell Fate During Development. J Orthop Res 33: 800-812.

316. Liu HH, Zhu SA, Zhang C, et al. 2014. Crucial transcription factors in tendon development and differentiation: their potential for tendon regeneration. Cell Tissue Res 356: 287-298.

317. Shwartz Y, Blitz E, Zelzer E. 2013. One load to rule them all: Mechanical control of the musculoskeletal system in development and aging. Differentiation 86: 104-111.

318. Killian ML, Cavinatto L, Galatz LM, et al. 2012. The role of mechanobiology in tendon healing. J Shoulder Elbow Surg 21: 228-237.

319. Ambrosio F, Wolf SL, Delitto A, et al. 2010. The Emerging Relationship Between Regenerative Medicine and Physical Therapeutics. Phys Ther 90: 1807-1814.

320. Ambrosio F, Russell A. 2010. Regenerative rehabilitation: A call to action. J Rehabil Res Dev 47: XI-XV.

321. Tan Q, Lui PPY, Lee YW. 2013. In Vivo Identity of Tendon Stem Cells and the Roles of Stem Cells in Tendon Healing. Stem Cells and Development 22: 3128-3140.

322. Badylak SE, Gilbert TW. 2008. Immune response to biologic scaffold materials. Semin Immunol 20: 109-116.

323. Wolf MT, Dearth CL, Ranallo CA, et al. 2014. Macrophage polarization in response to ECM coated polypropylene mesh. Biomaterials 35: 6838-6849.

324. Forbes SJ, Rosenthal N. 2014. Preparing the ground for tissue regeneration: from mechanism to therapy. Nat Med 20: 857-869.

325. Scotti C, Gobbi A, Karnatzikos G, et al. 2016. Cartilage Repair in the Inflamed Joint: Considerations for Biological Augmentation Toward Tissue Regeneration. Tissue Eng Part B 22: 149-159.

326. Lane SW, Williams DA, Watt FM. 2014. Modulating the stem cell niche for tissue regeneration. Nat Biotechnol 32: 795-803.

327. Qu F, Pintauro MP, Haughan JE, et al. 2015. Repair of dense connective tissues via biomaterial-mediated matrix reprogramming of the wound interface. Biomaterials 39: 85-94.

328. Vanden Berg-Foels WS. 2014. In Situ Tissue Regeneration: Chemoattractants for Endogenous Stem Cell Recruitment. Tissue Eng Part B 20: 28-39.

329. Andreas K, Sittinger M, Ringe J. 2014. Toward in situ tissue engineering: chemokine-guided stem cell recruitment. Trends Biotechnol 32: 483-492.

330. Lee CH, Lee FY, Tarafder S, et al. 2015. Harnessing endogenous stem/progenitor cells for tendon regeneration. J Clin Invest 125: 2690-2701.

331. Santo VE, Gomes ME, Mano JF, et al. 2013. Controlled release strategies for bone, cartilage, and osteochondral engineering-part I: recapitulation of native tissue healing and variables for the design of delivery systems. Tissue engineering Part B, Reviews 19: 308-326.

332. Santo VE, Gomes ME, Mano JF, et al. 2013. Controlled Release Strategies for Bone, Cartilage, and Osteochondral Engineering-Part II: Challenges on the Evolution from Single to Multiple Bioactive Factor Delivery. Tissue engineering Part B, Reviews 19: 327-352.

333. Mehta M, Schmidt-Bleek K, Duda GN, et al. 2012. Biomaterial delivery of morphogens to mimic the natural healing cascade in bone. Adv Drug Del Rev 64: 1257-1276.